

Universidade do Minho
Escola de Engenharia

Shama Parveen

Microstructure and Mechanical Properties
of Nanomaterial Reinforced Cementitious
Composites

Shama Parveen | Microstructure and Mechanical Properties
of Nanomaterial Reinforced Cementitious Composites

UMinho | 2016

December 2016



Universidade do Minho
Escola de Engenharia

Shama Parveen

Microstructure and Mechanical Properties
of Nanomaterial Reinforced Cementitious
Composites

Doctoral Thesis in

Science and Engineering of Polymers and Composites

Under the Supervision of
Professor Doutor Raul Manuel Esteves de Sousa
Fangueiro

And Co-Supervision of
Professora Doutora Maria da Conceição de Jesus Rêgo
Paiva

December 2016

STATEMENT OF INTEGRITY

I hereby declare having conducted my thesis with integrity. I confirm that I have not used plagiarism or any form of falsification of results in the process of thesis elaboration.

I further declare that I have fully acknowledged the code of Ethical Conduct of the University of Minho.

University of Minho, 30/12/2016

Full name: Shama Parveen

Signature: 

ACKNOWLEDGMENTS

This PhD work has been carried out at the Department of Civil Engineering and Institute for Polymers and Composites of University of Minho, Portugal under the supervision of **Professor Raul Figueiro** and co-supervision of **Professor Maria Conceição Paiva**.

I would like to express my special appreciation and thanks to my supervisor **Professor Raul Figueiro**; he has been a supportive mentor for me. I would like to thank him for encouraging my research work and allowing me to grow as a researcher. His advice and valuable suggestions for my research work as well as my career were invaluable.

I am deeply grateful to **Professor Maria Conceição Paiva** for her support and motivation throughout my research work. Her support helped me to complete my experiments and thesis writing on time. Also, I express my gratitude to both of my supervisors to allow me to do my research work without any pressure.

I would like to express my gratitude to **Dr. Sohel Rana** for his wonderful support and guidance. He is my mentor personally as well for my research work.

I would like to thank **Dr. Jose Xavier** from University of Trás-os-Montes e Alto Douro, Portugal, for his collaboration in performing tests with Digital Image Correlation technique.

I would also like to thank the technician of Civil Engineering laboratory, **Mr. Carlos Jesus** and Institute for Polymers and Composites, **Mr. Mauricio Malheiro** for their extreme efforts and assistance during my experimental work. I am also grateful to **Eunice Cunha** who has supported me during the execution of this research work.

Finally, I would like to dedicate this work to my **Father Shri Krishnendu Shankar Ghosh, late grandfather –in –law Md. Abdur Razzaque** and my **husband Dr. Sohel Rana** who supported me all the way until here. Special thanks to my son **Aman Rana**, for his tolerance and support during his mother's PhD.

Publications

Publications in International Journals:

1. Shama Parveen, Sohel Rana, and Raul Figueiro. A review on nanomaterial dispersion, microstructure and mechanical properties of carbon nanotube and nanofiber based cement composites. *Journal of Nanomaterials* 2013(2013): 1-19.
2. Shama Parveen, Sohel Rana, Raul Figueiro, and Maria Conceição Paiva. Microstructure and mechanical properties of carbon nanotube reinforced cementitious composites developed using a novel dispersion technique. *Cement and Concrete Research* 73 (2015): 215-227.
3. Shama Parveen, Sohel Rana, Raul Figueiro, and Maria Conceição Paiva. Characterizing dispersion and long term stability of concentrated carbon nanotube aqueous suspensions for fabricating ductile cementitious composites. *Powder Technology* 307 (2017): 1–9.
4. Shama Parveen, Sohel Rana, Raul Figueiro, and Maria Conceição Paiva. A Novel Approach of Developing Micro Crystalline Cellulose Reinforced Cementitious Composites with Enhanced Microstructure and Mechanical Performance. *Cement and Concrete Composites*. Under Review.

Publications in International Conferences:

1. S. Parveen, S. Rana, Raul Figueiro, “Microstructure and mechanical properties of carbon nanotube/cement nanocomposites”, IRF 2013, June 23-27, Funchal, Portugal.
2. S. Rana, S. Parveen, Raul Figueiro, “Nano-reinforced concrete: an intelligent and high performance construction material”, IRF 2013, June 23-27, Funchal, Portugal.
3. Shama Parveen, Sohel Rana, Raul Figueiro, A Review on Nanocellulose Composites: Preparation, properties and applications. ICNF2013, 9-10th June, Guimaraes, Portugal.
4. Shama Parveen, Sohel Rana, Raul Figueiro, M.C. Paiva, Aqueous dispersion of various types of carbon nanotubes at high concentrations using Pluronic F127, February 12-14, NanoPT2014, Porto, Portugal

5. Shama Parveen, Soheli Rana, Raul Figueiro, M.C. Paiva, Investigation on the homogeneity and stability of aqueous nano cellulose suspensions prepared using Pluronic F-127, ICNF2015, 27th-29th April 2015. Sao Miguel Portugal.
6. Soheli Rana, Shama Parveen, Raul Figueiro, M. C. Paiva, Development of Ductile Cementitious Composites Using Carbon Nanotubes. Nano PT, 11th-13th February 2015. Porto Portugal.
7. Shama Parveen, Soheli Rana, Raul Figueiro, M. C. Paiva, A Review on the Advancement of Nano cellulose as Reinforcement of Polymer Matrix. IRF2016, 24-28 July 2016. Porto Portugal (Accepted for Oral Presentation).

Book Chapters:

1. S. Parveen, S. Rana, R. Figueiro (2016). Influence of Carbon Nanotube Dispersion in Cementitious Composites. In: Dispersion of Carbon Nanotubes. Pan Stanford Publishing (In progress).
2. S. Parveen, S. Rana, R. Figueiro (2017). Macro and nano dimensional plant fibre reinforcements for cementitious composites. In: Sustainable & non-conventional construction materials using inorganic bonded fiber composites. Woodhead Publishing.

Abstract

Nanotechnology has now become a widely accepted technology to improve performance and functionality of materials. Like all other engineering disciplines, nanotechnology is emerging as a boon for civil engineering also. Considerable efforts have been directed towards using various nano and micro materials [e.g. carbon nanotubes (CNTs), nano TiO₂, nano SiO₂, nanocellulose, etc.] to improve cementitious materials, which are most widely used in construction all over the world. Despite of tremendous research attempts, most of these advanced cementitious materials could not be utilized at commercial scale, mainly due to the cost and processing difficulties of nano or micro materials (e.g. agglomeration, long dispersion time, energy consumption, health hazards, etc.).

This PhD work aims at improving the microstructure and mechanical performance of cementitious materials by dispersing CNT and micro crystalline cellulose (MCC) through short and industrially viable dispersion techniques. To achieve this objective, novel dispersion routes (using Pluronic F-127 as surfactant) have been explored for the fabrication of CNT and MCC reinforced cementitious composites. These two types of reinforcing materials were homogeneously dispersed within the cementitious matrix and their influence on the microstructure and mechanical properties (flexural and compressive properties and fracture energy) was thoroughly investigated. The effectiveness of the dispersion routes was characterized by studying the dispersion homogeneity and agglomeration (using optical microscopy), extractability (using UV-Vis spectroscopy) as well as short and long term storage stability. The optimum concentration of Pluronic F-127 (with respect to different CNT/MCC concentrations) and the best dispersion parameters were investigated.

In the first phase of this research, different types of CNT, namely single-walled (SWCNT), multi-walled (MWCNT), functionalized SWCNT (f-SWCNT) and functionalized MWCNT (f-MWCNT) were dispersed in water using Pluronic F-127 with the help of a short (1hr) and medium energy (80W) ultrasonication process at different concentrations (0.1 to 0.3 wt.%). A commonly used surfactant for CNT dispersion, sodium dodecyl benzene sulphonate (SDBS) was also used for the comparison purpose. Pluronic F-127 at optimum concentrations (1 wt.% for 0.1 wt.% CNT, 5 wt.% for 0.2 wt.% CNT and 5 wt.% for 0.3 wt.% CNT) provided highly homogeneous CNT dispersion with very less agglomerates. Overall, SWCNTs exhibited

higher extractability than MWCNTs with Pluronic and surface functionalization reduced the extractability, but enhanced the long term stability. Although SDBS could lead to higher extractability, the long term stability was considerably improved with Pluronic. Pluronic acted as superplasticizer and significantly improved the bulk density and mechanical properties of cement mortar. Further, dispersion of 0.1% SWCNT with Pluronic improved flexural modulus of mortar by 72% and flexural and compressive strengths by 7% and 19%, respectively after 28 days of hydration. Flexural and compressive strengths of cement mortar containing functionalized SWCNT increased with the hydration period up to 17% and 23% after 56 days, respectively. All CNT reinforced cementitious composites exhibited significantly higher stiffness, fracture energy and ductility as compared to plain mortar and composite samples prepared using SDBS.

In the second phase, MCC was dispersed homogeneously in water using Pluronic F-127 as a surfactant with the help of ultrasonication process (15 mins, 80W) and the aqueous suspensions were added to cement/sand mixture to prepare cementitious composites. A commonly used stabilizing agent for MCC, carboxy methyl cellulose (CMC) was also used for the comparison purpose. The influence of Pluronic and CMC concentration, superplasticizer, dispersion technique and dispersion temperature on cement mortar's mechanical performance was thoroughly studied to find out the optimum conditions. Overall, Pluronic (with Pluronic: MCC ratio of 1:5) led to better MCC dispersion as well as dispersion stability as compared to CMC. The best mechanical performance was achieved with Pluronic in combination with superplasticizer using ultrasonication process, resulting in improvement of 106%, 31% and 66% in flexural modulus, flexural strength and compressive strengths of cement mortar, respectively (highest values reported till date). The bulk density and degree of hydration of cementitious composites also improved significantly with the addition of MCC. However, the breaking strain of the cement mortar reduced significantly due to MCC incorporation.

This thesis explored the possibility of achieving excellent dispersion of CNT and MCC within cementitious matrices through a short and less energy intensive dispersion route involving Pluronic F-127 as surfactant, in order to develop high performance cementitious composites.

Resumo

Hoje em dia o uso de nanotecnologias e de nanomateriais é cada vez mais generalizado, com o objetivo de melhorar o desempenho e funcionalidade dos materiais. Tal como noutras áreas da engenharia, também na engenharia civil a utilização de nanomateriais se apresenta muito promissora. Têm-se verificado esforços consideráveis no sentido de utilizar materiais de dimensões nano e micro, como por exemplo nanotubos de carbono (CNT), nanopartículas de dióxido de titânio (TiO_2), de dióxido de silício (SiO_2), nanocelulose, etc., para melhorar cimentos, que são dos materiais mais amplamente utilizados em construção em todo o mundo. Apesar do grande esforço de investigação realizado nesse sentido, a maioria desses materiais avançados à base de cimento não podem ainda ser utilizados em escala comercial, principalmente devido ao custo das nanopartículas e à dificuldade no seu processamento (por exemplo aglomeração, tempo de dispersão no material à base de cimento, consumo de energia, os riscos para a saúde, etc.).

Neste trabalho de doutoramento procurou-se melhorar a microestrutura e o desempenho mecânico dos materiais à base de cimento por adição de CNT e celulose microcristalina (MCC), usando técnicas de dispersão eficientes e industrialmente viáveis. Para atingir este objetivo foram exploradas novas estratégias de dispersão usando Pluronic F-127 como agente tensioativo, permitindo a produção de suspensões aquosas estáveis das nano e micro partículas, para a preparação de compósitos de cimento contendo CNT e MCC. Estes dois tipos de materiais de reforço foram homogeneamente dispersos na matriz de cimento e sua influência sobre a microestrutura e propriedades mecânicas (flexão, compressão e energia de fratura) foi extensamente investigada. A eficácia das estratégias de dispersão foi caracterizada através do estudo da homogeneidade da dispersão e aglomeração (por microscopia óptica), da capacidade para estabilizar nanopartículas em suspensão aquosa (usando espectroscopia UV-Visível), bem como a estabilidade de armazenamento a curto e longo prazo. Foi investigada a concentração óptima de Pluronic F-127 (com respeito a diferentes concentrações CNT / MCC) assim como os melhores parâmetros de dispersão.

Na primeira fase da investigação estudou-se a dispersão em água de diferentes tipos de CNT, nomeadamente de CNT de parede única (SWCNT), de parede múltipla (MWCNT), SWCNT funcionalizados (f-SWCNT) e MWCNT funcionalizados (f-MWCNT), usando Pluronic F - 127. A dispersão foi realizada com auxílio de um banho de ultrassons, em condições suaves (durante 1 h a 80W), e com diferentes concentrações das nano ou micro partículas (0,1 a 0,3

de % em peso, ou wt%). Utilizou-se também um agente tensioativo comumente aplicado na dispersão CNT, o dodecil benzeno sulfonato de sódio (SDBS), para efeitos de comparação. A utilização de Pluronic F-127 em concentrações ótimas (1 wt% para 0,1 wt% CNT, 5 wt% para 0,2 wt% CNT e 5 wt% para 0,3 wt% CNT) permitiu a dispersão homogênea de CNT, livre de aglomerados. Em geral conseguiu-se maior concentração de SWCNT em suspensão relativamente a MWCNT usando Pluronic, e a funcionalização da superfície reduziu a capacidade de suspensão de CNT, mas aumentou a estabilidade a longo prazo. Embora a utilização de SDBS aumentasse a capacidade de extração (ou seja, a concentração de CNT em suspensão na água), a estabilidade a longo termo aumentou consideravelmente com a utilização de Pluronic. Este tensioativo apresentou uma ação de superplastificante, melhorando significativamente a densificação e as propriedades mecânicas da argamassa de cimento. Além disso, a incorporação de uma dispersão de 0,1 wt% de SWCNT em Pluronic induziu um aumento de 72% do módulo de flexão da argamassa, e de 7% e 19% da resistência à flexão e à compressão, respectivamente, após 28 dias de hidratação. A resistência à flexão e à compressão da argamassa de cimento contendo f-SWCNT aumentou até 17% e 23%, respectivamente, com o período de hidratação de 56 dias. Todos os compósitos à base de cimento com CNT mostraram aumento significativo do módulo, energia de fratura e deformabilidade, em comparação com argamassa simples e amostras de compósitos preparados com SDBS.

Na segunda fase, dispersou-se homogeneamente MCC em água usando Pluronic F-127 como um agente tensioativo, com a ajuda de ultrassons (15 minutos, 80 W) e as suspensões aquosas foram adicionados à mistura de cimento e areia para a preparação de compósitos. Para efeitos de comparação utilizou-se também um agente estabilizante para o MCC, a carboximetil celulose (CMC). Estudou-se detalhadamente a influência da concentração de Pluronic e CMC, de superplastificador, da técnica de dispersão e da temperatura de dispersão no desempenho mecânico argamassa de cimento, com o objetivo de identificar o melhor conjunto de condições. Concluiu-se que, em geral, o Pluronic (com Pluronic:MCC na razão de 1:5) conduziu a uma melhor dispersão da MCC, bem como estabilidade da dispersão, em comparação com CMC. O melhor desempenho mecânico foi alcançada com Pluronic em combinação com superplastificador usando dispersão por ultrassons, resultando no aumento de 106%, 31% e 66% no módulo de flexão, resistência à flexão e resistência à compressão da argamassa de cimento, respectivamente (valores mais elevados reportados até à data). A densidade e o grau de hidratação dos materiais compósitos à base de cimento também

melhoraram significativamente com a adição de MCC. No entanto, a deformação de rutura da argamassa de cimento reduziu significativamente com a incorporação da MCC.

Esta tese explorou a possibilidade de atingir uma excelente dispersão da CNT e MCC em matrizes à base de cimento através de um processo de dispersão simples e rápido, envolvendo Pluronic F-127 como agente tensioativo, a fim de produzir compósitos de cimento de alto desempenho.

TABLE OF CONTENTS

Acknowledgements	v
Publications	ix
Abstract	xi
Resumo	xiii
Table of Contents	xvii
List of Figures	xxi
List of Tables	xxvii
List of Acronyms	xxix
Chapter 1: Introduction	1
1.1. Aim	2
1.2. Cementitious Matrix.....	3
1.3. Carbon Nanotube and Its Properties.....	4
1.4. Nanocellulose and Its Properties.....	6
1.5. Motivation.....	8
1.6. Objectives.....	9
1.7. Outline of Thesis.....	11
Chapter 2: Literature Review	13
State of the Art: Carbon Nanomaterials Reinforced Cementitious Composites	
2.1. Dispersion of Carbon Nanotubes and Nanofibers	14
2.2. Dispersion of Carbon Nanotubes and Nanofibres within Cementitious Matrices.....	14
2.2.1. Physical Techniques	16
2.2.2. Chemical Methods	16
2.2.3. Novel Routes of CNT Dispersion.....	22
2.2.4. Large-Scale Production of CNT Dispersion.....	24
2.3. Microstructure of Carbon Nanomaterial/ Cement Nanocomposites.....	25

2.4.	Mechanical Properties of CNT/CNF Reinforced Cementitious Composites..	26
2.4.1.	Influence of Dispersion.....	26
2.4.2.	Influence of Nanomaterial Surface Treatment and Interface.....	28
2.4.3.	Influence of Microstructure.....	30
2.4.4.	Mechanical Properties of Hybrid Cement Nanocomposites.....	31
State of The Art: Nanocellulose Reinforced Cementitious Composites		
2.5.	Cellulose.....	33
2.6.	Structure of Cellulose.....	33
2.7.	Preparation of Cellulose Nanocrystal.....	34
2.8.	Dispersion of Nano Cellulose.....	37
2.8.1.	Chemical Modification of Nano Crystalline Cellulose.....	37
2.8.1.1.	Nano-Covalent Modification of Nano Crystalline Cellulose..	38
2.8.1.2.	Covalent Functionalization of Nano Crystalline Cellulose...	39
2.9.	Dispersion of Nanocellulose within Cementitious Matrix.....	44
2.10.	Effect of Nanocellulose on Cementitious Matrix.....	45
2.10.1.	Influence of Nanocellulose on Flow Behaviour of Cement Paste...	45
2.10.2.	Influence of Nanocellulose on Mechanical Properties of Cement...	46
2.10.3.	Influence of Nanocellulose on Microstructure of Reinforced Cement.....	48

Chapter 3: Dispersion of Carbon Nanotubes in Aqueous

Suspension.....	51	
3.1.	Introduction.....	52
3.2.	Materials and Methods	53
3.2.1.	Raw Materials and Characterization.....	53
3.2.2.	CNT Dispersion Route.....	55
3.2.3.	Characterization of CNT Dispersion.....	55
3.2.3.1.	Visual Observation.....	56
3.2.3.2.	Optical Microscopy.....	56
3.2.3.3.	Quantitative Analysis of Agglomerates.....	57
3.2.3.4.	UV-Vis Spectroscopy.....	57
3.2.3.5.	Transmission Electron Microscopy.....	57
3.3.	Results and Discussion.....	58

3.3.1. CNT Morphology and Properties.....	58
3.3.2. Visual Inspection of Sedimentation.....	58
3.3.2.1. Sedimentation after Ultracentrifugation.....	59
3.3.3. Optical Microscopy: Qualitative Analysis.....	60
3.3.3.1. Quantitative Analysis of Agglomerates.....	62
3.3.4. UV-Vis Spectroscopy: Extractability.....	65
3.3.5. Long Term Storage Stability.....	67
3.3.6. Detection of Surfactant on CNT Surface.....	69
3.3.7. Discussion: Carbon Nanotube Dispersion in Aqueous Surfactant Solutions.....	70
3.4. Conclusions.....	71

Chapter 4: Development of Carbon Nanotube Reinforced Cementitious

Composites	73
4.1. Introduction.....	74
4.2. Materials and Methods	75
4.2.1. Raw Materials	75
4.2.2. Preparation of CNT Aqueous Suspension	75
4.2.3. Preparation of Plain Mortar and CNT/Mortar Composites.....	75
4.2.4. Characterization of Plain Mortar and CNT/Mortar Composites.....	76
4.3. Results and Discussion.....	77
4.3.1. Consistence of Mortar Paste	77
4.3.2. Effect of Pluronic on Dry Bulk Density	78
4.3.3. Mechanical Properties	79
4.3.3.1. Effect of Surfactant and CNT Type on Flexural Properties... 79	
4.3.3.2. Effect of surfactant and CNT Type on Compressive Properties.....	82
4.3.3.3. Effect of Hydration Period on Mechanical Properties	82
4.3.4. Microstructure.....	88
4.3.5. Fracture behaviour.....	89
4.4. Comparison with Previous Studies.....	90
4.5. Conclusions.....	92

Chapter 5: Development of Micro Crystalline Cellulose Reinforced Cementitious Composites.....93

5.1. Introduction.....94

5.2. Materials and Methods.....95

5.2.1. Raw Materials.....95

5.2.2. Preparation of MCC aqueous suspensions.....95

5.2.3. Characterization of Aqueous MCC Suspensions through UV-Vis Spectroscopy.....96

5.2.4. Characterization of Aqueous MCC Suspensions through Optical Microscopy.....96

5.2.5. Fabrication of MCC/Cement Composites.....96

5.2.6. Characterization of Mechanical Performance and Dry Bulk Density..99

5.2.7. Thermo-gravimetric Analysis of MCC/Cement Composites.....99

5.2.8. Microstructural Characterization of MCC/Cement Composites.....99

5.3. Results and Discussion.....99

5.3.1. Aqueous Dispersion of MCC: Visual Inspection.....99

5.3.2. Characterization of MCC Dispersion Quality using UV-Vis Spectroscopy.....101

5.3.3. Characterization of Dispersion Quality through Optical Microscopy.....102

5.3.4. Dry Bulk Density of Cement and MCC/Cement Composites.....104

5.3.5. Mechanical Properties of MCC/Cement Composites104

5.3.5.1. Influence of Processing Parameters on Mechanical Properties.....107

5.3.6. Influence of MCC on Cement Hydration.....109

5.3.7. Microstructure of MCC/Cement Composites.....110

5.3.8. Main Findings.....110

5.4. Conclusions.....112

Chapter 6: Conclusions and Future Work.....115

References.....119

LIST OF FIGURES

Figure 1.1 The molecular model of C-S-H: the blue and white spheres are oxygen and hydrogen atoms of water molecules, respectively; the green and gray spheres are inter- and intralayer calcium ions, respectively; the yellow and red sticks are silicon and oxygen atoms in silica tetrahedral	3
Figure 1.2 Schematic representation of the structure of graphene (a), SWCNT (b) and MWCNT (c)	4
Figure 1.3 Preparation routes of nanocellulose	6
Figure 1.4 SEM micrograph of concrete showing cracks (a) and collapse of structure due to extensive crack formations (b)	8
Figure 2.1 SEM image of CNT/cement paste after hydration	15
Figure 2.2 Dispersion of MWCNT within cementitious composites prepared using different surfactant to MWCNT weight ratio: (a) 0, (b) 1.5, (c) 4.0, and (d) 6.25	17
Figure 2.3 Fracture surface of CNF/cement nanocomposites, showing individually dispersed CNFs	17
Figure 2.4 TEM image of MWCNTs showing presence of acrylic acid polymer on the surface at magnifications of 13000x (a) and 800000x (b)	19
Figure 2.5 TEM image of MWCNT dispersion in water without any treatment (a) and with acrylic acid polymer and sonication (b)	19
Figure 2.6 SEM image of cement nanocomposites with untreated CNTs ((a), (b)) and acid-treated CNTs ((c), (d))	21
Figure 2.7 TEM image of CCF-free FWCNTs after hydration for 1 hour (a) and 5.5 hour (b)	22
Figure 2.8 Schematic diagram showing concept of incorporating CNTs/CNFs within cementitious composites by their direct growth on	23

cement particles	
Figure 2.9 TEM image showing complete coverage of cement particles by carbon nanomaterial (a), formation of MWCNT (b), and CNF formation (c)	24
Figure 2.10 SEM images of pristine silica particles (a), growth of CNTs on silica particles at 600°C (b), and TEM image of CNTs grown on silica particles at 600°C (c)	24
Figure 2.11 SEM micrographs of 1wt.% CNT/cement paste after 28 days of hydration at different magnifications	25
Figure 2.12 SEM image of hardened cement paste (28 days) after mechanical test at different magnifications	27
Figure 2.13 Post-compression testing structural integrity of plain cement paste (a) and cement paste containing 0.5 wt.% surface-treated CNFs (b)	29
Figure 2.14 Comparison of compressive behaviour of cement paste and CNF/cement composites before and after decalcification	29
Figure 2.15 Structure of cement-foam concrete: (a) without nanotubes, (b) with 0.05% CNT (pore walls), (c) without CNT (perforated), and (d) stabilized with addition of 0.05% CNT	31
Figure 2.16 Load-CMOD curves for (a) plain cement paste and cement paste containing CNFs, (b) cement paste and cement paste containing PVA microfibers, (c) cement paste containing PVA microfibers and hybrid cement paste, and (d) cement paste containing CNFs, cement paste containing PVA microfibers, and hybrid cement paste for CMOD values less than 0.04mm	32
Figure 2.17 Structure of cellulose: (a) chemical structure, (b) crystalline and amorphous regions and (c) cellulose nano crystals	34
Figure 2.18 Cellulose nano crystals in the form of rods (a and b) and spheres (c and d)	35
Figure 2.19 (a): Acid hydrolysis mechanism; (b): Esterification of cellulose nanocrystal surface	36
Figure 2.20 Classification of NCC dispersion techniques.	37

Figure 2.21 Single step synthesis and functionalization of NCC through Fischer esterification process	40
Figure 2.22 Scheme for functionalization of NCC with FITC	41
Figure 2.23 Model explaining the silane functionalization of NCC at: (a) low DS showing onset of surface functionalization, (b) moderate DS showing surface functionalization and (c) high DS showing disruption of NCC core	42
Figure 2.24 Schematic of TEMPO-mediated oxidation of NCC	43
Figure 2.25 Influence of NCC vol.% on the yield stress of mortar paste	46
Figure 2.26. Improvement of mortar's flexural strength due to CNC addition	47
Figure 2.27. Schematic diagram explaining the short circuit diffusion mechanism	47
Figure 2.28 FE-SEM image of cement based materials with 3 wt.% of MCC. (a) cement mortar with 3 wt.% of MCC. (b) cement paste with 3 wt.% of MCC. (c) FE-SEM image of cement paste with 3 wt.% of MCC	48
Figure 3.1 Morphology of CNTs: (a) MWCNT, (b) f-MWCNT, (c) SWCNT and (d) f-SWCNT	54
Figure 3.2 Chemical structure of (a) Pluronic F-127 and (b) SDBS	55
Figure 3.3 Different techniques used to characterize the quality of CNT suspensions	56
Figure 3.4 Visual observation of sedimentation of various CNT suspensions prepared using Pluronic and SDBS	58
Figure 3.5 Inspection of sedimentation of various CNT suspensions after ultracentrifugation: (a) 0.1% SWCNT-1% Pluronic, (b) 0.1% MWCNT-1% Pluronic, (c) 0.1% f-SWCNT-1% Pluronic, (d) 0.1% f-MWCNT-1% Pluronic, (e) 0.3% SWCNT-5% Pluronic, (f) 0.3% MWCNT-5% Pluronic, (g) 0.3% f-SWCNT-5% Pluronic and (h) 0.3% f-MWCNT-5% Pluronic, (a1) to (h1): same CNT conc. as (a) to (h), dispersed using SDBS	59
Figure 3.6. Optical micrographs of MWCNT suspensions prepared using Pluronic F-127 and SDBS	60

Figure 3.7. Optical micrographs of SWCNT suspensions prepared using Pluronic F-127 and SDBS	61
Figure 3.8. Total area of agglomerates (a) and max. agglomerate size (b) of CNT suspensions	62
Figure 3.9 Cumulative area ratio of (a) MWCNT and (b) SWCNT suspensions (P denotes Pluronic F-127)	64
Figure 3.10 UV-Vis absorption spectra of (a) MWCNT and (b) SWCNT suspensions prepared using Pluronic F-127	65
Figure 3.11. Long term stability of CNT suspensions over a period of 4 years: (a) 0.2% SWCNT with 0.8% SDBS, (b) 0.2% SWCNT with 5% Pluronic and (c) 0.04-0.0025% SWCNT suspensions prepared through dilution of (b)	68
Figure 3.12 TEM micrograph of 0.2% SWCNT suspensions prepared with 5% Pluronic: pristine SWCNT (a) and functionalized SWCNT (b)	68
Figure 3.13 ATR curves of Pluronic F-127 and various nanotubes	69
Figure 4.1 Determination of flow diameter	76
Figure 4.2 Flexural stress-strain curves of plain mortar and CNT/cement composites	79
Figure 4.3 Comparison between predicted and experimental values of flexural modulus	81
Figure 4.4 Comparison of flexural strength of plain mortar and CNT/mortar samples at different periods of hydration	84
Figure 4.5 Comparison of compressive strength of plain mortar and CNT/mortar samples at different periods of hydration	85
Figure 4.6 FTIR curves of plain mortar and CNT/mortar samples	86
Figure 4.7 DTG curves of plain mortar and CNT/mortar composites	87
Figure 4.8 Fracture surface of plain mortar (a) and CNT/mortar samples (b, c, d, e, f) at different	88

Figure 4.9 Load-CTOD curves (a) and fracture energy (b) of plain cement mortar and CNT/cement composites	89
Figure 5.1 Aqueous suspension of MCC with Pluronic (a) and CMC (b)	100
Figure 5.2 MCC suspensions prepared using Pluronic: (a) 0% Pluronic and (b) 1% Pluronic and (c) 2% Pluronic	101
Figure 5.3. UV-Vis absorption spectra for (a) Pluronic and (b) CMC suspensions	102
Figure 5.4. Optical micrographs of MCC suspensions: (a) 0.5% MCC, (b) 1% MCC, and (c) 1.5% MCC	103
Figure 5.5. Optical micrographs of MCC suspensions prepared using CMC: (a) 0.5% MCC, (b) 1% MCC and (c) 1.5% MCC	103
Figure 5.6. Flexural stress-strain curves of plain mortar and MCC/cement composites	105
Figure 5.7. Flexural strength of plain mortar and MCC/cement composites	107
Figure 5.8 Compressive strength of plain mortar and MCC/cement composites	108
Figure 5.9. Derivative weight loss curves for plain cement mortar and mortar containing MCC	109
Figure 5.10. Microstructure of MCC reinforced cementitious composites	110

LIST OF TABLES

Table 1.1 Comparison of Properties of Carbon Nanotubes with High Performance Fibers	5
Table 1.2 Comparison of Conductivity of Carbon Nanotubes with other Conductive Materials	5
Table 1.3 Comparison of Properties of Nanocellulose with other Material	7
Table 3.1. Properties of Different Types of CNT	54
Table 3.2 Properties and Concentrations of Surfactants	55
Table 3.3 Concentration and Extractability of Various Types of CNT Dispersed in Aqueous Solution using Pluronic F-127 and SDBS	66
Table 3.4. Extractability of 0.2% SWCNT Suspensions after Storage for 4 years	67
Table 4.1 Consistence of Plain Mortar and CNT/Mortar Pastes	78
Table 4.2 Dry Bulk Density of Plain Mortar with and without Pluronic	79
Table 4.3 Flexural Properties of Plain Mortar and CNT/Mortar Samples	80
Table 4.4 Compressive Strength of Plain Mortar and CNT/Mortar Composites	83
Table 4.5 Flexural Strength (MPa) of Plain Mortar and CNT/mortar samples at 28, 42 and 56 Days of Hydration	83
Table 4.6 Compressive Strength (MPa) of Mortar and CNT/Mortar Samples at 28, 42 and 56 Days of Hydration	85
Table 4.7 Comparison of Present Results with Those of CNT/Cement Composites Prepared Using Other Dispersion Routes	91

Table 5.1 Properties of Raw Materials	95
Table 5.2 Details of Samples Prepared using CMC	97
Table 5.3 Details of Samples Prepared using Pluronic	98
Table 5.4 Bulk Density of Plain Mortar and MCC/Mortar Composites	104
Table 5.5 Flexural Modulus and Fracture Energy of Plain Cement Mortar and MCC/Cement Composites	105
Table 5.6 Improvement of Flexural and Compressive Strengths of Mortar due to MCC Addition	106
Table 5.7 Comparison of Main Findings of Present Research with the Previous Studies on Nanocellulose, MCC and CNT Reinforced Cementitious Composites	111

LIST OF ACRONYMS

AG	Gum Arabic
CMC	Carboxy Methyl Cellulose
CMOD	Crack Mouth Opening Displacement
CNF	Carbon Nanofiber
CNT	Carbon Nanotube
C-S-H	Calcium Silicate Hydrate
CTAB	Cetyl Trimethyl Ammonium Bromide
CVD	Chemical Vapour Deposition
DIC	Digital Image Correlation
f-MWCNT	Functionalized Multi Walled Carbon Nanotube
f-SWCNT	Functionalized Single Walled Carbon Nanotube
FT-IR	Fourier Transform- Infra Red
MS	Magnetic Stirring
MCC	Micro Crystalline Cellulose
MFC	Micro Fibrillar Cellulose
MWCNT	Multi Walled Carbon Nanotube
NaDC	Sodium deoxycholate
NCC	Nano Crystalline Cellulose
NFC	Nano Fibrillar Cellulose
SDBS	Sodium Dodecyl Benzene Sulphonate
SEM	Scanning Electron Microscope
SWCNT	Single Wall Carbon Nanotube
TEM	Transmission Electron Microscope
TX10	Triton X-100
UV-Vis	Ultra Violet- Visible

Chapter 1

Introduction

1.1 Aim

Concrete is considered as the building block for civil engineering structures like buildings, highways, bridges, runways, and so on. Concrete is known for its strength and also it is one of the oldest materials used for construction starting from the Roman era. Though concrete is considered as a strong material, reinforcements are required to reduce its brittleness and improve ductility [1]. Nowadays, nanomaterials are being extensively researched for different industrial applications due to promising characteristics of various nano particles and fibers. Nanomaterials such as nanofibres and nanotubes have been successfully utilized in various polymeric matrices to improve mechanical, thermal and electrical performances, as well as to introduce smart functionalities such as strain and damage sensing, self-healing, self-cleaning, etc [2-7]. Exploring nanotechnology for civil engineering structures is gaining attention due to possibility of introducing various desirable functionalities with the help of nanomaterials. To achieve the target of developing high performance nano reinforced cementitious composites, the first and foremost requirement was identified to be the efficient dispersion of nanomaterials. Till now, various scientists worked with the general dispersion routes which were also followed in case of polymeric matrices, such as ultrasonication, surfactant-assisted dispersion, nanomaterial functionalization, etc. with only limited success [8-18]. Proper selection of nanomaterials as well as dispersion routes was found to be crucial in case of cementitious composites, as they can have strong effects on the hydration behaviour of cement, which in turn, controls the performance of cementitious composites.

The focus of this PhD work is to develop a short and effective route to introduce nano and micro reinforcements within cementitious matrices in order to reduce the time and energy consumption associated with the conventional dispersion processes and to disperse nano/micro materials effectively without losing the beneficial properties of these reinforcing materials as well as cementitious matrix. By ensuring homogeneous dispersion of nano/micro reinforcements, this PhD work mainly focuses on achieving considerable improvement in the microstructure and mechanical properties of cementitious composites. Therefore, the present research work aims at finding suitable dispersing agents and developing a short and less energy intensive process for dispersing nano/micro materials such as carbon nanotubes (CNTs) and micro crystalline cellulose (MCC) within cementitious materials. The research activities undertaken in this thesis are divided into mainly three phases:

- Development of an effective dispersion route for CNT and MCC,
- Development and characterization of CNT reinforced cementitious composites, and
- Development and characterization of MCC reinforced cementitious composites.

1.2 Cementitious Matrix

Concrete generally consists of Ordinary Portland Cement (OPC, which is known as the principal binding agent), coarse aggregates, and fillers such as sand, admixtures, and water. Portland cement is mainly composed of tricalcium silicate (20 - 65%), dicalcium silicate (10 - 55%), tricalcium aluminate (0 - 15%) and tetra calcium aluminoferrate (5 - 15%). These materials react with water with an exothermic reaction forming a mineral glue (known as “C-S-H” gel), calcium hydroxide, ettringite, monosulfate, unhydrated particles, and air voids. Molecular structure of C-S-H gel was not fully understood till recent past. Researchers at the Massachusetts Institute of Technology (MIT, USA) [19] recently proposed a structure, and according to that, cement hydrate consists of a long tetrahedral silica chain and calcium oxide in long range distances, where water causes an intralayer distortion in otherwise regular geometry (Figure 1. 1). The distortion in the structure due to addition of water makes the cement hydrate robust. The density of C-S-H has been determined as 2.6 g/cc [20].

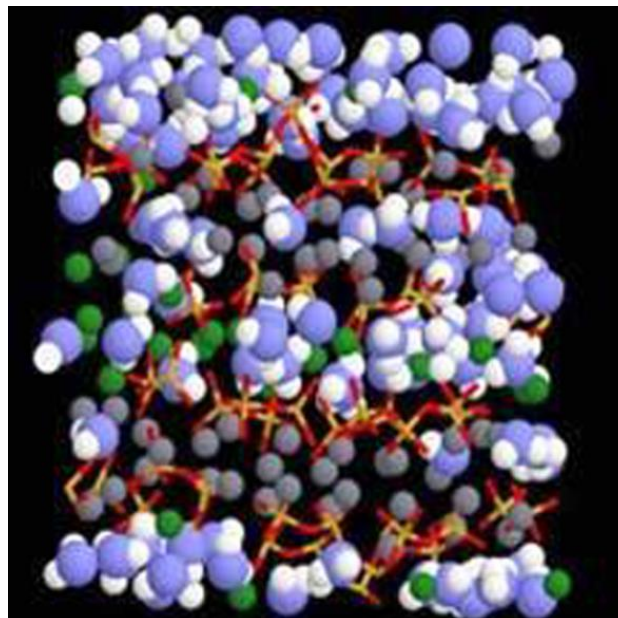


Figure 1. 1 The molecular model of C-S-H: the blue and white spheres are oxygen and hydrogen atoms of water molecules, respectively; the green and gray spheres are inter- and intralayer calcium ions, respectively; the yellow and red sticks are silicon and oxygen atoms in silica tetrahedral [19].

Cementitious materials are characterized by quasi-brittle behaviour and are susceptible to cracking. The cracking process within concrete begins with isolated nanocracks, which then conjoin to form microcracks and in turn macrocracks. Reinforcement is required because of this brittle nature of concrete, and as reinforcements, polymeric fibers as well as glass and carbon fibers were used during the 1970s, 80s, and 90s, respectively [1].

Recently, the use of microfiber reinforcements has led to significant improvement in the mechanical properties of cement-based materials by delaying the transformation of microcracks into macroforms, but they could not stop the crack growth. This fact encouraged the use of nanosize fibers or particles for concrete reinforcement in order to prevent the transformation of nanocracks into microcracks [21,22]. Nanoparticle addition to cement paste was found to improve mechanical, chemical, and thermal properties of cementitious matrix.

1.3 Carbon Nanotube and Its Properties

Buckyball (or Buckminsterfullerene, a spherical molecule made only of carbon atoms in sp^2 hybridization) was discovered in 1985 by Kroto et al. [23], reactivating the interest in carbon-based nanostructures, with emphasis for the synthesis of CNT by Iijima [24], based on a similar carbon structure with tubular shape. These nanotubes (called multiwalled carbon nanotubes or MWCNTs) consisted of up to several tens of graphitic shells with adjacent shell separation of ~ 0.34 nm, diameters of a few nanometers, and high length/diameter ratio. About two years later, Iijima reported the observations of single-walled carbon nanotubes (SWCNTs), which consist of a single graphite sheet seamlessly wrapped into a cylindrical tube [25], as shown in Figure 1. 2.

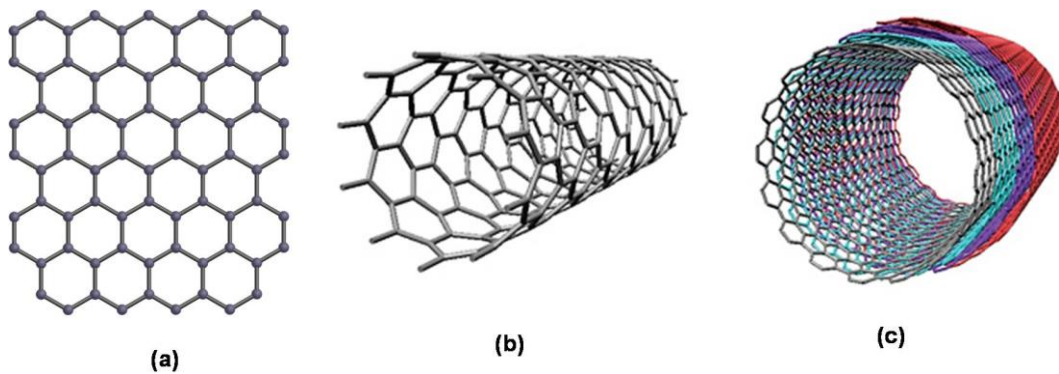


Figure 1. 2 Schematic representation of the structure of graphene (a), SWCNT (b) and MWCNT (c) [25].

CNTs can be characterized as metals or semiconductors based on three different kinds of structure, namely zig-zag, armchair or chiral. CNTs show extraordinary high strength and modulus (Table 1. 1) because of sp^2 bonding similar to graphite, but in case of CNT graphene sheets are rolled forming a tubular structure.

Table 1. 1 Comparison of Properties of Carbon Nanotubes with High Performance Fibers

Fiber Material	Density (g/cm ³)	Young's Modulus (TPa)	Strength (GPa)	Strain at break (%)
Carbon Nanotube	1.3-2	1	10-60	10
HS Steel	7.8	0.2	4.1	<10
Carbon fiber-PAN	1.7-2	0.2-0.6	1.7-5	0.3-2.4
Carbon Fiber – Pitch	2-2.2	0.4-0.96	2.2-3.3	0.27-0.6
E/S Glass	2.5	0.07-0.08	2.4-4.5	4.8
Kevlar-49	1.4	0.13	3.6-4.1	2.8

Source: <http://www.nanocyl.com/CNT-Expertise-Centre/Carbon-Nanotubes>

In addition, CNTs possess excellent thermal and electrical conductivity, as shown in Table 1. 2. CNTs can be produced by various techniques such as arc discharge, laser ablation, thermal and plasma enhanced chemical vapor deposition (CVD), and many other recently developed methods [23-28].

Table 1. 2 Comparison of Conductivity of Carbon Nanotubes with other Conductive Materials

Material	Thermal Conductivity (W/m.K)	Electrical Conductivity (S/m)
Carbon Nanotube	>3000	10^6 - 10^7
Copper	400	6×10^7
Carbon Fiber-PAN	8-105	6.5 - 14×10^6
Carbon Fiber-Pitch	1000	2 - 8.5×10^6

Source: <http://www.nanocyl.com/CNT-Expertise-Centre/Carbon-Nanotubes>

1.4 Nanocellulose and Its Properties

Cellulose is an abundant biopolymer, and with the progress in nanotechnology the nano form of cellulose, i.e. nanocellulose has gained tremendous attention. The terminology micro fibrillar cellulose (MFC) was first coined in early 1980s when ITT Rayonier issued patents and publications based on a totally new nanocellulose composition [29-31]. In later years MFC was modified by acid hydrolysis to obtain nano crystalline cellulose (NCC). Nanocellulose has now become a good alternative for other nanomaterials in various applications due to its remarkable mechanical properties, transparency, ability to form chiral nematic structures and above all, owing to its lower health risk, environment friendliness and biodegradability. Researchers are working with nanocellulose in diverse fields. It can act as reinforcing agent for various matrices because of excellent mechanical properties as well as due to presence of free hydroxyl groups which can be modified according to the needs. Nanocellulose is also being explored in biomedical field for drug delivery, enzyme immobilization, tissue culture, etc. Due to transparency and barrier properties it can be utilized in packaging and as transparent flexible films [32,33]. Nanocellulose can be obtained by mainly two different approaches: top down approach and bottom up approach, as presented in Figure 1. 3.

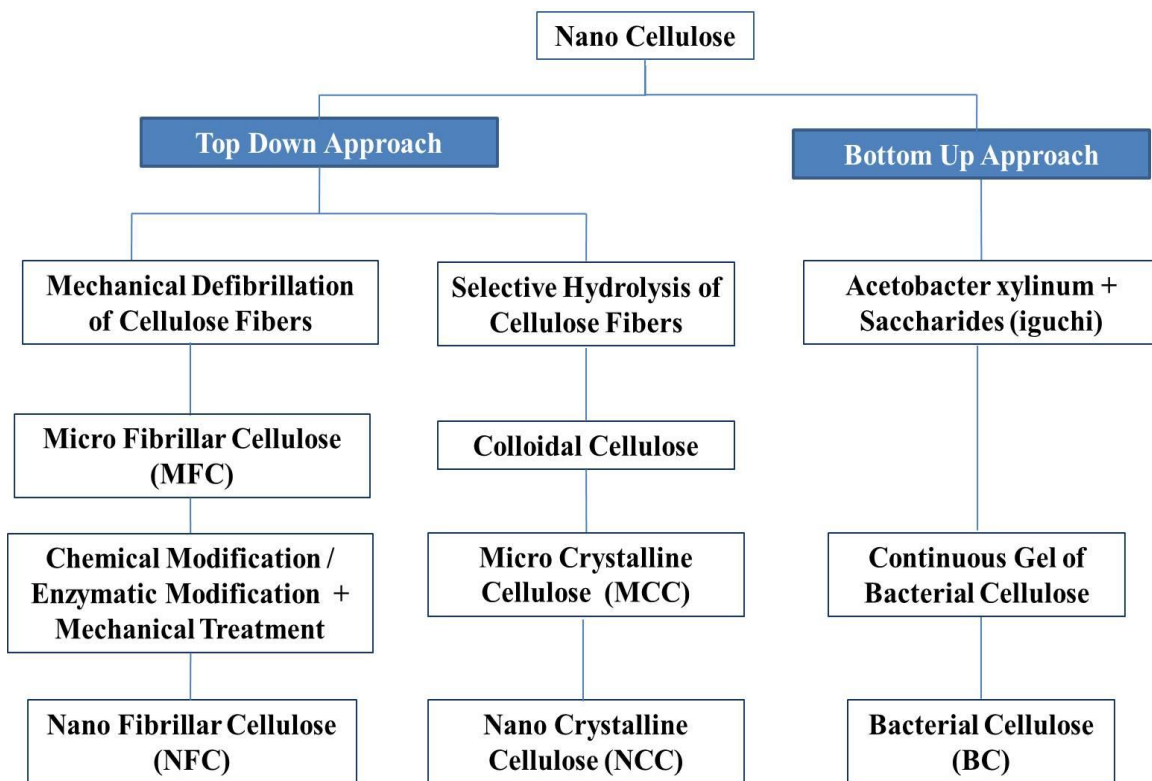


Figure 1. 3 Preparation routes of nanocellulose [32].

The top down approach involves enzymatic or chemical/physical processes to isolate nanocellulose from wood and forest/ agriculture residues. In bottom up approach nanocellulose is obtained from glucose by bacteria. The isolated cellulosic materials with one dimension in the nanometer range are referred as nanocellulose. Nanocellulose can be categorized as nano whiskers or NCC and nano fibrillar cellulose (NFC). When plant products are subjected to strong acid conditions combined with sonication, they produce nano whiskers or NCC. Nano whiskers are rod like structures resulted from hydrolysis of non-crystalline domains. Dimension of nano whiskers depends on the source of cellulose; their length ranges between 100-300 nm. On the other hand, when plant products are subjected to high mechanical shearing without undergoing the hydrolysis steps, it results in NFC. The lateral dimension of NFC lies in the range of 10-30 nm. They are generally present in bundles, in which the individual fibril's lateral dimension is 5 nm [32-40]. The production method of nanocellulose is presented in Figure 1.3 and properties of nanocellulose have been compared with other materials in Table 1. 3.

Table 1. 3 Comparison of Properties of Nanocellulose with other Materials

Material	Density (g/cm ³)	CTE (10 ⁻⁶ /K) Axial	Tensile Strength (GPa) Axial	Elastic Modulus (GPa)	
				Axial	Transverse
Crystalline Cellulose	1.6	0.1	7.5	120-220	11-57
Kevlar-49 Fiber	1.4	2	3.5	124-130	2.5
Glass Fiber	---	4	4.8	86	---
Carbon Fiber	1.8	1.6-2.1	1.5-5.5	150-500	---
Steel Wire	7.8	9-17	4.1	210	---
Clay Nanoplatelets	---	---	---	170	---
Carbon Nanotubes	---	---	11-63	270-950	0.8-30
Boron Nanowhiskers	---	6	2-8	250-360	---

Source: <https://engineering.purdue.edu/nanotrees/cellulose.shtml>

1.5 Motivation

Due to the quasi brittle nature of cement, it is highly susceptible to crack formation. The cracks formed within a cementitious matrix are shown in Figure 1. 4

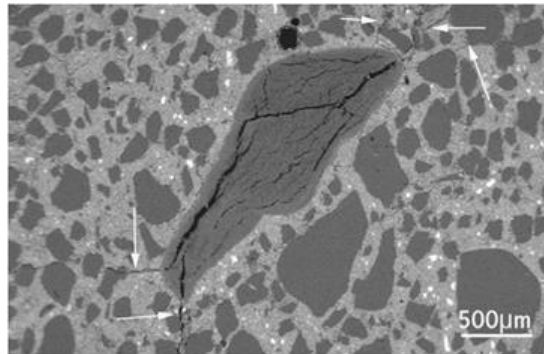


Figure 1. 4 SEM micrograph of concrete showing cracks.

Formation and growth of cracks lead to loss of mechanical performance with time and also make concrete accessible to water and other degrading agents such as CO_2 , chlorides, sulfates, etc. leading to strength loss, corrosion of steel rebars and ultimately, failure of the concrete structures [41]. To decrease brittleness of concrete, reinforcements such as polymeric as well as glass and carbon fibers have been used, and microfibers improved the mechanical properties significantly by delaying (but could not stop) the transformation of micro-cracks into macro forms [1]. This fact encouraged the use of nano-sized fillers in concrete to prevent the growth of nano-cracks and to stop their transformation into micro and macro forms.

Nanomaterials with exceptional properties like CNTs have been incorporated within cementitious matrix to improve mechanical performance and toughness and to introduce electrical conductivity and piezoresistivity [42, 43]. Additionally, at the nano-scale, CNTs exhibited the possibility to restrict the growth of nano-cracks through crack-bridging mechanism [44], thereby, enhancing the durability of concrete. However, the improvement of above properties was found to be strongly dependent on the dispersion of CNT within cementitious matrix, since improper dispersion and nanotube agglomeration even resulted in deterioration of various properties [43]. Therefore, there exists an enormous need for an efficient dispersion route to achieve homogeneous CNT dispersion, and besides mechanical treatments (ultrasonication, stirring, etc.), various chemical dispersants (surfactants and polymers) have been suggested to prepare well dispersed CNT aqueous suspensions for mixing with cement [45-

48]. Recently, natural nano and micro materials like MFC and MCC/NCC are also becoming very attractive due to non-toxicity, good mechanical properties and biocompatibility [49, 50]. Few studies have been conducted to incorporate these materials within concrete with promising results [51, 52]. However, to successfully utilize cellulose nanomaterials within concrete, considerable research is necessary to understand their dispersion behaviour and their influence on cement hydration, microstructure and properties. Therefore, although CNTs have been widely investigated as reinforcements of cementitious matrix, and nanocellulose to some extent, the practical application of this technology is only possible after development of a simple, less energy intensive and industrially viable dispersion techniques for these nano/micro materials. Also, the interaction of these nano/micro structures with cementitious matrix and the influence of various materials and process parameters on the resulting composite's properties should be well understood. Therefore, within this Ph.D. work, Pluronic F-127 has been used, for the first time, as a surfactant to disperse CNTs and MCC within cementitious matrix, in order to develop a short and effective dispersion method. Additionally, to explore the potential of CNTs and MCC for reinforcement of cementitious matrix, various aspects of incorporating CNT/MCC within cementitious matrix (such as dispersion route, influence on hydration, microstructure and mechanical properties) has been thoroughly investigated.

1.6 Objectives

The main objective of this research is to develop high performance cementitious composites with improved microstructure and mechanical properties through incorporation of CNTs and MCC using an effective dispersion route. To achieve this objective, this research has been planned to carry out in the following steps:

1. Literature Review

2. Preparation and Characterization of Homogeneous and Stable Aqueous Suspensions of Carbon Nanotubes

- Preparation of homogeneous and stable aqueous suspensions of CNT using ultrasonication technique in presence of Pluronic F-127.
- Preparation of aqueous suspensions of CNT using ultrasonication in presence of a commonly used surfactant (SDBS) for comparison with Pluronic F-127.

- Detailed characterization of homogeneity and stability of CNT suspensions using various qualitative and quantitative methods, in order to optimize the concentration of Pluronic F-127 with respect to CNT concentration.

3. Preparation of Homogeneous and Stable Aqueous Suspensions of Micro Crystalline Cellulose

- Preparation of homogeneous and stable aqueous suspensions of MCC using ultrasonication technique in the presence of Pluronic F-127.
- Preparation of aqueous suspensions of MCC using ultrasonication in presence of a commonly used stabilizing agent (CMC) for comparison with Pluronic F-127
- Detailed characterization of homogeneity and stability of MCC suspensions using different qualitative and quantitative methods, in order to optimize the concentration of Pluronic with respect to MCC concentration.

4. Development and Characterization of CNT Reinforced Cementitious Composites

- Preparation of cementitious composites incorporating CNT and setting for different hydration periods
- Characterization of workability of mortar paste containing CNT
- Characterization of bulk density, mechanical properties (compressive and flexural properties and fracture energy) and microstructure of cementitious composites
- Investigating the influence of various parameters such as CNT type and concentration, surfactant type, dispersion parameters and hydration time on the microstructure and mechanical performance of cementitious composites.

5. Development and Characterization of MCC Reinforced Cementitious Composites

- Preparation of MCC incorporated cementitious composites
- Characterization of workability of MCC added mortar paste
- Characterization of bulk density, mechanical properties (compressive and flexural properties and fracture energy) and microstructure of MCC reinforced cementitious composites
- Investigating the influence of various parameters such as MCC concentration, dispersant type and dispersion parameters on the microstructure and mechanical performance of cementitious composites.
- Comparison of processing and performance of cementitious composites reinforced with CNT and MCC.

1.7 Outline of Thesis

This thesis is divided into the following 6 chapters:

Chapter 1. Introduction: This chapter discusses the aim of this research, brief introduction about cementitious materials, CNT and nanocellulose, motivation, research objectives and thesis outline.

Chapter 2. Literature Review: This chapter includes a comprehensive discussion on the available literature published in the field of carbon nanomaterial and NCC/MCC reinforced cementitious composites. Existing dispersion techniques and microstructure and mechanical properties of reported cementitious composites are discussed in detail. An extensive part of the literature review has been published in “A review on nanomaterial dispersion, microstructure, and mechanical properties of carbon nanotube and nanofiber reinforced cementitious composites”. *Journal of Nanomaterials* 2013 (2013): 80.

Chapter 3. Dispersion of Carbon Nanotubes in Aqueous Suspension

This chapter discusses the dispersion of different types of CNT (SWCNT, MWCNT, both pristine and functionalized) in aqueous medium using Pluronic F-127 and SDBS. Various characteristics of prepared suspensions such as homogeneity, agglomeration, extractability as well as short and long term stabilities are discussed and the optimum surfactant concentration for achieving highly homogeneous and stable CNT suspensions is reported. An extensive part of the results presented in this chapter has been submitted for publication as “Characterizing Dispersion and Long Term Stability of Concentrated Carbon Nanotube Aqueous Suspensions for Fabricating Ductile Cementitious Composites” in *Colloids and Surfaces A: Physicochemical and Engineering Aspects*, Elsevier.

Chapter 4. Development of Carbon Nanotube Reinforced Cementitious Composites

This chapter discusses the microstructure and mechanical properties of cementitious composites reinforced with CNTs. The effects of CNT type, its concentration, surfactant type (Pluronic F-127 or SDBS) and hydration period on flexural and compressive properties as well as fracture energy of cementitious composites are discussed. The optimum conditions to maximize mechanical performance of cementitious composites are highlighted. An extensive part of the results presented in this chapter has been reported in the publication, “Microstructure and

mechanical properties of carbon nanotube reinforced cementitious composites developed using a novel dispersion technique”. *Cement and Concrete Research* 73 (2015): 215-227.

Chapter 5. Development of Micro Crystalline Cellulose Reinforced Cementitious

Composites: This chapter discusses the preparation and characterization of MCC dispersion in aqueous medium using Pluronic F-127 and CMC, used for comparison purpose. The optimum Pluronic concentration to achieve homogeneous and stable MCC dispersion is reported and the microstructure and mechanical properties (flexural and compressive) of resulting cementitious composites are discussed. The performance of cementitious composites reinforced with CNT and MCC is also compared. An extensive part of the results presented in this chapter has been submitted for publication as “A Novel Approach of Developing Micro Crystalline Cellulose Reinforced Cementitious Composites with Enhanced Microstructure and Mechanical Performance” in *Cement and Concrete Composites*, Elsevier.

Chapter 6. Conclusions and Future Work

This chapter presents the summary and conclusions of different chapters and also the overall conclusion of the thesis. The future scope of this research is also highlighted.

Chapter 2

Literature Review

This chapter is based on the article:

Shama Parveen, Sohel Rana, and Raul Figueiro. A review on nanomaterial dispersion, microstructure and mechanical properties of carbon nanotube and nanofiber based cement composites. *Journal of Nanomaterials* 2013(2013): 1-19.

State of the Art: Carbon Nanomaterials Reinforced Cementitious Composites

2.1 Dispersion of Carbon Nanotubes and Nanofibres

Dispersion of CNTs and CNFs is one of the major factors that strongly influence the properties of nanocomposites. These nanomaterials have strong tendency to agglomerate due to presence of attractive forces (Van der Waals), originated from their polarizable extended π electron system. Infiltration of agglomerates with matrices is very difficult and their presence is therefore the source of potential defects in nanocomposites. The process of de-agglomeration and subsequent distribution of nanomaterials within matrices or solvents is called dispersion. Dispersion can occur either due to abrupt splitting up of agglomerates into small fragments under high stress (rupture) or due to continuous detachment of small fragments from the agglomerate surface at a comparatively lower stress (erosion). The dispersion behaviour of CNF and CNT depends on a few critical factors such as length of nanomaterials, their entanglement density, attractive forces, volume fraction and matrix viscosity. Different chemical methods have been tried till date to achieve homogeneous dispersion of carbon nanomaterials in water and various polymers such as using solvents [53], surfactants [8,13,14,54], functionalization with acids [55], amines [56], fluorines [15], plasma [57,58], microwave [16] and matrix moieties [59], non-covalent functionalization [60], using block co-polymers [17,18], wrapping conjugated polymers [61] and other techniques [62,63]. On the other hand, the basic physical technique used for carbon nanomaterial dispersion is the ultrasonication, which is often used in combination with the other methods mentioned above [64-70].

2.2 Dispersion of Carbon Nanotubes and Nanofibres within Cementitious Matrices

Similar to polymeric matrices, dispersion of carbon nanomaterials in cementitious matrices is also a critical issue which strongly influences the properties of cement based nanocomposites. The approach of dispersing CNF/CNT directly within cement paste during mixing is not feasible, as the thickening of cement paste begins within a short period after addition of water [44]. The mixing process using a Hobart mixer, commonly used to prepare mortar paste, cannot ensure proper dispersion of CNT within cementitious matrix [71], resulting in large CNT clusters within the hydrated paste (Figure 2. 1). To avoid this situation, the strategy commonly employed for mixing CNTs/CNFs with cementitious matrices is to disperse these nanomaterials first in water, followed by mixing of nanomaterial/water dispersion with cement using a

conventional mixer. However, the methods of dispersing nanomaterials in water should be carefully selected so that they do not interfere with the hydration and processing of cement nanocomposites. Many surfactants that are successfully used to disperse carbon nanomaterials in polymeric matrices have been reported to create problems in cement hydration, entrap air in the cement paste or react with the water reducing admixtures [72].

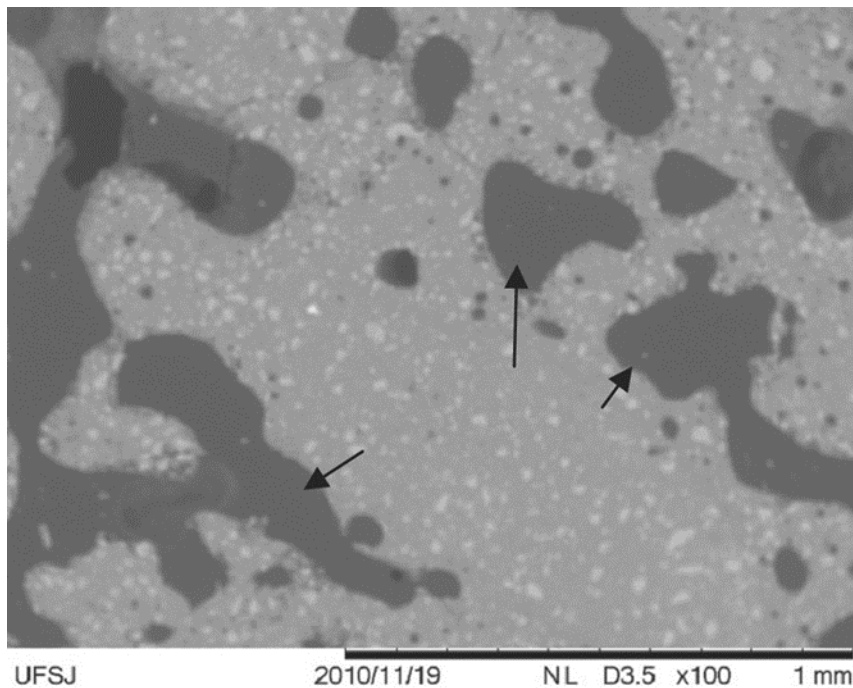


Figure 2. 1 SEM image of CNT/cement paste after hydration [44].

Dispersion of CNF/CNT in cement is even more difficult as compared to the polymeric matrices. One of the reasons for poor dispersion may be the size of cement grains. As CNFs or CNTs are separated by the cement grains, the presence of larger grains than the average leads to absence of CNFs/CNTs in some areas, whereas they can be present in higher quantity in other areas where the cement grains are much smaller in size [73]. Although reduction of cement particle size using ball milling can improve nanomaterial dispersion, small grain cement has many other disadvantages such as high water consumption, thermal cracking, more chemical and autogenous shrinkage, etc. [74]. Recently performed 3D simulation study suggested that a homogeneous distribution of nanomaterials within cement is possible only when the cement particles are also distributed homogeneously without any agglomeration [75]. Therefore, to improve carbon nanomaterial dispersion in cementitious matrices various approaches have been employed till date, carefully considering the issues discussed above and, can be broadly categorized into physical and chemical techniques, as discussed in the following sections. However, it should be

noted that the various chemical routes (such as using surfactant, polymers or functionalization) cannot directly disperse nanomaterials in water; instead they help in the dispersion process by wetting the nanomaterials with water and improving the dispersion stability. Therefore, these chemical routes are always used in combination with the mechanical routes (such as ultrasonication), which can directly disperse the nanomaterials.

2.2.1 Physical Techniques

Ultrasonication

In an ultrasonic processor, electrical voltage is converted to mechanical vibrations, which are transferred to the liquid medium (water or solvent) and lead to formation and collapse of microscopic bubbles. During this process (known as cavitation) millions of shock waves are created and a high level of energy is released [44], leading to dispersion of nanomaterials in the liquid. A short duration of ultrasonic treatment (15 minutes at 20 kHz frequency and amplitude setting of 50%) using a titanium probe was found successful to prepare homogeneous aqueous dispersion of VCNFs (1.14 wt.%) [73]. However, this technique could not ensure homogeneous distribution of CNTs within cement, meaning that a homogeneous nanomaterial dispersion in water does not guarantee a good dispersion in the nanocomposites as well. This fact necessitates the use of various chemical routes in combination with ultrasonication to improve the dispersion stability, thus preserving the nanomaterial dispersion up to the composite stage.

2.2.2 Chemical Methods

Use of surfactant

Surfactants can improve aqueous dispersion of nanomaterials by reducing surface tension of water and moreover, lead to stable dispersion as a result of electrostatic and/or steric repulsions between the surfactant molecules adsorbed on the nanomaterials surface. However, the dispersion capability of surfactants strongly depends on their concentration and an optimum surfactant to nanomaterials ratio should be used for preparing cementitious composites. Among the various concentrations studied, it was observed that surfactant/CNT ratios of 4.0 and 6.25 (by weight) were efficient in preparing homogeneous aqueous dispersion of 0.16 wt.% MWCNT using ultrasonication process (operated at 500W, amplitude of 50%, energy of 1900-2100 J/min and at cycles of 20s) [76]. Moreover, the dispersion homogeneity was preserved in the nanocomposites as well as due to the better dispersion stability and only individual nanotubes were observed in the fracture surface (Figure 2. 2). Lower surfactant/CNT ratios (0 and 1.5),

however, could not disperse CNTs well, leading to presence of large CNT clusters within the composites. Similarly, VCNFs (0.048 wt. % with respect to cement weight) could also be dispersed homogeneously (Figure 2. 3) using a surfactant/CNF ratio of 4.0 [77].

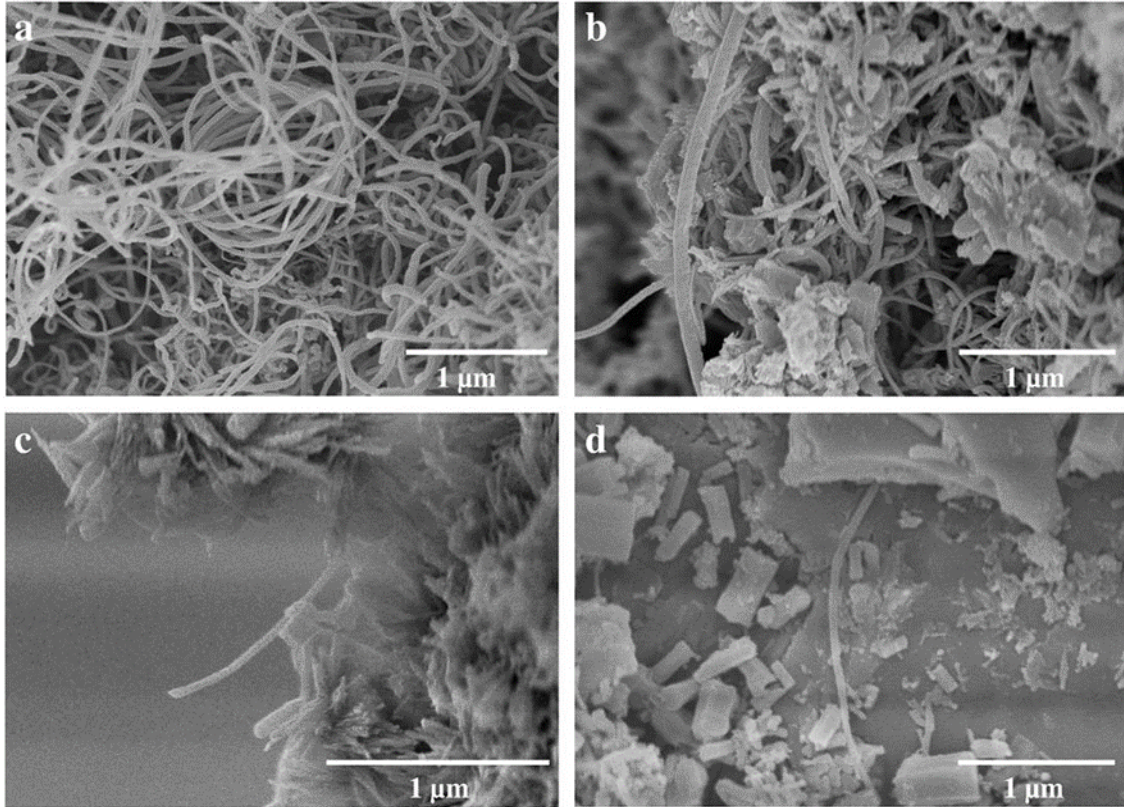


Figure 2. 2 Dispersion of MWCNT within cementitious composites prepared using different surfactant to MWCNT weight ratio: (a) 0, (b) 1.5,(c) 4.0, and (d) 6.25 [76].

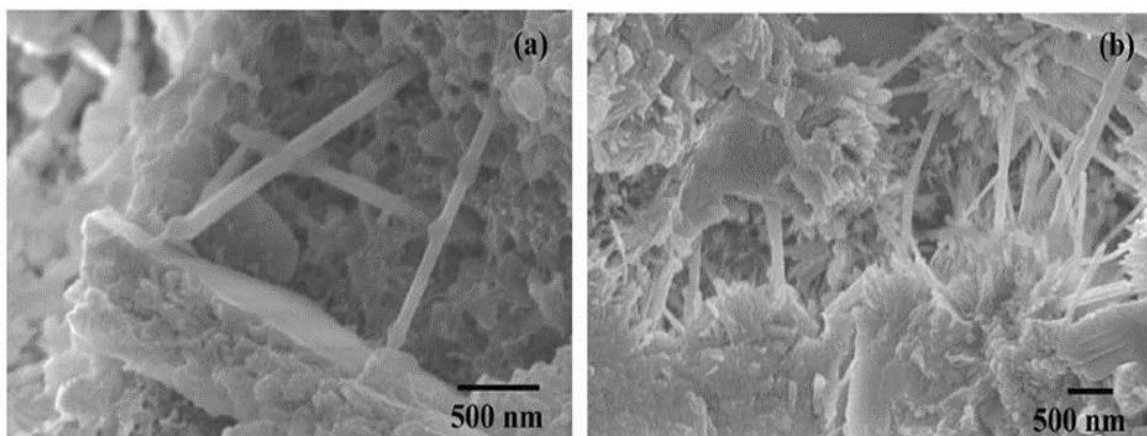


Figure 2. 3 Fracture surface of CNF/cement nanocomposites, showing individually dispersed CNFs [77].

Besides concentration, it has been observed that the type and structure of surfactant also have significant influence on the dispersion of carbon nanomaterials in water and subsequently within cementitious composites. Among the various surfactants such as benzene sulfonate (SDBS), sodium deoxycholate (NaDC), Triton X-100 (TX10), Arabic gum (AG), and cetyltrimethyl ammonium bromide (CTAB), the anionic one (SDBS) provided the best aqueous dispersion of MWCNTs (prepared using surfactant concentration of 2 wt.% and magnetic stirring for 10 min at 300 rpm combined with ultrasonication using a tip sonicator at 40W for 90 rounds, each of 90s and 10s rest in-between), which was stable after 70 minutes of ultracentrifugation and 60 days of sitting [45]. The result was even better when SDBS was used in combination with Triton X-100 (non-ionic) in the weight ratio of 3:1. The better stabilization in case of SDBS was attributed to the benzene ring in the hydrophobic chain, smaller charged SO_3^{2-} head group, and relatively longer alkyl hydrophobic chain [78]. The dispersion ability of various surfactants was found in the following order: SDBS & TX10 > SDBS > NaDC & TX10 > NaDC > AG > TX10 > CTAB. The cationic surfactant CTAB showed the lowest dispersion capability because of the absence of benzene ring on the long chain and the positive charge which might have neutralized the negative charge of MWCNTs in aqueous solution. The fracture surface of cement nanocomposite containing 0.2 wt.% MWCNTs dispersed using SDBS/TX10 combination showed very uniform distribution of CNTs. Sodium dodecyl sulfate (SDS) has also been reported as an effective anionic surfactant for fabricating CNT/cement nanocomposites [79]. However, one drawback of using surfactants as nanomaterial dispersant is the lack of connectivity of nanomaterials within cementitious matrix due to blocking by surfactant molecules and this fact affects the electrical and piezoresistive properties of nanocomposites [79].

Surface decoration of carbon nanomaterials using polymeric surfactants has been reported to introduce steric repulsion between the nanomaterials, leading to their homogeneous dispersion. The surface of MWCNTs could be covered with acrylic acid polymer through ultrasonication in water, as can be seen from Figure 2. 4[46] and this led to very good aqueous dispersion of CNT (Figure 2. 5). Methylcellulose is another polymer which has been used to prepare highly stable aqueous dispersion of CNT for fabricating cementitious nanocomposites [80-82].

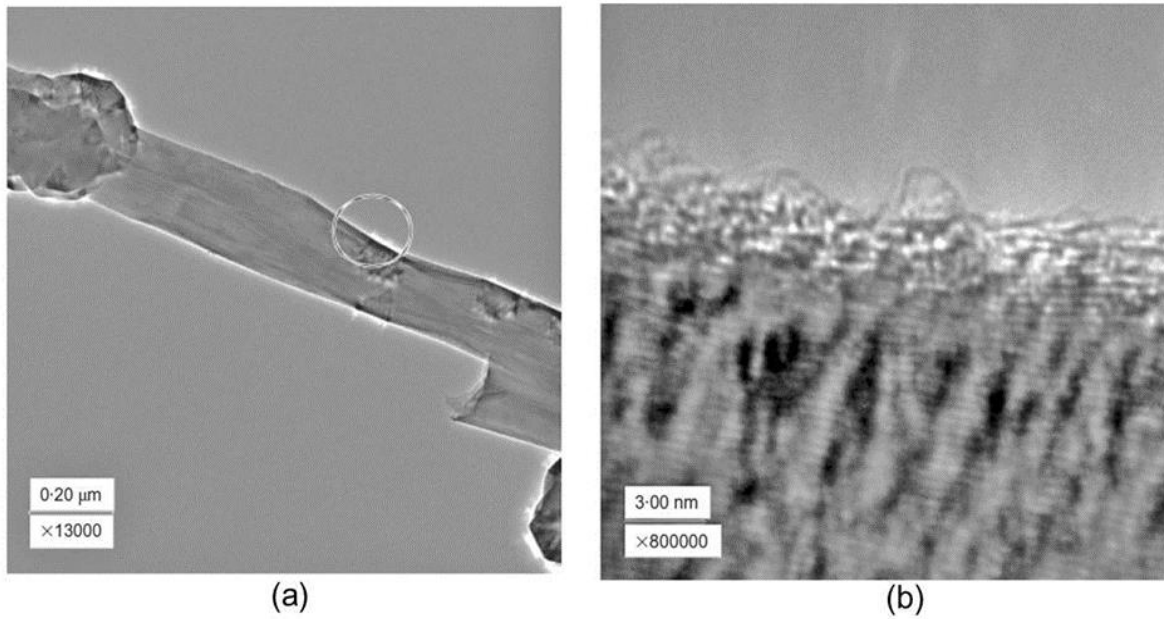


Figure 2. 4 TEM image of MWCNTs showing presence of acrylic acid polymer on the surface at magnifications of 13000x (a) and 800000x (b) [46].

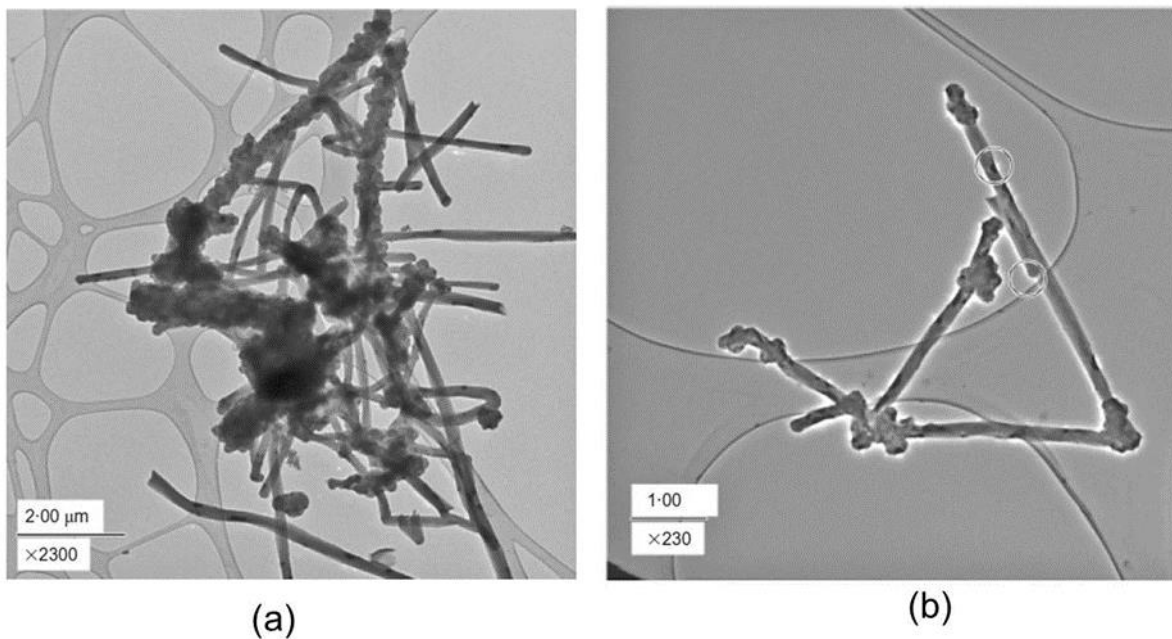


Figure 2. 5 TEM image of MWCNT dispersion in water without any treatment (a) and with acrylic acid polymer and sonication (b) [46].

Use of cement admixtures

Polycarboxylate, which is commonly used as a superplasticizer within cement paste, was also found to be an effective dispersant of CNT [47]. Among the various cement admixtures such as alkylbenzene sulfonic acid (air entraining agent), styrene butadiene rubber co-polymer latex,

aliphatic propylene glycol ether including ethoxylated alkyl phenol, polycarboxylate, calcium naphthalene sulfonate, naphthalene sulphonic acid derivatives and lignosulfonate, very stable dispersions stable up to 9 days were obtained with the air entrainer, polycarboxylate and lignosulfonate in the sedimentation test. However, the use of high concentration of lignosulfonate required for good CNT dispersion is not recommend to avoid delay in the setting time of Portland cement [83]. Also, despite of a good aqueous dispersion, the use of alkylbenzene sulfonic acid could not lead to a homogeneous CNT dispersion in the hardened cement paste. On the contrary, the use of polycarboxylate resulted in a very good dispersion of MWCNT in water as well as in the hardened cement paste and therefore, proved to be the best dispersant among the various admixtures used in cement.

Silica fume, an amorphous polymorph of silicon dioxide, is also used as a pozzolanic material in concrete production [84-86]. Silica fume consists of spherical particles with average diameter of 150 nm and has been found to improve microfiber dispersion within cement [87,88]. The influence of silica fume on carbon nanomaterial dispersion has also been studied [89]. It was observed that the cement nanocomposites prepared through dry mixing of 2 wt.% CNFs with cement and silica fume (10 wt.%) using a conventional three speed mixer (followed by water addition) showed both CNF agglomerates as well as individually dispersed nanofibres. However, in absence of silica fume only CNF agglomerates were observed, indicating positive influence of silica fume [89]. The better dispersion in the presence of silica fume was attributed to the smaller size (100 times smaller as compared to anhydrous cement particles) of silica fume particles which could disrupt the Van der Waals forces between individual CNFs, thereby mechanically separating some of them during the dry mixing process and reducing the CNF clumps. Additionally, the silica fume particles present within the CNF clumps as well as individual CNFs could also act as the silicon source for the formation of Ca-Si rich phases and nucleation sites for the self-assembly of Ca-Si rich phases.

Covalent functionalization

The most common approach to improve the dispersion ability of CNTs/CNFs in water or polymeric matrices is the covalent functionalization. Frequently, carbon nanomaterials have been treated with strong acids such as nitric acid or mixture of sulfuric and nitric acid (3:1) to oxidize the surface and create functional groups such as carboxylic [90]. Covalent functionalization using acid mixture has been found successful to disperse CNTs individually

within cementitious matrix [91]. Moreover, CNTs became tightly wrapped by the C-S-H phase of cement, due to covalent bonding between COOH or C-OH groups of nanotubes and C-S-H. Similar observations were also made in case of surface functionalized CNFs using 70% nitric acid [92]. However, although surface treated CNTs could be homogeneously dispersed within cementitious matrix, the dispersed CNTs could not form a well connected three dimensional network (as evident from Figure 2. 6) required for good electrical conductivity or piezoresistive properties due to fewer contact points and covering of surface by C-S-H phases [48].

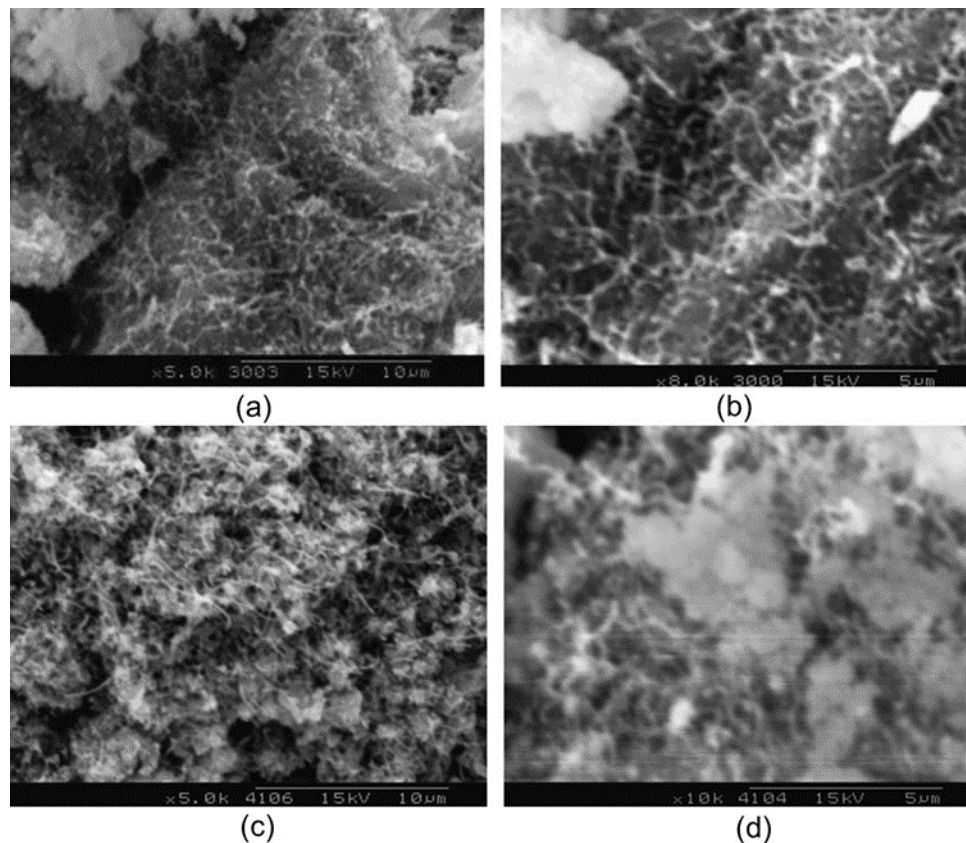


Figure 2. 6 SEM image of cement nanocomposites with untreated CNTs ((a), (b)) and acid-treated CNTs ((c), (d)) [48].

Functionalization of CNTs with strong acids forms carboxylated carbonaceous fragments (CCFs), which are organic molecules consisting condensed aromatic rings with several functional groups [93]. Although CCFs have functional groups which can react with cement, but they do not contribute to the mechanical properties as they are only small fragments and do not have proper structure to carry mechanical loads. CCFs can be removed through washing of functionalized CNTs using acetone. CNTs, either containing CCFs or free from CCFs resulted in floccules formation when $\text{Ca}(\text{OH})_2$ was added to the dispersion, indicating reaction between the

surface functional groups of CNT and Ca^{2+} ions. The hydration of cement on the surface of functionalized CNTs was also observed, as shown in Figure 2. 7.

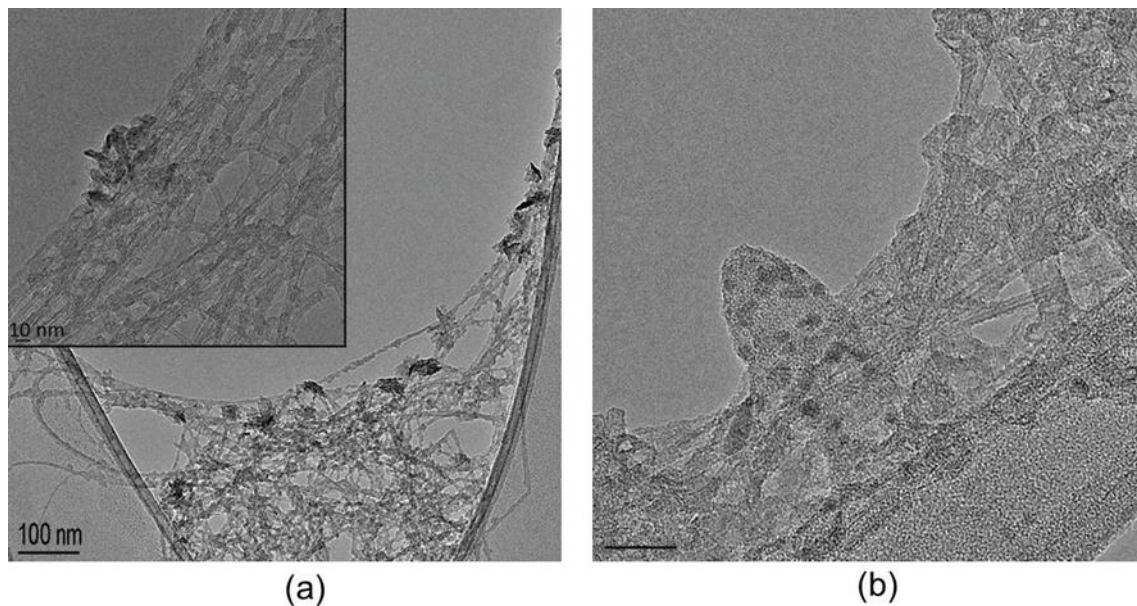


Figure 2. 7 TEM image of CCF-free FWCNTs after hydration for 1 hour (a) and 5.5 hour (b) [93].

Combination of various chemical methods

The combination of surface functionalization with polymers has been found to provide more stable aqueous dispersion of CNT than using only polymers or functionalized CNTs [46]. The dispersions of non-functionalized MWCNTs using acrylic acid polymer or gum arabic were found stable only up to 2 hours after which sedimentation was observed. Similarly, aqueous dispersion of functionalized nanotubes also showed poor long term stability. On the contrary, functionalized MWCNT dispersion prepared using acrylic acid polymer showed stability for more than 2 months. The long polyacrylic acid polymer chains were adsorbed on the surface of functionalized nanotubes and increased the steric barrier towards their agglomeration. In a similar way, use of surfactant (sodium dodecylbenzene sulfonate) to homogeneously disperse carboxyl functionalized MWCNTs within cementitious matrix was found to be very effective [94].

2.2.3 Novel Routes of CNT Dispersion

In order to avoid the problematic and time consuming process of dispersing CNTs within cementitious matrix, an innovative method of fabricating cementitious nanocomposites through

growth of CNTs on to the cement particles has been recently reported [95]. CNTs were grown in a chemical vapour deposition (CVD) reactor at 400-700°C using acetylene as the main carbon source and carbon monoxide and dioxide as the additives to enhance the yield. Cement powder was feed in the reactor continuously at a speed of 30 g/h and the oxides (Fe_2O_3) present in the cement acted as catalysts for CNT growth, without the need for an additional catalyst support used in the conventional CVD process. The concept of preparing cement nanocomposites using this route has been illustrated in Figure 2. 8. The TEM images of CNT grown cement particles showed complete coverage of cement particles by carbon nanomaterials and formation of MWCNTs as well as CNFs, as shown in Figure 2. 9. More recently, CNTs were also grown on the silica fume particles, impregnated with iron salt, using acetylene as the carbon source [96]. CNTs with 5-10 walls and diameters of 10-15 nm were grown at 600°C and with 12-20 nm diameters were produced at 750°C (Figure 2. 10). Silica fume, which is used as an admixture, can therefore be utilized to introduce CNTs within cementitious matrices.

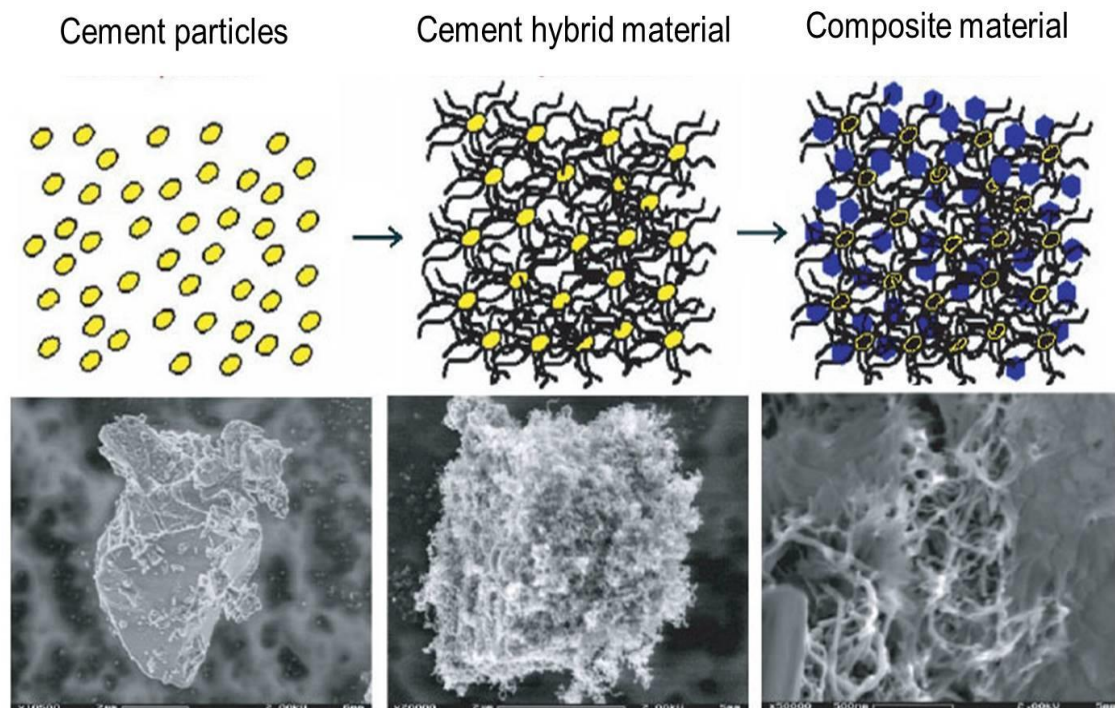


Figure 2. 8 Schematic diagram showing concept of incorporating CNTs/CNFs within cementitious composites by their direct growth on cement particles [95].

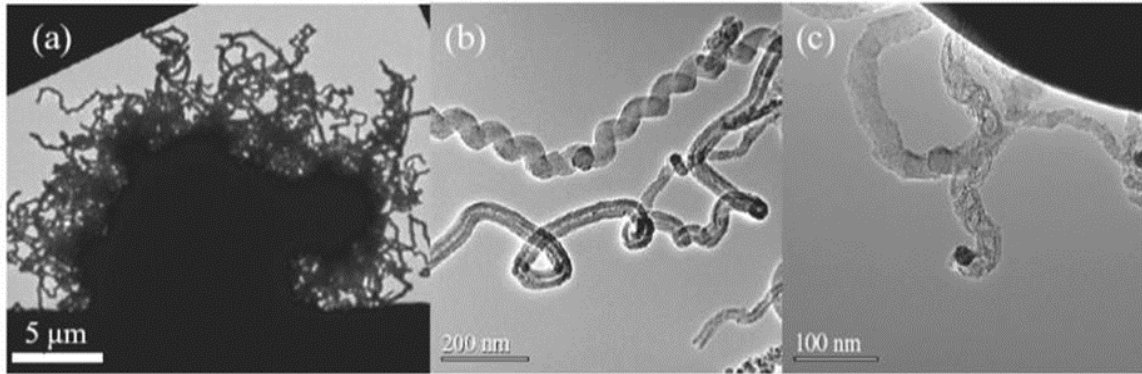


Figure 2. 9 TEM image showing complete coverage of cement particles by carbon nanomaterial (a), formation of MWCNT (b), and CNF formation (c) [95].

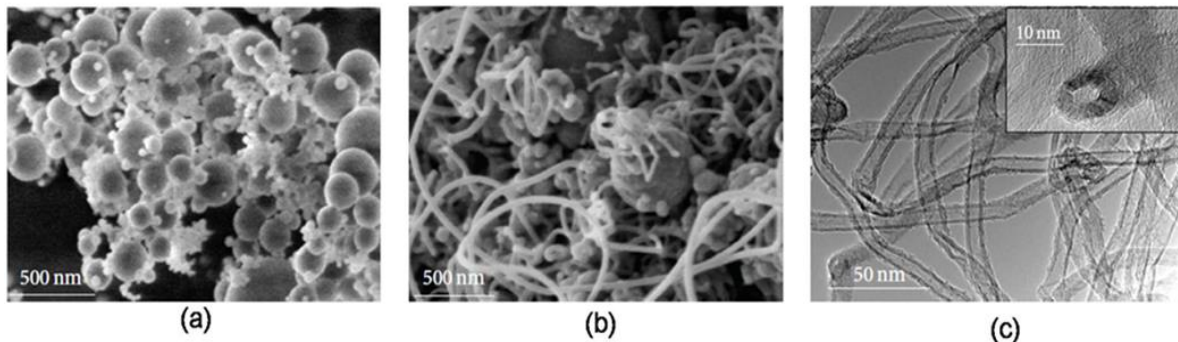


Figure 2. 10 SEM images of pristine silica particles (a), growth of CNTs on silica particles at 600°C (b), and TEM image of CNTs grown on silica particles at 600°C (c)[96].

2.2.4 Large-Scale Production of CNT Dispersion

A technique for producing highly concentrated MWCNT/water suspensions that can be used for developing cement nanocomposites at large scale has been recently developed [97]. In this process, MWCNTs were homogeneously dispersed in water using surfactant (MWCNT to surfactant weight ratio of 4.0) using a tip sonicator. When this CNT dispersion was centrifuged at 28,000 rpm using a swing bucket rotor, the dispersed MWCNTs started precipitating at the bottom of the tube and complete sedimentation was achieved after 11 hours. The supernatant solution was then decanted down to keep only 20% of the initial volume of the solution and CNTs were re-dispersed in this solution through ultrasonication for 40 minutes. The concentration of MWCNTs increased 5 times using this process, as revealed by optical absorbance spectroscopy. The concentrated MWCNT solution, when diluted by adding the same amount of water previously decanted, showed same concentration as the reference non-concentrated MWCNT suspension. Moreover, it was quite interesting to note that, the

cementitious nanocomposites prepared using the concentrated MWCNT suspension (after dilution) exhibited similar mechanical properties as that obtained using the reference non-concentrated MWCNT suspensions, indicating that the dispersion of MWCNTs was preserved even after the concentration process through centrifugation. Therefore, this process can be utilized to prepare large scale production of CNT admixtures for developing cementitious nanocomposites.

2.3 Microstructure of Carbon Nanomaterial/Cement Nanocomposites

It has been reported by several researchers that carbon nanomaterials can significantly change the microstructure of cement, and this is one of the principal reasons for improvement in mechanical properties. Significant difference between the porosity of Portland cement and cement/CNT nanocomposites was observed [98]. The total porosity and surface area both decreased with CNT addition. This was attributed to the fact that CNTs filled in the pores, mainly the mesopores (size less than 50 nm), between the hydration products and, thereby produced a denser microstructure than the unreinforced cement. Moreover, this also resulted in very good interaction between the hydration products and dispersed CNTs, which were seen densely inserted between the C-S-H and CH phases of cement (Figure 2. 11). Similar findings were also made in case of cement containing 0.5 wt.% surface treated MWCNTs [92], which resulted in 64% lower porosity and 82% lower pores with size more than 50 nm. On the contrary, cement composites containing micro-scale fibres such as carbon showed much higher porosity than the Portland cement samples. Nanoindentation tests also showed lower probability of porous phase in a cement nanocomposite containing 0.08 wt.% MWCNT than Portland cement, indicating lower porosity in case of nanocomposites [76].

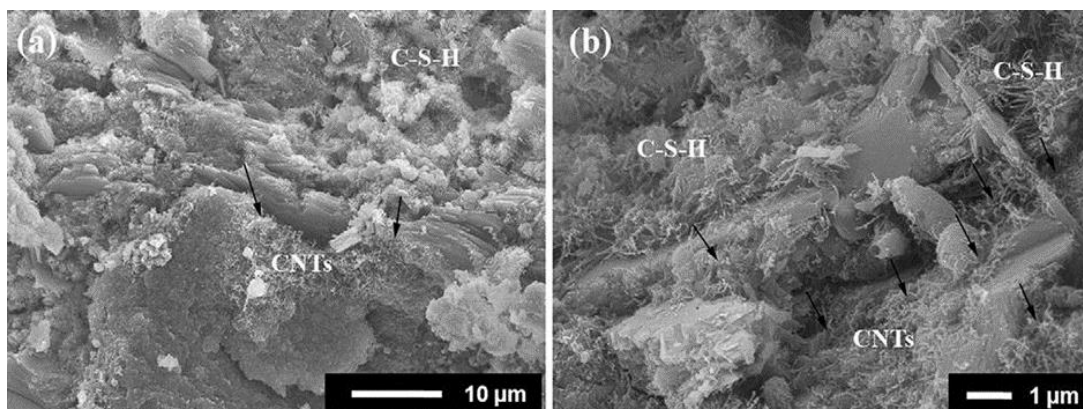


Figure 2. 11 SEM micrographs of 1wt.% CNT/cement paste after 28 days of hydration at different magnifications [98].

2.4 Mechanical Properties of CNT/CNF Reinforced Cementitious Composites

Early investigations showed that CNTs have strong influence on the hydration process and hardness of cementitious composites [99]. In spite of non-homogeneous CNT dispersion in nanocomposites with cement/CNT ratio of 0.02 (by weight), Vickers hardness improved up to 600% in case of 0.4 and 0.5 water/cement ratios in the early hydration stages, although no improvement in hardness was observed after 14 days of hydration. These early results reflected the potential of CNT for improving mechanical properties of cement. However, as in case of polymer, the reinforcing efficiency of CNT/CNF in cementitious matrices and the resulting mechanical properties of nanocomposites also depend on several critical factors, as discussed in the following sections.

2.4.1 Influence of Dispersion

Dispersion of nanomaterials has been identified as one of the principal factors which influence the mechanical properties most. Therefore, the parameters which control the dispersion behaviour also have a strong influence on the mechanical properties. For example, the type and structure of surfactant were found to be very important with respect to the mechanical properties. Among the various surfactant such as SDBS, NaDC, TX10, AG and CTAB, the highest flexural and compressive properties were achieved with NaDC, whereas the lowest variation as well as second best flexural and compressive strengths were obtained in case of 3:1 mixture of SDBS and TX10. The improvements in case of NaDC were 35.45% and 29.5% as compared to plain cement paste. The highest improvement in case of NaDC was due to good dispersion of MWCNTs as well as formation of strong interface between cement matrix and MWCNTs. Similarly, better mechanical properties in case of SDBS and TX10 mixture resulted from the best dispersion ability of this combination and also good bonding between MWCNTs and matrix. Microscopy study in case of this surfactant combination suggested that MWCNTs were well distributed within the cement matrix as a net like structure and acted as bridges between the micro-cracks, resulting in superior mechanical performance [45]. Similarly, among the various cement admixtures, improved dispersion of CNT in water as well as within cement was observed only in case of polycarboxylate and therefore, the cement paste containing 0.8% polycarboxylate and 0.5% CNT showed very good flow behaviour even with low water ratio (0.35) and presented a compressive strength 25% higher than the control cement samples [47]. The length and

concentration of CNTs also influence their dispersion behaviour and therefore, are controlling factors for mechanical properties of nanocomposites [76]. It was noticed that short MWCNTs (10-30 μm) provided better dispersion and flexural properties even when used at higher concentrations (0.08 wt.%), whereas long MWCNTs (10-100 μm) should be used at lower concentrations (0.048 wt.%) to maintain better dispersion and to achieve good flexural properties. It was also observed that short CNTs at higher concentrations were better in terms of mechanical properties due to relatively better dispersion, reduced CNT free volume of cement paste and better filling of nano sized voids [100]. However, reduction of CNF's aspect ratio due to either de-bulking process or ultrasonication was found detrimental to mechanical properties and it was observed that a higher ultrasonication energy than optimum led to reduction in nanomaterials' aspect ratio and deterioration of mechanical properties [101].

Homogeneous dispersion of CNTs/CNFs achieved through their growth on to cement particles was reported to provide 2 times higher compressive strength than the pristine cement composites after 28 days of hydration [95]. This dispersion process led to good distribution of CNTs and CNFs embedded in to the hydration products of C-S-H phases and therefore, bridged the adjacent cement particles (Figure 2. 12), resulting in strong improvements in compressive strength. Although a homogeneous dispersion of carbon nanomaterials is extremely necessary for enhancing mechanical performance of cementitious composites, it has been observed that even when they are poorly dispersed, they can prevent the formation of shrinkage cracks and significantly improve the mechanical performance especially when curing is done in absence of moisture for first 24 hours [102].

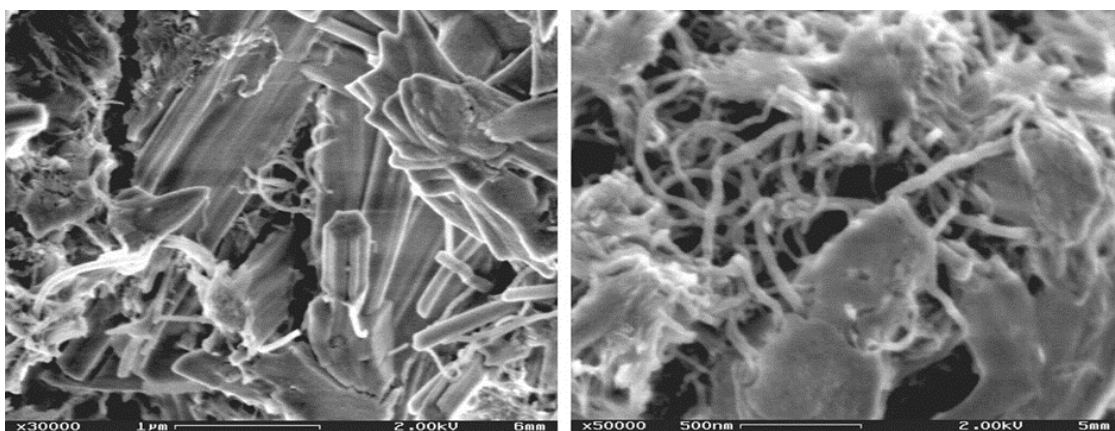


Figure 2. 12 SEM image of hardened cement paste (28 days) after mechanical test at different magnifications [95].

2.4.2 Influence of Nanomaterial Surface Treatment and Interface

The interface between nanomaterials and cementitious matrix controls the load transfer between them and therefore, significantly influence the mechanical properties of composites. Formation of covalent bonding between COOH or C-OH groups of functionalized CNTs and C-S-H phases of cement matrix has been observed through FTIR studies [91] and was also supported by microscopy studies which showed tight wrapping of functionalized CNTs by C-S-H phases. Cement nanocomposites containing surface treated MWCNTs presented much better flexural and compressive properties as compared to plain cement paste. Flexural and compressive strength improved up to 25% and 19% respectively using 0.5 wt.% functionalized CNT. It has been observed that ensuring a good dispersion through acrylic acid polymer wrapping does not ensure improved mechanical properties of composites, due to improper load transfer at the interface [46], whereas 0.045% of functionalized MWCNTs showed nearly 50% increase in compressive strength when dispersed using the same process, indicating strong influence of the interface. Improvement of mechanical properties using functionalized nanomaterials can be further enhanced through removal of CCFs from the nanomaterials surface [93]. It has been reported that the incorporation of functionalized CNTs (0.01 wt.%) containing CCFs resulted in only 13% improvement in compressive strength, whereas after removal of CCFs using acetone resulted in very strong improvement in compressive strength, up to 97% using only 0.03 wt.% CNT. This was attributed to the fact that functionalized CNTs became less accessible for the reaction with cement hydration products and their nucleation, due to presence of these CCFs. Similarly the presence of surfactant molecules on the nanomaterial surface was also found detrimental to the mechanical properties, due to blocking of direct contacts between surface functional groups and cement hydration products and, a reduction of 65% in compressive strength was observed using 4% SDS.

Use of surface treated CNTs/CNFs also improves the post testing mechanical integrity of cement nanocomposite [92] Cement samples containing 0.5 wt.% surface treated CNFs were found to maintain better structural integrity than the control samples after compression testing, as shown in Figure 2. 13. Better structural integrity in case of CNF/cement composites resulted due to the restriction in crack propagation by the entangled clumps of CNF inside cement cavities, leading to bridging of cracks and also due to individually dispersed CNFs within the cement matrix. It was also observed that after decalcification using ammonium nitrate solution for 95 days, the samples containing CNFs showed better ductile behaviour with slow load dissipation after

failure, as presented in Figure 2. 14. This indicates better durability of CNF/cement nanocomposites as compared to the plain cement paste.

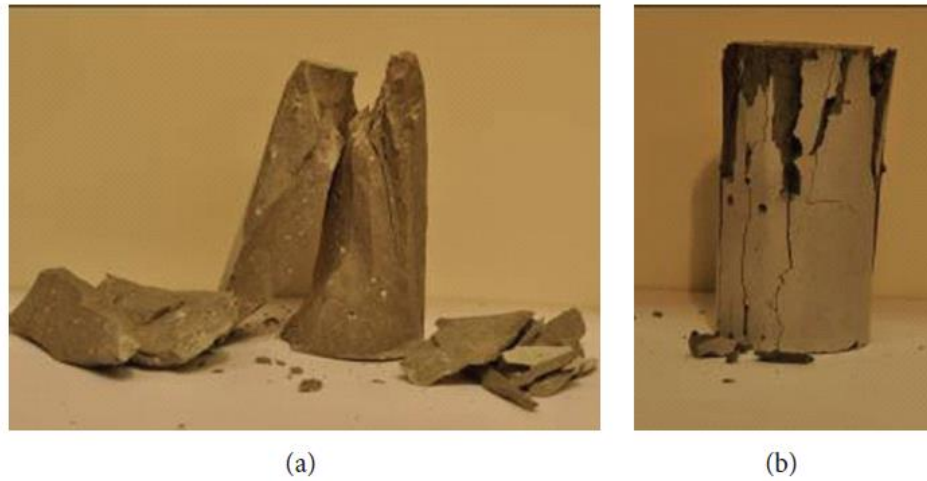


Figure 2. 13 Post-compression testing structural integrity of plain cement paste (a) and cement paste containing 0.5 wt.% surface-treated CNFs (b) [92].

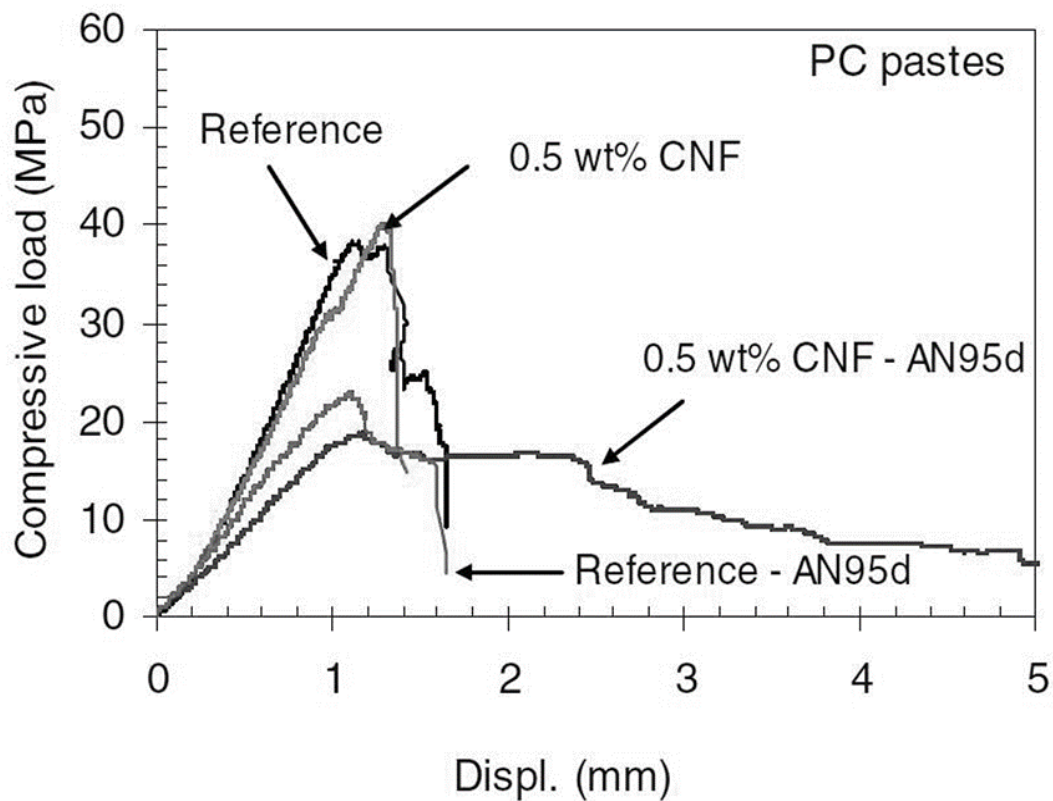


Figure 2. 14 Comparison of compressive behaviour of cement paste and CNF/cement composites before and after decalcification [92].

In spite of several benefits of using functionalized nanomaterials, surface functionalization method should be used carefully in case of cementitious matrices. There is a possibility that functionalized CNTs can absorb water present in the cement paste due to their hydrophilic nature and may adversely affect the cement hydration. It has been noticed that the cement nanocomposites containing 0.5 wt.% carboxyl functionalized MWCNTs led to formation of lower amount of tobermorite gel due to improper hydration process and significantly deteriorated the mechanical properties [103].

Besides surface functionalization, the interface in a carbon nanomaterial/cement composite also depends on the surface feature of nanomaterials. The CNF variety with rougher surface containing conically shaped graphitic planes was found to be very effective in enhancing mechanical properties as compared to the CNFs having smoother surface [101].

2.4.3 Influence of Microstructure

The improvement of mechanical properties achieved in case of well dispersed MWCNT/cement nanocomposites has been found to be much higher than that predicted using theoretical equations [76]. There may be several possible reasons for this fact; the decrease in cement porosity and improvement of its microstructure is certainly one of them. The increase in the amount of high stiffness C-S-H phases in presence of CNT, as revealed from the nanoindentation tests is another reason for such strong improvement in mechanical properties. Improvement of microstructure is also the primary cause for mechanical property enhancements in case of non-autoclave foam concrete. It was found that the use of CNTs (0.05% by mass) as the reinforcement of foam concrete stabilized its structure by decreasing the pore wall percolation and ensuring better pore size uniformity (Figure 2. 15) [104]. This resulted in strong improvement in the compressive strength (70%) associated with a decrease in the average density of concrete from 330 kg/m³ to 309 kg/m³. Improvement of microstructure and resulting enhancements in mechanical properties due to CNT addition has also been noticed in case of fly-ash cement [105-110]. Fly-ash cement samples containing CNTs presented higher density than control fly-ash and PC samples, due to filling of cement pores by CNTs, and a denser microstructure [111]. The compressive strength of fly-ash cement composites containing 1 wt.% CNT reached that of PC at 28 days and 60 days, which are usually higher than the compressive strength of fly-ash cement due to its slow hydration rate.

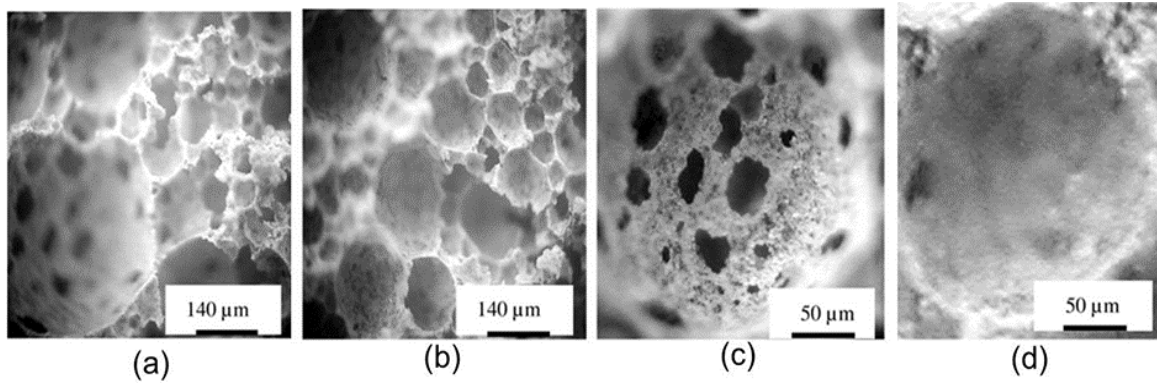


Figure 2. 15 Structure of cement-foam concrete: (a) without nanotubes, (b) with 0.05% CNT (pore walls), (c) without CNT (perforated), and (d) stabilized with addition of 0.05% CNT [104].

2.4.4 Mechanical Properties of Hybrid Cement Nanocomposites

Hybrid cement nanocomposites are analogous to the multi-scale polymer nanocomposites containing reinforcements of different scales such as micro and nano. Hybrid cement nanocomposites containing both CNTs and nano metakaolin (NMK) have been reported [112]. NMK is a silica based material, which can react with $\text{Ca}(\text{OH})_2$ to produce C-S-H gel at room temperature and incorporation of NMK into concrete was found to significantly improve the early strength, increase resistance to alkali-silica reaction and sulfate and can increase toughness and durability [113-116]. Additionally, homogeneous dispersion of exfoliated NMK was found to significantly improve the compressive strength of cement (18% using 6 wt.% NMK) due to reduction of porosity and improvement in the solid volume and bond strength of cement through pozzolanic reaction between silicon and alumina elements present in NMK and the elements of calcium oxide and hydroxide in cement. Also, the presence of NMK could probably disrupt the attractive forces between CNTs during dry mixing process and could separate them leading to their individual dispersion. Additionally, the presence of NMK particles mixed with the dispersed CNTs could act as a Si source for the formation of Ca-Si rich phases and, CNTs could further act as the nucleation sites for the self-assembly of Ca-Si phases. Due to these reasons, addition of up to 0.02% CNT resulted in 11% higher compressive strength as compared to the mortar containing only NMK.

Hybrid cement nanocomposites containing Polyvinyl alcohol (PVA) micro-fibres and CNFs were also developed and reported to have higher Young's modulus, flexural strength and toughness than plain cement, cement containing only PVA micro-fibres or CNFs [77]. It was observed that cement containing CNFs presented much higher load carrying capability at the

same CMOD (crack mouth opening displacement) during the early stages of loading (Figure 2.16).

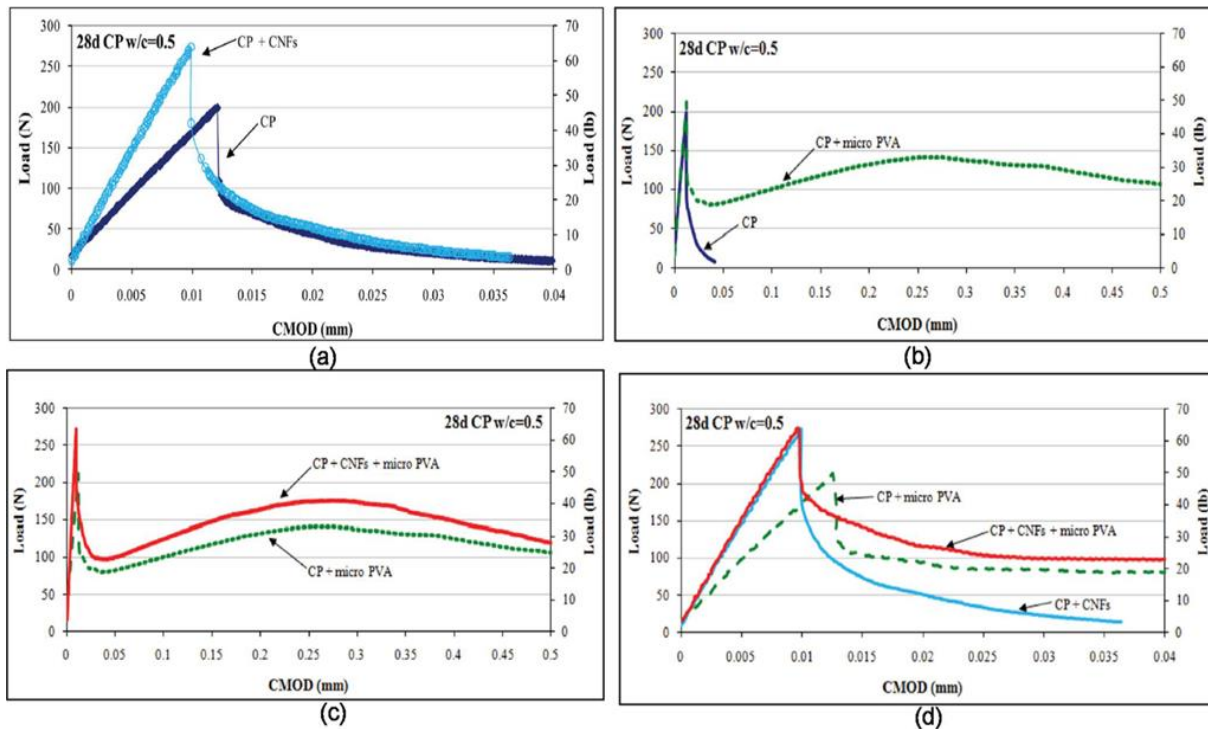


Figure 2.16 Load-CMOD curves for (a) plain cement paste and cement paste containing CNFs, (b) cement paste and cement paste containing PVA microfibers, (c) cement paste containing PVA microfibers and hybrid cement paste, and (d) cement paste containing CNFs, cement paste containing PVA microfibers, and hybrid cement paste for CMOD values less than 0.04mm [77].

Using only 0.048% CNFs, Young’s modulus, flexural strength and toughness improved up to 75%, 40% and 35% respectively. On the contrary, use of PVA micro-fibres improved the Young’s modulus and flexural strength only marginally, but the fracture toughness increased tremendously, retaining the load for ten times higher CMOD than plain cement. Therefore, in the hybrid composites, the pre-peak behaviour was mainly controlled by CNFs, whereas the post-peak behaviour was influenced by mainly PVA micro-fibres. The fracture surface study suggested good bonding between cement and both CNFs and PVA micro-fibres and bridging of micro-pores by PVA fibres and pores at nano level by CNFs. The hybrid cementitious composites showed up to 50% improvement in flexural strength, 84% improvement in Young’s modulus and 33 times (3351%) improvement in fracture toughness over plain cement matrix. Similarly, hybrid cement nanocomposite bar containing 2.25% short carbon fibres and 0.5% MWCNT were found to have much higher tensile modulus (60%), load carrying capacity (54%) and failure strain (44%) as compared to plain cement bars [117].

Besides mechanical properties, degradation behaviour of cement is another important characteristic that influences the durability of concrete structures. Although some initial studies demonstrated a higher corrosion rate of steel bars inside a CNF reinforced mortar, subjected to aggressive environments such as carbonation and chloride attack [118], more research is necessary in this direction to understand the degradation behaviour and durability of nano reinforced concrete and the steel reinforcements present inside the concrete sections.

State of The Art: Nanocellulose Reinforced Cementitious Composites

2.5 Cellulose

Cellulose is a naturally available bio-polymer. The abundance, bio-degradability, renewability, and remarkable physical and mechanical properties made cellulose an attractive material for paper, textile, cosmetics and building industries [119-121]. Nowadays, nanotechnology and nanoscience have become highly attractive research fields for production of tailorable nano particles and fibres with extraordinary properties. Exploring nanotechnology in biopolymers for producing bio-nanomaterials proved highly beneficial for different applications including reinforcement, sensing, drug delivery, and so on. Nanocellulose is derived from cellulose by two processes, top down process and bottom up process, as presented in Figure 1.3 (Chapter 1). Top down process breaks cellulose into NFC and NCC through various steps. Bottom up process produces NFC using bacteria (acetobacter) in a favourable atmosphere of nitrogen and carbon or by tunicates [32,122-130].

2.6 Structure of Cellulose

Cellulose is one of the most abundant and renewable resources. It is classified as carbohydrate since it is made up of carbon, hydrogen and oxygen. The structure of cellulose (Figure 2. 17) is comprised of repeating D-anhydroglucose units, in which glucose units are formed of 6 membered rings known as pyranoses. The C1 of one pyranose ring is attached to C4 of another pyranose ring resulting in β 1-4 glycosidic linkage. β 1-4 glycosidic linkage in cellulose provides stability as well as ribbon like extended structure. The alternating pyranose rings are attached to each other at 180° turns and they form hydrogen bonds between the monomers of same fibrils and also with the monomers of neighbouring fibrils. The Van der Waal forces and

intermolecular hydrogen bonds between the hydroxyl groups and oxygen of monomers result in parallel stacking of cellulose chains, leading to the formation of microfibrils of 5-50 nm in diameter [121,128,129]. The structure of cellulose microfibrils contains highly ordered arrangement of cellulose chains forming the crystalline part of cellulose microfibrils as well as disordered arrangements of cellulose chains forming the amorphous region.

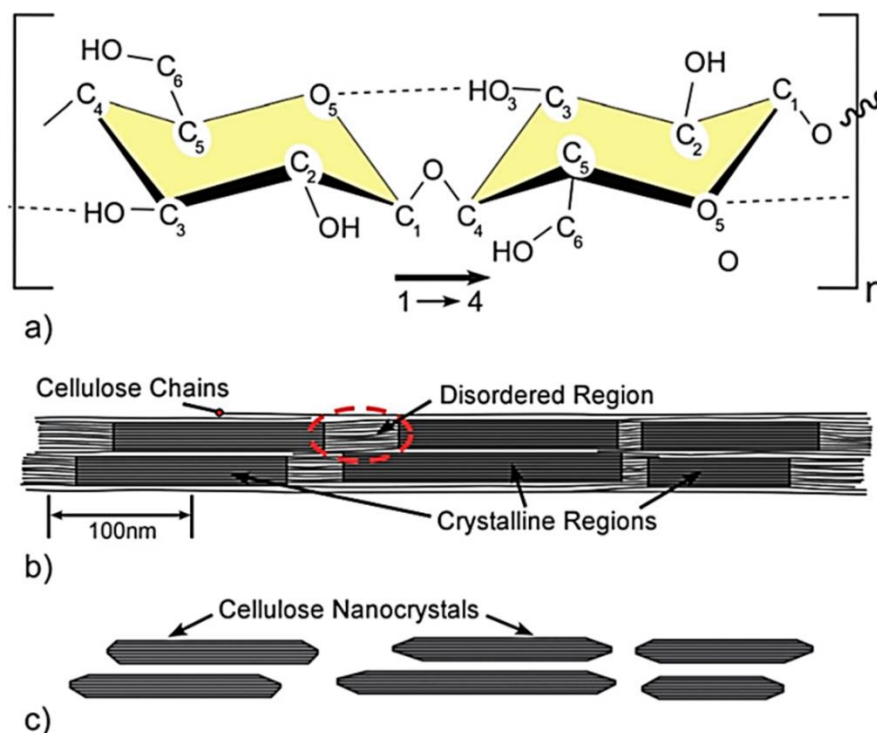


Figure 2.17 Structure of cellulose: (a) chemical structure, (b) crystalline and amorphous regions and (c) cellulose nanocrystals [131].

2.7 Preparation of Cellulose Nanocrystal

Nanocellulose crystals (NCC) are obtained by top down process via the acid hydrolysis mechanism. The amorphous region of MFC is susceptible to chemical reactions; this region breaks and releases the crystalline region when treated with acid. This process is divided in to two steps: (1) diffusion of acid into the amorphous region, (2) cleavage of glycosidic bonds [132]. The mechanism of glycosidic bond cleavage proceeds through two paths (a) rapid protonation of glycosidic oxygen or (b) rapid protonation of cyclic oxygen, followed by addition of water to break down the glycosidic bonds [133]. The typical production process of NCC by acid hydrolysis method involves addition of adequate quantity of strong acid to cellulosic materials at controlled temperature while keeping the mixture in an ice bath for specific reaction duration. The mixture is stirred during this period. The mixture is then subjected to

centrifugation to separate the supernatant and the suspension is washed with deionised water to remove the excess acid. The process is repeated several times until the supernatant becomes turbid. The final suspension is subjected to dialysis with deionised water to remove the acid completely. The hydrolysis of cellulosic materials is usually done either by sulphuric acid or with hydrochloric acid or mixture of both acids [130,133,134]. Many researchers investigated the optimum concentration of sulphuric acid, reaction time and ultrasonication period required to produce NCC. In general, researchers preferred to use 65 wt% of sulphuric acid, keeping the reaction temperature between 20°C-70°C and reaction time between 30 minutes to overnight. Revol et al. found that the optimum concentration of sulphuric acid was between 60 wt % and 70 wt% [132]. According to Bondeson et al., an acid concentration of 63.5 wt.%, 29.6 minutes of sonication time, temperature of 44°C and 130.3 hours of reaction time were the optimum conditions for sulphuric acid hydrolysis to produce NCC [130]. Jackson et al. also reported that the use of 64 wt% sulphuric acid resulted in the formation of NCC with high crystallinity [135]. Likewise, Lu et al. used 64-65% (w/w) sulphuric acid, temperature of 45°C and reaction time of 60 minutes to produce NCC, as presented in Figure 2. 18[133].

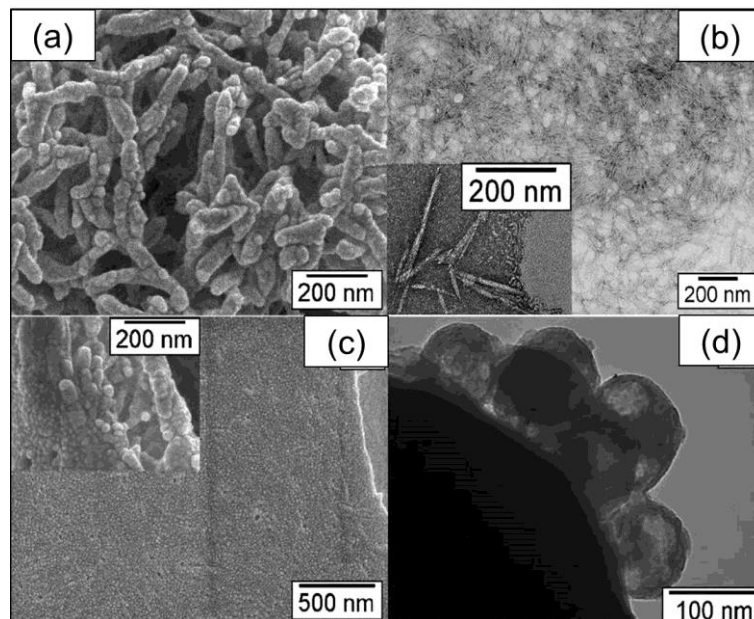


Figure 2. 18 Cellulose nano crystals in the form of rods (a and b) and spheres (c and d) [133].

The acid hydrolysis mechanism of cellulose is shown in Figure 2.19a. The hydrolysis of cellulose with sulphuric acid results in the formation of sulphate ester, as shown in Figure 2. 19.

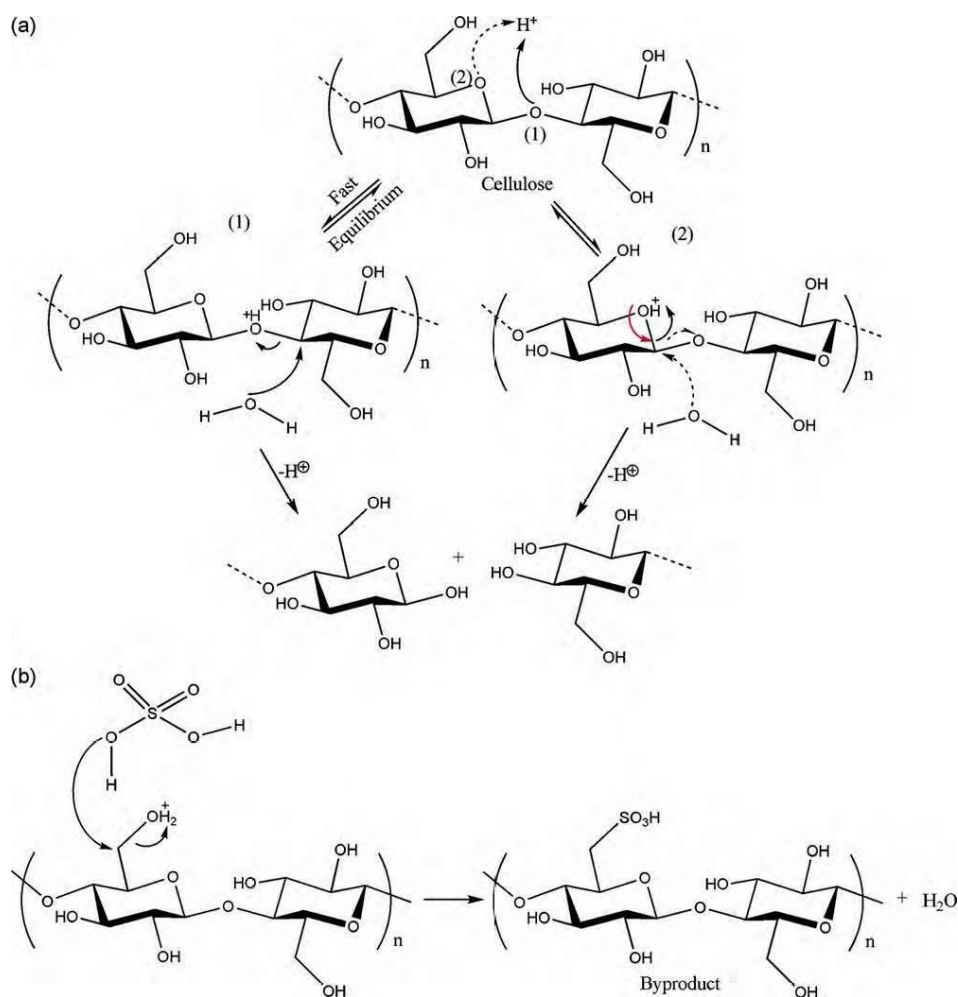


Figure 2. 19 (a): Acid hydrolysis mechanism; (b): Esterification of cellulose nanocrystal surface [133].

The sulphate groups present on NCC surface stabilise them in water due to the formation of repulsive electric double layers which minimize the agglomeration of cellulose crystals in water [123]. NCC obtained by hydrochloric acid treatment does not possess charged double layers and therefore, the crystals tend to flocculate in water [136]. NCC produced by sulphuric acid treatment is less thermally stable than that produced by hydrochloric acid [136]. Wang et al developed spherical cellulose nanocrystals by hydrolysing MCC with the mixture of hydrochloric acid and sulphuric acid. The concentration of acids was kept mild in order to avoid breakage of cellulose into nano rods. The mixture was ultrasonicated, which resulted in the hydrolysis of MCC surface as well as the inner amorphous region simultaneously, facilitating the formation of micro meter sized fragments. The fragments were further hydrolysed to obtain spherical nanocellulose. The spherical nanocellulose was then desulfated by keeping the supernatant, obtained after repeated washing and centrifugation, for dialysis against distilled water for several days. Some samples were also neutralized by NaOH and then washed until

neutral pH was obtained. The spherical nanocellulose thus obtained was more thermally stable due to less surface charges as compared to NCC obtained from pure sulphuric acid hydrolysis [137].

2.8 Dispersion of Nanocellulose

NCC has excellent mechanical and physicochemical properties. NCC can be used in various sectors due to its advantageous properties (such as high surface area, interesting mechanical and optical properties), renewability and abundance. The properties of nanomaterials can be fully explored when they are well dispersed within the matrix. Incorporation of NCC in polymeric resin is carried out using physical or chemical techniques, as shown in Figure 2. 20. In some cases, both physical and chemical techniques are used to obtain better dispersion in the matrix. Typically, NCC is produced as aqueous suspensions. The dispersion of NCC in hydrophobic resins, therefore, requires evaporation of water. Drying of NCC can be achieved through freeze drying or spray drying process [138-144]. However, NCC tends to agglomerate during the drying process. The formation of agglomerates can be reduced by optimizing the rate, time period and temperature of drying, and also by surface modification of NCC [138-144]. Figure 2.20 shows the available NCC dispersion techniques.

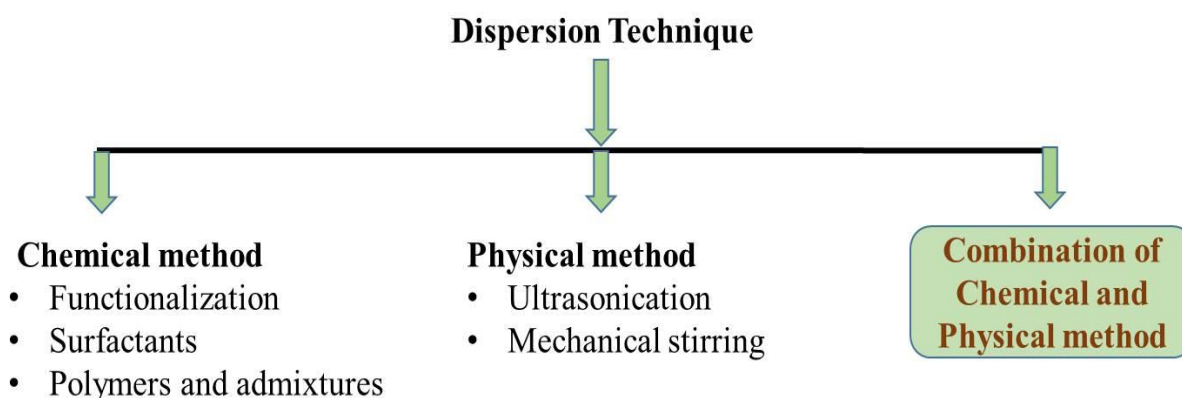


Figure 2. 20 Classification of NCC dispersion techniques.

2.8.1 Chemical Modification of Nano Crystalline Cellulose

Chemical modification of NCC is performed to make desirable changes on the surface to widen its application in various matrices and solvents. Surface modification of NCC increases its compatibility with hydrophobic matrices and non-polar solvents by decreasing the surface

energy. NCC contains three hydroxyl groups in each pyranose ring. The hydroxyl group present on the 6th position is the primary hydroxyl group, which is more susceptible to any type of chemical modification [145]. The chemical modification techniques can be classified as non-covalent and covalent techniques. Non-covalent modifications are mostly carried out using surfactant or polymer coating. Surfactants/polymer coatings are adsorbed on the surface of NCC without affecting the chemical morphology and therefore, securing the integrity and strength of NCC. Covalent modifications include acetylation, esterification, cationization, silylation, fluorescence labelling, polymer grafting, etc.

2.8.1.1 Non-Covalent Modification of Nano Crystalline Cellulose

Non-covalent modification of MCC was first reported by Heux et al. MCC was dispersed in aqueous suspension with the help of an anionic surfactant (acid phosphate ester of alkyl phenol ethoxylate) using MCC-surfactant ratio of 4:1. The resultant surfactant coated MCC was freeze dried in the form of pallets. The surfactant coated MCC pallets were easily dispersed in non-polar solvents using ultrasonication energy for small duration [146]. Similar procedure was also followed by Ljungberg et al. and Fortunati et al. for the dispersion of NCC [147,148]. Researchers also used cationic surfactants to form stable dispersion in organic solvents. Kaboorani et al. and Salajkova et al. used quaternary ammonium surfactant, hexadecyltrimethylammonium (HDTMA) bromide in aqueous medium to obtain surfactant coated NCC. Surfactant coated NCC suspensions were then centrifuged to eliminate excess surfactant from NCC surface and then freeze dried to obtain dried NCC powder [149,150]. Cationic surfactant coated NCC can be easily dispersed in low polar solvents like tetrahydrofuran (THF). Another quaternary ammonium surfactant, cetyltrimethylammonium bromide (CTAB) has also been utilized due to its good adsorption onto NCC surface. According to Beaupré et al., almost 60% of surface hydroxyl groups were covered by CTAB when used at 5-7.5 wt % with respect to NCC. CTAB coated NCC has been used for drug deliveries [151]. Nano metal synthesis can also be done on NCC surface using CTAB [152]. The density and particle size of metal nanomaterials synthesised on NCC surface were controlled by CTAB concentration, pH and the reduction time [135,151-153]. The use of cationic alkyl ammonium surfactants, didecyldimethylammonium bromide (DMAB) and CTAB have also been reported to prepare NCC Pickering emulsions [154]. The use of non-ionic surfactant is also common to disperse NCC in hydrophobic matrices. Kim et al. used sorbitan monostearate to improve the dispersion of NCC in THF. Sorbitan monoesterate was found to improve the stability of NCC dispersion within hydrophobic polystyrene matrix [155]. Recently, 2,2,6,6-

tetramethylpiperidine-1-oxyl (TEMPO) oxidised NCC whiskers were dispersed using Pluronic surfactants (Pluronic L61 and L121) for fabrication of epoxy nanocomposites [156]. The use of Pluronic lead to better NCC dispersion and NCC/epoxy interfacial interactions resulting in improved mechanical and thermal properties of the nanocomposites.

2.8.1.2 Covalent Functionalization of Nano Crystalline Cellulose

Acetylation and Esterification

Acetylation and esterification of NCC have been carried out using a number of methods. In one of these techniques, acetylation was performed by treating fibrous as well as homogeneous NCC with acetic anhydride and acetic acid [157]. In case of fibrous NCC, acetylation only occurred in the cellulose chains present on the surface of NCC, which surrounded the unreacted NCC core. On the other hand, uniform acetylation was obtained in case of homogeneous NCC due to the progress of acetylation reaction into the core, owing to dissolution of surface acetylated cellulose. In another method, an NCC suspension was mixed with an aqueous emulsion of alkyenyl succinic anhydride and the mixture was subjected to freeze drying and heating to perform acetylation of NCC [158]. Reaction with vinyl acetate in the presence of potassium carbonate catalyst has also been used to perform surface acetylation of NCC whiskers [159]. An increase in the reaction time, however, led to complete destruction of the crystalline structure of NCC whiskers. A combined method of NCC synthesis and functionalization has also been developed recently [160]. A mixture of acetic acid, HCl and organic acids was used for the single step synthesis and functionalization of NCC through Fischer esterification process, as presented in Figure 2. 21. Gas phase esterification of NCC through evaporation in large excess of palmitoyl chloride has also been reported [161]. Refluxing of hydrolysed NCC in organic acid chloride is another approach for esterification of NCC [162]. This method did not affect the crystalline core of NCC and resulted in grafting of NCC with organic fatty acids of different aliphatic chain lengths.

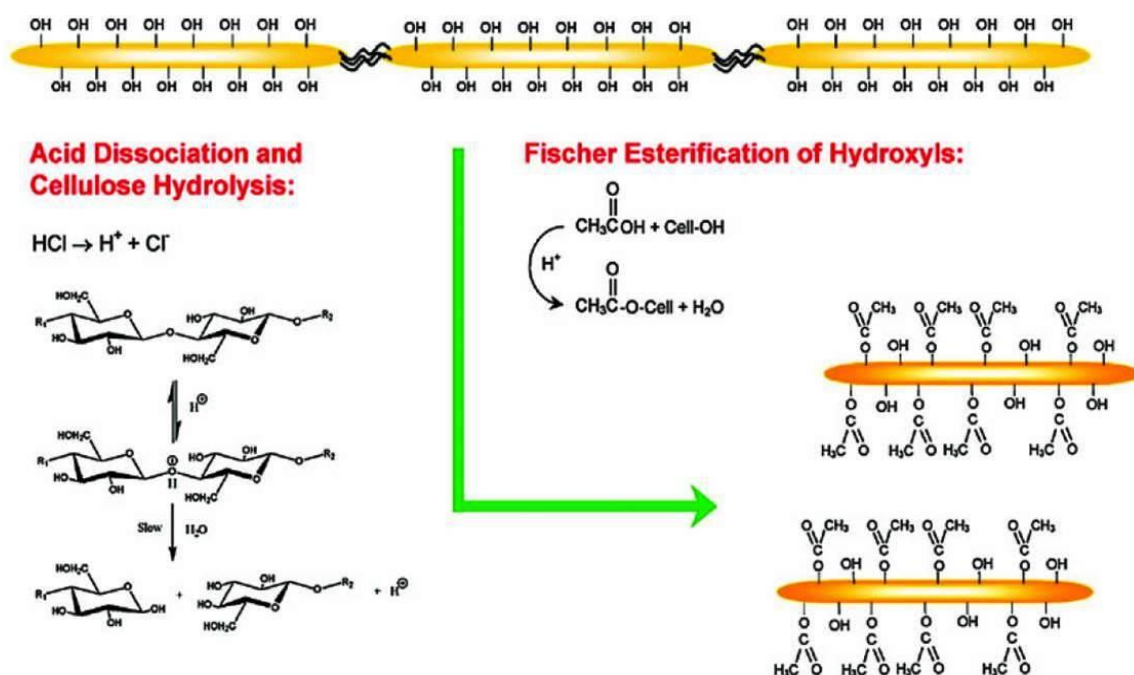


Figure 2. 21 Single step synthesis and functionalization of NCC through Fischer esterification process [160].

Cationisation

Recently, a one-step process of cationisation of NCC surface has been developed. In this process, epoxypropyltrimethylammonium chloride (EPTMAC) was grafted to the NCC surface [163]. The grafting occurred due to nucleophilic addition reaction of alkali activated hydroxyl groups of NCC to the epoxy group of EPTMAC. The surface charge of NCC changed from negative to positive due this grafting process and as a result of positive surface charges, a stable aqueous suspension was obtained. The use of mild alkaline conditions in this process did not affect the original morphology or crystal structure of NCC.

Functionalization of NCC with Fluorescein Isothiocyanate

For fluorescence bioassay and bioimaging applications, which are based on tracking of localization of the fluorophores, NCC has been covalently functionalized with fluorescein-5'-isothiocyanate (FITC) [164]. For this covalent functionalization, a three step reaction route has been used, as shown in Figure 2. 22.

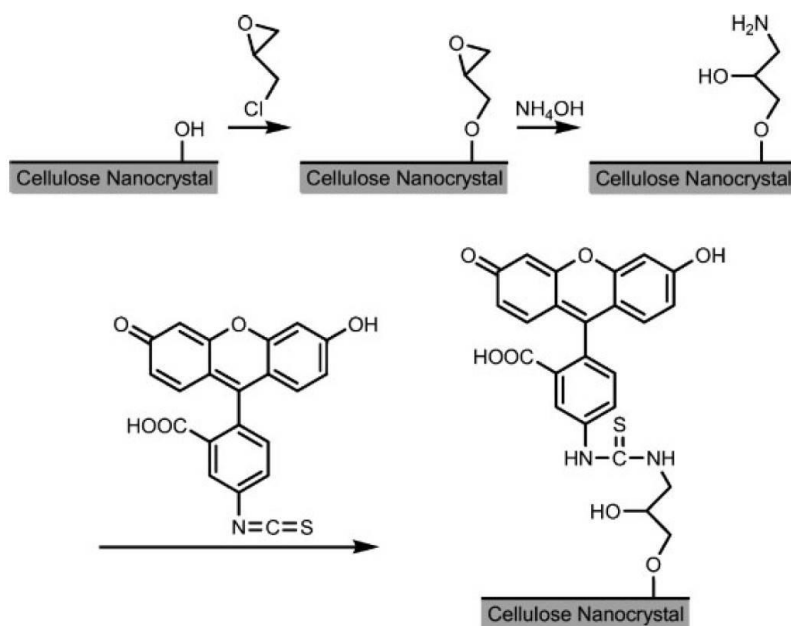


Figure 2. 22 Scheme for functionalization of NCC with FITC [164].

In the first step, NCC surface was functionalized with epoxy functional groups through reaction with epichlorohydrin. In the second step, primary amino groups were introduced by opening the epoxy rings through reaction with ammonium hydroxide. In the final step, covalent bonding of FITC with NCC was achieved through reaction of primary amino groups of NCC with isothiocyanate groups present in FITC. The functionalization of NCC with FITC was confirmed through UV-Vis spectroscopy from the absorption peaks of FITC in the wavelength range of 450–500 nm.

Functionalization with Silanes

Partial silylation of NCC whiskers has been carried out using a series of alkyldimethylchlorosilanes containing alkyl groups ranging from isopropyl to n-butyl, n-octyl and n-dodecyl [165]. When degree of substitution (DS) was between 0.6 and 1, the silylated NCC whiskers were dispersed easily in medium polarity solvents like acetone and tetrahydrofuran (THF). No change in morphology or crystal structure was observed when DS was maintained below 0.6. However, when DS was increased above 1, the structural integrity was disrupted. According to the model developed by the researchers, as shown in Figure, silylated NCC at low DS maintained its structural integrity and was hydrophilic (Figure 2. 23). When the DS was moderate, the surface of NCC was hydrophobic and it could be dispersed in THF (Figure 2. 23). And lastly, when the DS was high, the surface chains were solubilized and

silylation progressed into the NCC core, resulting in disruption of crystal structure of NCC (Figure 2. 23). In addition to the above process, trimethyl silylation of NCC surface, derived from bacterial cellulose, has also been reported [39].

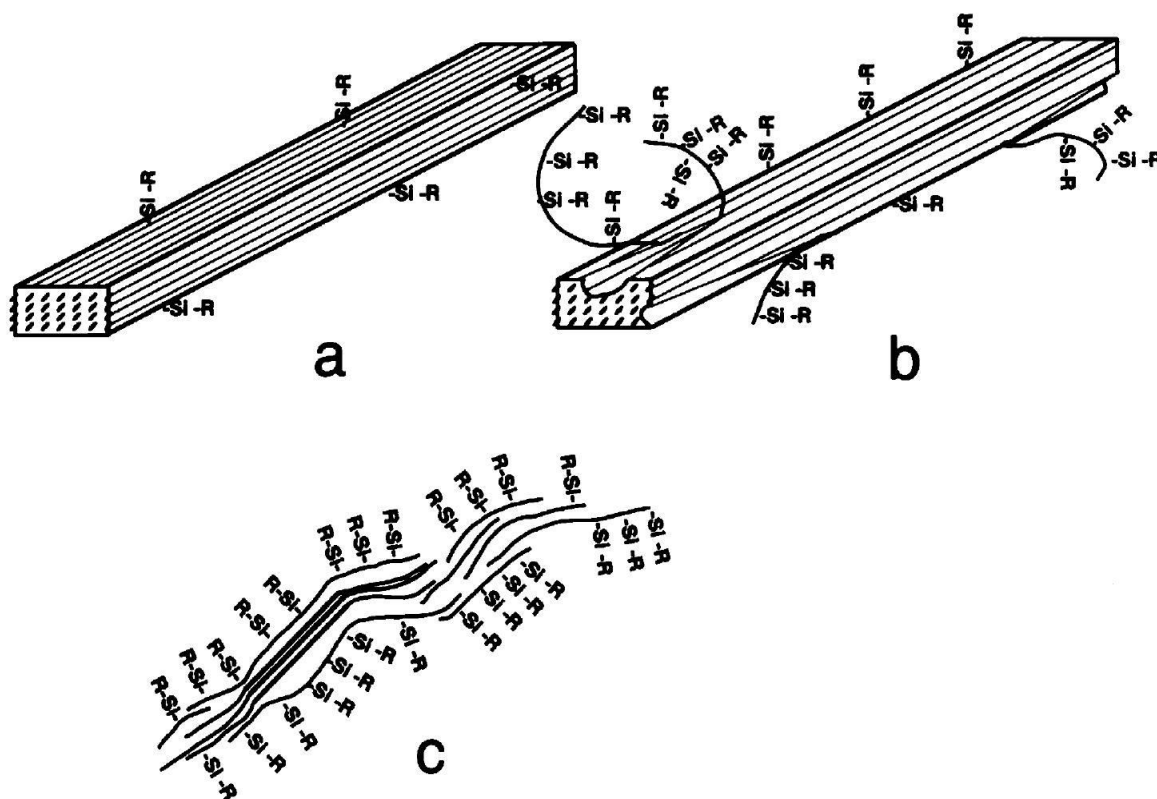


Figure 2. 23 Model explaining the silane functionalization of NCC at: (a) low DS showing onset of surface functionalization, (b) moderate DS showing surface functionalization and (c) high DS showing disruption of NCC core [39].

TEMPO-mediated Oxidation and Functionalization of NCC

TEMPO-mediated oxidation has been used to functionalize NCC with carboxylic groups [166-168]. This functionalization is carried out using TEMPO reagent in NaBr and NaOCl environment by specifically oxidising the primary hydroxymethyl groups [169]. Only 50% of the surface hydroxymethyl groups are oxidised in TEMPO-mediated oxidation, keeping the secondary hydroxyl groups intact. TEMPO-mediated oxidation is shown schematically in Figure 2. 24. This functionalization resulted in better aqueous dispersion of NCC due to electrostatic repulsion between the carboxylic groups and the resulting suspension showed a liquid-crystal like behaviour.

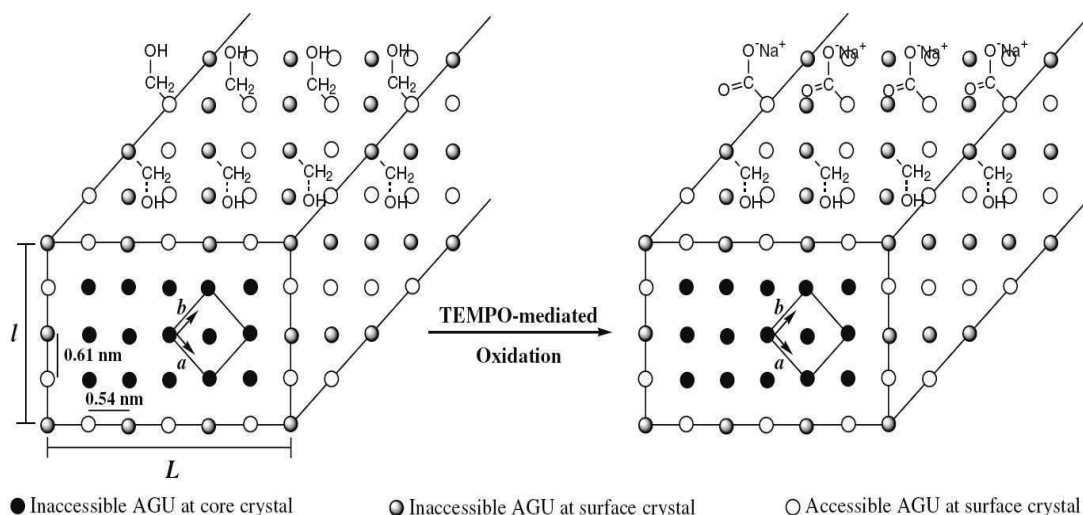


Figure 2. 24 Schematic of TEMPO-mediated oxidation of NCC [169].

The degree of oxidation of NCC in TEMPO-mediated oxidation process could be controlled by varying the molar ratio of NaOCl over the anhydroglucose unit of hydrolysed cellulose. Higher NaOCl molar ratio resulted in higher oxidation degree and carboxyl content; however, excessive oxidation led to the degradation of amorphous region of NCC affecting the structural integrity [170]. Once NCC is functionalized with carboxyl groups, it can be further grafted with various polymers to obtain different functionalities. Preparation of a ‘brush polymer’ through grafting of poly (ethylene glycol) on to carboxyl functionalized NCC (obtained from TEMPO oxidation) has been reported [171]. In a recent study NCC, after TEMPO-oxidation and amine grafting with tuned charge density, was used to control the morphology and stability of silver nanoparticles in aqueous suspensions [172].

NCC Functionalization through Polymer Grafting

Functionalization of NCC surface through polymer grafting has been frequently reported. In one approach, polymer chains were grafted to the NCC surface (known as ‘grafting to’ approach), whereas in the second approach, polymer chains were grown on the NCC surface (known as ‘grafting-from’ approach) through graft polymerization process. In the first approach, polycaprolactone (PCL) of different molecular weights was grafted to NCC through the isocyanate-mediated coupling reaction [36]. At higher grafting density, crystallization of PCL on NCC surface was observed. Grafting of polyurethane onto NCC surface using the same approach has also been reported [173]. Carboxylated NCC, obtained through TEMPO oxidation, could be grafted with polymers through the peptide coupling reaction. Through this approach, grafting of

PEG-NH₂ on to TEMPO oxidized NCC surface was carried out through EDC/NHS [1-Ethyl-3-(3-dimethylaminopropyl)-carbodiimide/N-hydroxysuccinimide] carbodiimide chemistry at room temperature [171]. The same approach has also been utilized for grafting of DNA to the NCC surface [174]. Grafting of maleated polypropylene onto NCC surface has also been reported [147]. NCC with thermos reversible aggregation behaviour, which can be used for designing stimuli-responsive bio-based materials, was prepared through grafting of thermo-responsive polymers onto NCC surface via a peptidic coupling reaction [175].

In the graft polymerization approach (i.e. 'grafting-from'), polymer chains have been grown on the NCC surface through the atom transfer radical polymerisation (ATRP) process. In this process, first the hydroxyl groups of NCC surface were esterified with 2-bromoisobutyryl bromide (BIBB). In the second step, the selected monomers were polymerized. The grafting process on NCC surface could be controlled very precisely using this surface initiated ATRP technique [176]. The monomers which have been graft polymerized on NCC surface include styrene and N, N-dimethylaminoethyl methacrylate [177-179]. Azobenzene polymers were also grafted to NCC surface to produce a novel amphotropic hairy rod-like system exhibiting thermotropic and lyotropic liquid crystalline properties [180]. Another approach which has been tried for graft polymerization on NCC surface was through ring-opening polymerisation. Polycaprolactone (PCL) was grafted to NCC through this approach using stannous octoate (Sn(Oct)₂) as the grafting and polymerising agent [36]. The use of microwave irradiation was also used to improve the grafting efficiency onto the NCC surface [181,182]. Attempts were also made to use novel in-situ solvent exchange method for grafting of long chain isocyanate groups onto NCC whiskers [183].

2.9 Dispersion of Nanocellulose within Cementitious Matrix

Due to lack of research studies in the field of nanocellulose reinforced cementitious composites, very brief information could be obtained on the dispersion of nanocellulose within cementitious matrix. The hydrophilic nature and water retention capability of NCC and MCC influence the yield stress of cement paste and hydration kinetics of cementitious composites. A suspension of MCC in water was prepared by C.G. Hoyos [51] to study the amount of water absorbed by MCC. The aqueous suspension of MCC was prepared by mixing 0.5g of MCC in 3 ml of water. The suspension was kept for three days at 25°C and centrifuged at 3000 rpm for 25 minutes to segregate two phases. The saturated MCC samples were then quantified for the absorbed water.

It was observed that MCC absorbed 230% water with respect to its mass and 100% with respect to its volume. Similar procedure of MCC saturation was also adopted to prepare MCC reinforced cementitious composites. Saturated MCC suspensions were prepared by adding MCC in adequate amount of water and storing the suspension for two days. Then saturated MCC suspension was mixed with cement in Hobart mixer and additional water was added during the mixing process [51]. Cao et al used dispersed NCC (5.38 wt.% CNCs in water) obtained from the sulphuric acid hydrolysis of cellulose fibres. 0.81% surface of NCC was grafted by sulphate groups, which ensured homogenous dispersion of NCC in aqueous suspension. NCC reinforced cement composites were prepared by mixing diluted NCC suspensions (0.1 wt.% -3.8wt.% w.r.t. cement) and water with cement with the help of a vacuum mixer. The vacuum mixer was set at the speed of 400 rpm for 180s, and there was a pause after 90s for scrapping the mixture from the bowl. The vacuum mixer was used to minimize the air entrapment during the mixing process and it also maintained the consistency of cement pastes [52].

2.10 Effect of Nanocellulose on Cementitious Matrix

2.10.1 Influence of Nanocellulose on Flow Behaviour of Cement Paste

Mini slump test is performed for the analysis of flow behaviour of cement to check the workability. In the freshly prepared cement paste, small particles interact via colloidal forces such as Van-der Waals, electrostatic repulsion, steric hindrance, hydrogen bonding, and some bigger particles interact via direct contact like friction or collisions. The yield stress (τ_0) is the stress necessary to break those interactions and separate the particles. MCC (3 wt% w.r.t. cement) reinforced cement paste showed an increase of τ_0 by 2.6 times over plain cement paste. This may result in increase of energy costs in construction. However, for certain construction applications, higher τ_0 is necessary; for example, in rigid pavements where the fresh paste should retain its shape. Therefore, for these applications MCC reinforcement will be ideal [51]. Cao et al. studied the influence of NCC [or cellulose nano crystal (CNC)] % on yield stress, as shown in Figure 2. 25. According to them, at lower NCC concentration (0.02 wt%-0.04 wt% w.r.t. cement), the yield stress decreased as compared to plain cement paste with the increase in NCC concentration. But on further increase in the NCC concentration, the yield stress again started to increase and at 0.3 wt. % of NCC (w.r.t. cement) the yield stress reached the value similar to that of plain cement. With further increase of NCC (1.5 wt% w.r.t. cement) the yield stress increased significantly as compared to plain cement paste. This contradictory behaviour could be explained based on various interactive forces present between NCC particles during mixing with

cement. At lower concentration, NCC particles behaved like cement admixtures (e.g. polycarboxylate) and promoted the degree of cement hydration by dispersing cement particles through steric stabilization mechanism. This resulted in lower yield stress as compared to plain cement paste. But, with the increase in NCC concentration, NCC particles started to agglomerate and the force required to break these agglomerates was very high, resulting in high yield stresses [52].

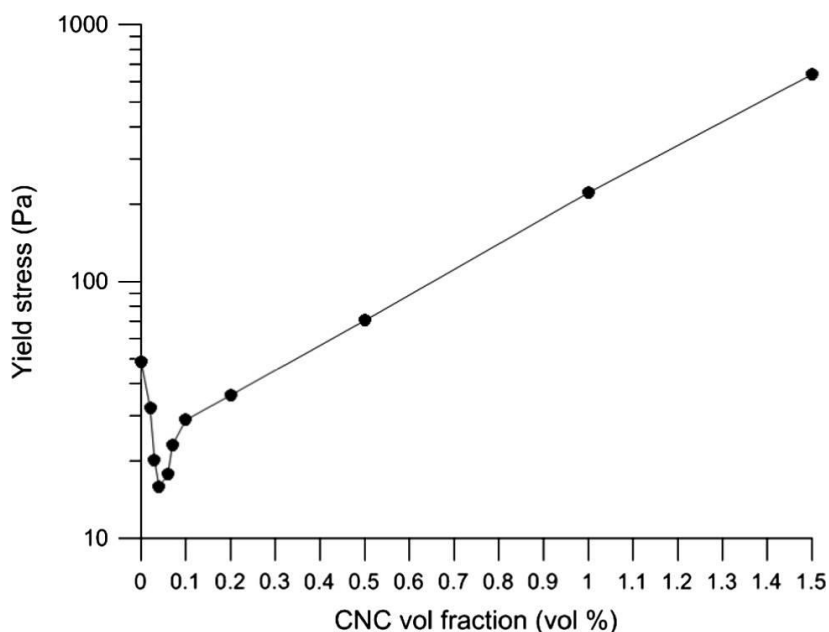


Figure 2. 25 Influence of NCC vol.% on the yield stress of mortar paste [52].

2.10.2 Influence of Nanocellulose on Mechanical Properties of Cement

It was observed that incorporation of 3 wt% of MCC decreased the mechanical properties of cementitious composite in a normal curing period of 28 days [51]. During accelerated curing conditions, which resulted in higher degree of cement hydration, mechanical properties of MCC reinforced cement just reached the values of plain cement mortar. As MCC could retain water due to its hydrophilic nature, at higher temperature (during accelerated curing) it released water leading to more formation of hydration products [51]. According to Cao et al, NCC behaved as water reducing agent at lower concentration (0.2 vol. %) and helped to disperse cement particles. The degree of hydration increased with the addition of adequate amount of NCC. It was observed that NCC% could only be increased up to 0.5 % as further increase resulted in segregation of particles. The increase in flexural strength was 20% and 30% in 3 days and 7 days, respectively with the addition of 0.2% of NCC (Figure 2. 26).

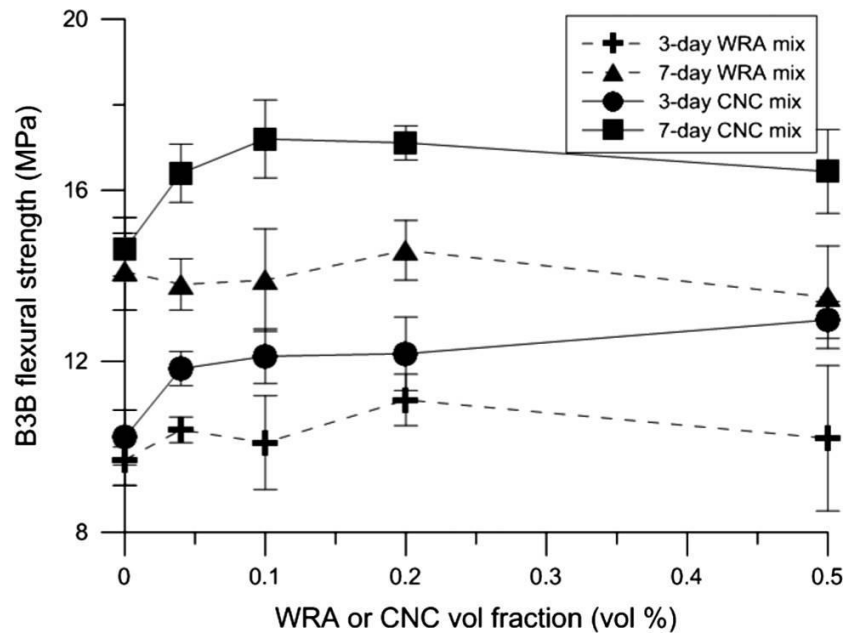


Figure 2. 26 Improvement of mortar's flexural strength due to CNC addition [52].

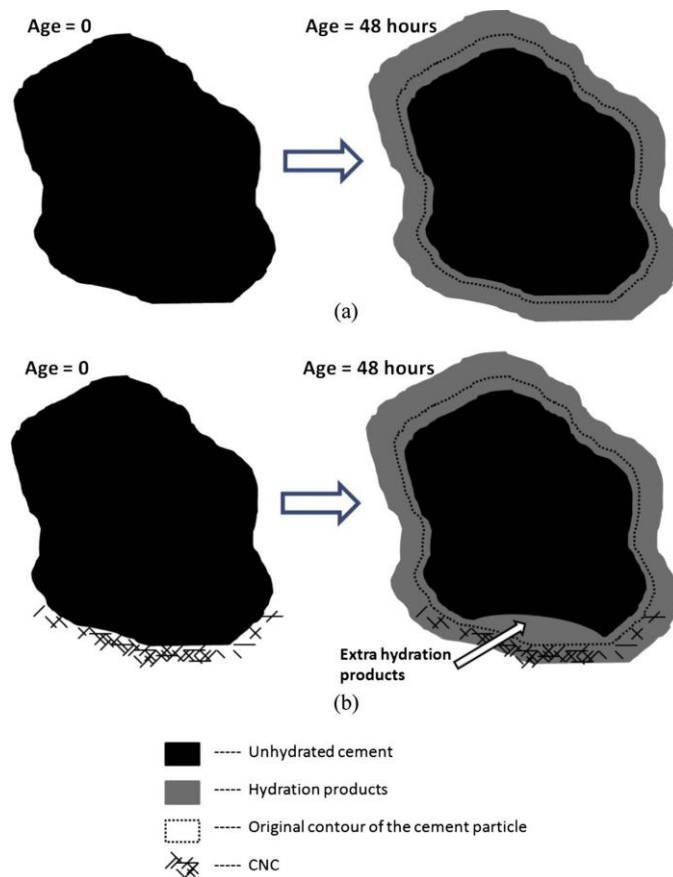


Figure 2. 27 Schematic diagram explaining the short circuit diffusion mechanism [52].

The improvement of flexural strength due to NCC addition was attributed to improved hydration of cement owing to the steric stabilization of cement particles and short circuit moisture

diffusion. The short circuit diffusion was the penetration of water from hydrated part of CSH (more dense part) to the unhydrated part with the help of NCC particles leading to better hydration, as shown in Figure 2. 27.

2.10.3 Influence of Nanocellulose on Microstructure of Reinforced Cement

According to C. G. Hoyos et al. [51], MCC cement composites possess good microstructure due to availability of free hydroxyl groups on MCC. The available hydroxyl groups of MCC can form hydrogen bonding with the hydration products of cement. MCC remains saturated with water and therefore, the CSH phase (cement hydration product) growing near MCC can utilize the water bound with MCC. Moreover, the size distribution of MCC is similar to CSH crystals making MCC a suitable reinforcement for cementitious matrix. The microstructure of MCC reinforced cement is presented in Figure 2. 28.

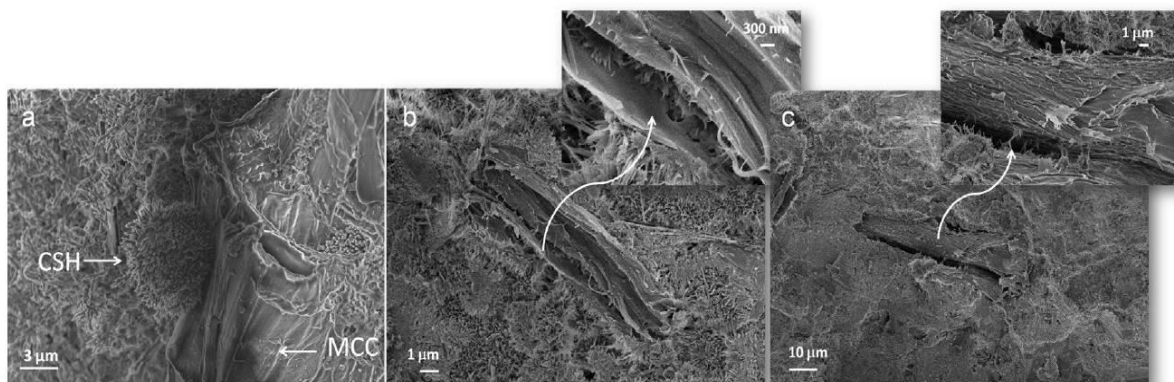


Figure 2. 28 FE-SEM image of cement based materials with 3 wt.% of MCC. (a) cement mortar with 3 wt.% of MCC. (b) cement paste with 3 wt.% of MCC. (c) FE-SEM image of cement paste with 3 wt.% of MCC [51].

In summary, the dispersion of CNTs/CNFs is the main factor which controls the microstructure as well as the mechanical performance of cement nanocomposites. The conventional method of mixing nanomaterials within mortar paste using a standard mixer cannot ensure homogeneous dispersion and therefore, deteriorates the mechanical properties. Addition of admixtures such as silica fume during the mixing process can significantly improve the nanomaterial dispersion. However, the best route to achieve homogeneous nanomaterial dispersion is to disperse the nanomaterials first in water, followed by mixing of aqueous suspensions with mortar paste. Various chemical techniques attempted to achieve uniform and stable CNT/CNF aqueous dispersion are using surfactants, polymers, cement admixtures, functionalization and

combination of various techniques. Anionic surfactants such as SDBS, polymers such as acrylic acid, cement admixtures such as polycarboxylates, acid functionalization and combination of functionalized nanomaterials with acrylic acid polymers were found to provide very good aqueous dispersion as well as strong enhancement in the mechanical properties of cementitious composites. Alternatively, carbon nanomaterials can be grown directly on to cement or silica fume particles to fabricate cement nanocomposites with homogeneous dispersion and significantly improved mechanical performance. Nevertheless, most of these dispersion techniques and processing routes are time consuming and energy intensive. Therefore, despite of achieving promising results with carbon nanomaterial reinforced cementitious composites, practical application of these materials is still challenging. There exists a strong need for a short and simple processing technique for application of these advanced materials in construction industry. In contrast to CNTs, the application of nano and microcrystalline cellulose in cementitious materials has been studied to much lesser extent, although these materials are already finding numerous applications in other industrial sectors. The initial studies indicated the need for developing effective techniques to ensure homogeneous dispersion of MCC/NCC within cementitious matrix and to understand different properties of the reinforced cementitious composites. To answer to these existing needs, as identified from this literature review, this PhD work has applied a new short and less energy intensive surfactant based dispersion route for developing CNT and MCC reinforced cementitious composites and thoroughly characterized the microstructure and mechanical properties of the resulting composites.

Chapter 3

Dispersion of Carbon Nanotubes in Aqueous Suspension

This chapter is based on the article:

Shama Parveen, Sohel Rana, Raul Figueiro, and Maria Conceição Paiva. Characterizing dispersion and long term stability of concentrated carbon nanotube aqueous suspensions for fabricating ductile cementitious composites. *Powder Technology* 307 (2017): 1–9.

3.1 Introduction

CNTs are finding widespread applications in various fields including catalyst supports, optical devices, quantum computers, biomedical sensors and composite reinforcement due to their unique electronic, thermal, optical, and mechanical properties [28,42,184,185]. Most of these applications require stable suspensions of high concentration of CNTs. The non-covalent functionalization technique of producing CNT suspensions does not alter the inherent electrical, optical or mechanical properties of CNT. In this route, CNTs are commonly dispersed using various surfactants, polymers or biomacromolecules [11,13,17,78,186-193]. Currently, among various surfactants, Pluronic F-127 is finding a special attention due to its biocompatibility and lower toxicity as compared to other surfactants [12,194-196]. Pluronic F-127 is a non-ionic triblock copolymer composed of a central hydrophobic chain of polyoxypropylene (PPO) flanked by two hydrophilic chains of polyoxyethylene (PEO). As Pluronic F-127 possesses an amphiphilic structure, it has been proved to be an effective surfactant for CNT dispersion [195]. It has high solubility in water at room temperature (up to 10 wt% at 20°C), allowing to prepare CNT suspensions at high surfactant concentration. The dispersion of CNT in Pluronic solution is attributed to the steric stabilization induced by the PEO chains which extend into the water. Recently, MWCNTs suspensions with up to 0.016 wt.% were obtained in water using 0.1% Pluronic F-127 and 8h magnetic stirring at 70°C followed by 16h of ultrasonication [194]. Good dispersion of 0.1 wt.% SWCNT in water using Pluronic was also achieved applying ultrasonication for 1 hour, followed by ultracentrifugation for another 1 hour [195]. The prepared SWCNT suspensions exhibited stability up to 3 months. Pluronic surfactants were also found to disperse MWCNTs better in highly acidic or basic aqueous media, as compared to ionic surfactants [11]. MWCNTs were also effectively dispersed in the mixture of ethoxy-modified trisiloxane (a silicone surfactant) and Pluronic F127 [196].

In general, research studies on the preparation of concentrated CNT aqueous suspensions are very few. The dispersion process requires either intensive ultrasonication (longer time/higher energy), which is detrimental for CNT's inherent properties, or needs high surfactant concentrations (above the critical micelle concentration or CMC), which may result in CNT flocculation due to micelle formation. Good dispersion of high concentration of SWCNTs up to 2 wt.% has been achieved using ionic surfactants such as SDBS with the help of a long ultrasonication treatment (24h) and high surfactant concentrations [193]. However, studies of CNT/Pluronic aqueous suspensions at high CNT concentrations are rarely reported and most of

the research studies focus on low CNT wt% at Pluronic concentrations below their CMC [10]. Extensive research studies have been reported on the study of water dispersions of CNT at low concentration using different surfactants [188-190, 10, 42]. However, the dispersability of CNT at high concentration using Pluronic and the influence of different factors such as CNT type, its functionalization, as well as CNT and surfactant concentrations in such systems have not been reported in the literature. For fabrication of cementitious composites at commercial scale, highly stable and concentrated aqueous CNT suspensions are the prerequisite. Therefore, in this PhD work the dispersion behaviour of different types of CNT at relatively higher concentrations (up to 0.3 wt.%) using Pluronic F-127 has been studied. The effect of different factors influencing CNT dispersion quality (i.e. agglomeration, extractability and stability) such as CNT type, functionalization, CNT and surfactant concentrations has been investigated and optimized to achieve the best dispersion quality. In addition to that, the dispersion quality of optimized CNT suspensions using Pluronic F-127 has been compared with that prepared using SDBS at previously reported recommended concentrations (CNT:SDBS ratio of 1:4) for ionic surfactants [201].

3.2 Materials and Methods

3.2.1 Raw Materials and Characterization

Four different types of CNT have been used in this research work, namely SWCNT, MWCNT, f-SWCNT and f-MWCNT. Nanotubes were purchased from Nanostructured & Amorphous Materials, Inc. (Houston, USA). Table 3. 1 lists the dimension, surface area and purity of these CNTs and their morphology is shown in Figure 3. 1. Morphology of CNTs was characterized using Scanning Electron Microscope (SEM, FEG-SEM, NOVA 200 Nano SEM, FEI) at accelerating voltage of 5 kV. The purity of used CNTs was determined using Energy dispersive X-ray Spectroscopy (EDS using EDAX Si(Li) detector) using an acceleration voltage of 5 kV. Two types of surfactants were used in this study: Pluronic F-127, which was the primary surfactant and SDBS, which was used only for the comparison purpose. The surfactants were purchased from Sigma Aldrich (Portugal). Their chemical structures are presented in Figure 3. 2 and properties are listed in Table 3. 2. Raw CNTs and CNTs extracted from surfactant solutions were studied using Attenuated Total Reflection Spectroscopy (ATR) to investigate the surfactant adsorption on CNT surface.

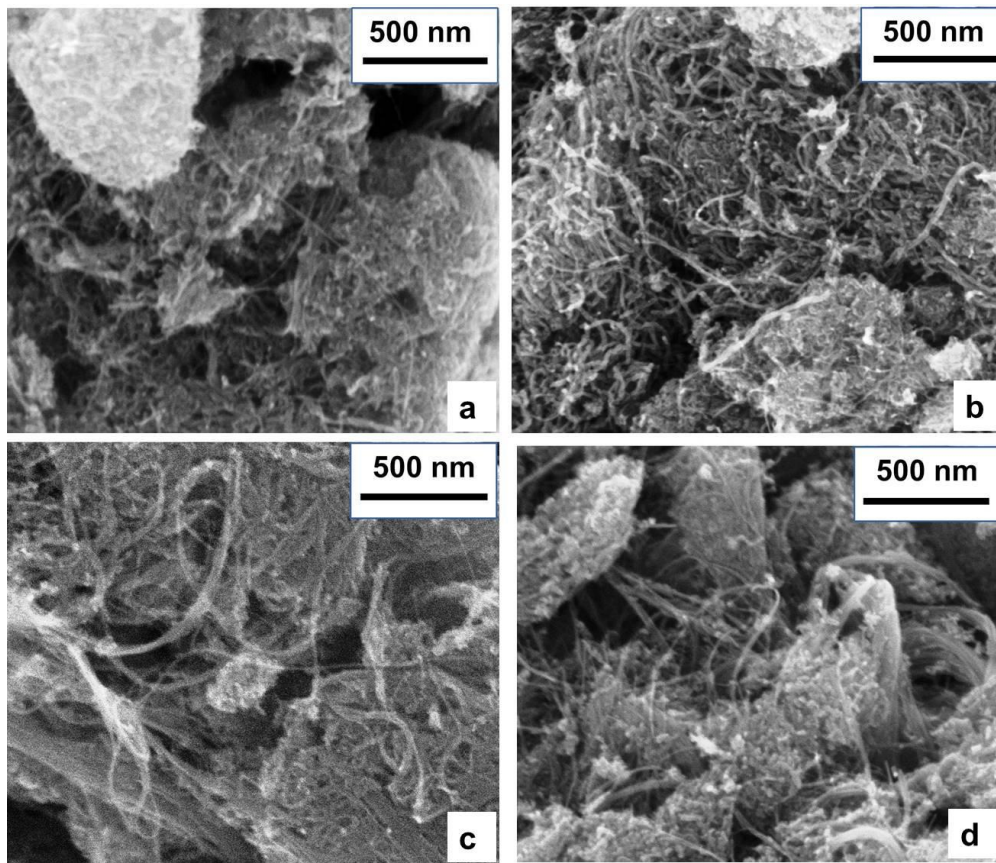


Figure 3. 1 Morphology of CNTs: (a) MWCNT, (b) f-MWCNT, (c) SWCNT and (d) f-SWCNT.

Table 3. 1 Properties of Different Types of CNT

Type of CNT	Diameter (nm)*		Length (μm)*	Surface Area* (m ² /g)	Elements (wt. %)**		Impurity (%)**
					C	O	
SWCNT	1-2		5-30	300-380	91.1	5.0	3.9
f-SWCNT	1-2		5-30	300-380	88.4	11.6	0
MWCNT	2-5nm (inner)	<8nm (outer)	10-30	350-420	92.1	7.9	0
f-MWCNT	2-5 (inner)	<8nm (outer)	10-30	350-420	88.2	11.8	0

Source: *Manufacturer's data, **elements and impurity were determined by EDX

Table 3. 2 Properties and Concentrations of Surfactants

CNT conc. (wt.%)	Type of surfactant	Mol. Wt. (gmol ⁻¹)*	Aqueous Solubility (at 25° C)*	CMC (wt.% at 25°C)**	Surfactant conc. (wt.%)
0.1, 0.2, 0.3	Pluronic F-127	12600	>10%	0.004–0.091	1, 3, 5
0.1, 0.2, 0.3	SDBS	348.5	20%	0.056–0.105	0.4, 0.8, 1.2

*Sigma Aldrich, ** Ref. [186]

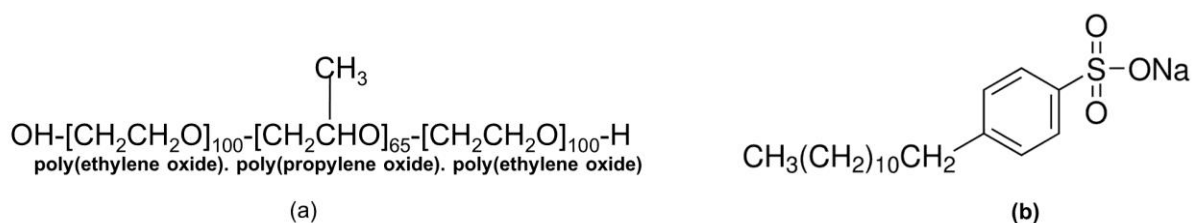


Figure 3. 2 Chemical structure of (a) Pluronic F-127 and (b) SDBS.

3.2.2 CNT Dispersion Route

A short and medium energy intensive process was used to disperse the nanotubes. The process is advantageous for practical applications due to short duration and ability to preserve inherent properties of CNTs. For this purpose, CNT powder was mixed in water along with the required amount of surfactant and subjected to magnetic stirring for 5-10 min. Then ultrasonication was carried out at room temperature using a bath sonicator (CREST Ultrasonicator, CP 230T) for 1h at 45 kHz frequency and 80 W power. The concentrations of CNT and surfactants are listed in Table 3.2.

3.2.3 Characterization of CNT Dispersion

Different techniques used for characterizing prepared CNT suspensions are shown schematically in Figure 3. 3. The main characteristics of the suspensions which have been studied are: (a) sedimentation (b) homogeneity and presence of CNT agglomerates, (c) concentration of well (or individually) dispersed CNTs, (d) stability under ultracentrifugation and (e) long term storage stability.

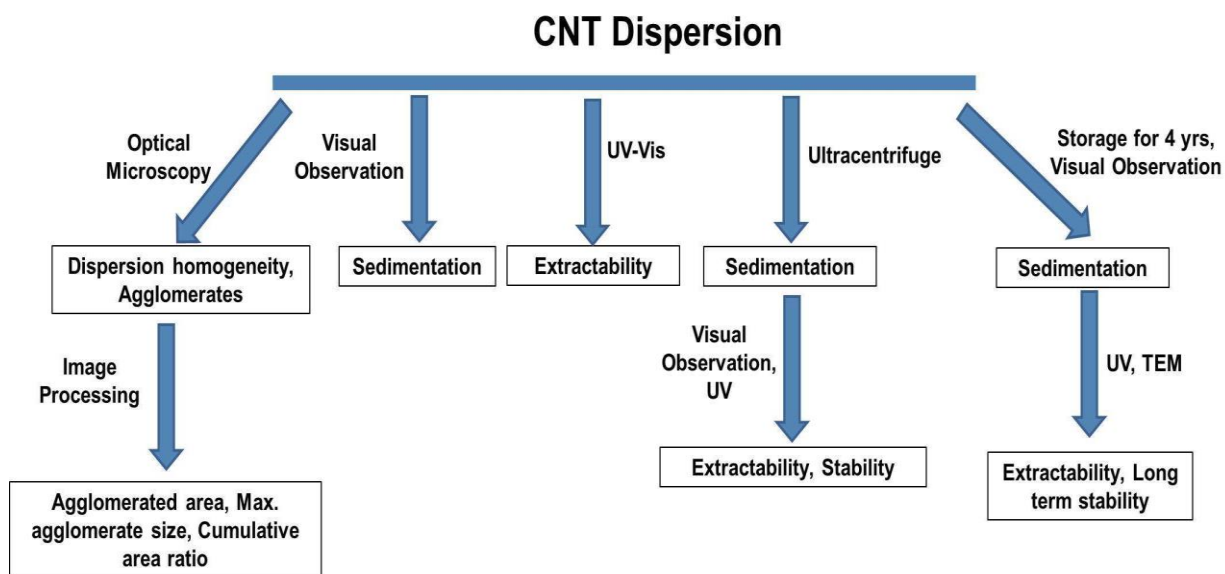


Figure 3. 3 Different techniques used to characterize the quality of CNT suspensions.

3.2.3.1 Visual Observation

The prepared CNT suspensions were kept in small vials and observed for any sedimentation immediately (within 24 hours) after their preparation. Large CNT clusters which were not dispersed will flocculate immediately under gravity forming sediment at the bottom of the vials. Also, sedimentation under ultracentrifugation at 3000 rpm (for 20 min) was observed to study the stability of prepared CNT suspensions. Relatively large suspended CNT bundles will flocculate during ultracentrifugation. Some well dispersed CNTs can also re-agglomerate and form bigger clusters and flocculate. Therefore, inspection of sedimentation due to ultracentrifugation is a qualitative measure of the stability of CNT suspensions. In addition, long term storage stability of CNT suspensions was also studied by storing the vials for 4 years and observing the sedimentation phenomena.

3.2.3.2 Optical Microscopy

An optical microscope was used to study the overall homogeneity or uniformity of CNT dispersion in various CNT suspensions. The presence of large CNT clusters was also observed. For this purpose, a small drop of suspension was put on a glass slide and covered with a cover slip and analyzed. Pictures were taken at different locations of the same suspension (prepared repeated times) and at different magnifications to get clear idea about the dispersion quality.

3.2.3.3 Quantitative Analysis of Agglomerates

Optical micrographs of CNT suspensions were analysed by image processing (using ImageJ software) to calculate total area of agglomerates, maximum agglomerate size and cumulative area ratio. The last parameter represents the contribution of different agglomerate size to the total area of agglomerates and can be helpful to identify CNT suspensions containing higher number of large agglomerates.

3.2.3.4 UV-Vis Spectroscopy

The dispersed CNTs in aqueous suspension are active in UV-Vis region owing to additional absorption due to 1D van Hove singularities [17, 198,199]. Thus, UV-Vis spectroscopy (UV 2401 PC, Shimadzu) was used to determine the concentration of well dispersed CNTs in various suspensions. Bundled CNTs, however, are hardly active in the wavelength region between 200 and 1200 nm due to photoluminescence quenching, originating a weak and broad signal. To measure the concentration, a calibration curve of absorbance vs. concentration was prepared for each type of CNT and the concentration of the various suspensions was calculated using these calibration curves. For the preparation of calibration curves, reference samples with different known CNT concentrations were prepared by diluting a known concentrated CNT suspension prepared using the same method as discussed in section 3.2.2. During each measurement, surfactant solutions of same concentration were used as blank sample to eliminate the peaks due to surfactant. The UV absorption of CNTs at 253 nm was registered [199]. The concentration was measured after ultracentrifugation and after 4 years of storage to investigate the long term storage stability. The concentration of dispersed CNTs was used to calculate extractability, which is the ratio of dispersed CNT concentration (concentration of CNT effectively suspended in solution) and the initial CNT concentration (concentration based on the overall amount of CNT initially added) expressed in percentage, as defined below:

$$\text{Extractability} = 100 * \left(\frac{\text{Conc. of well dispersed CNT}}{\text{Original conc. of CNT}} \right)$$

3.2.3.5 Transmission Electron Microscopy

Selected CNT suspensions with very high stability were characterized using Transmission Electron Microscope (TEM, LEO 906E) to get deeper insight on the dispersion state of CNTs as well as interaction between CNTs and surfactant molecules.

3.3 Results and Discussion

3.3.1 CNT Morphology and Properties

Morphology of MWCNT and SWCNT, as observed by SEM, is presented in Figure 3.1. It can be noticed that CNTs were highly entangled with each other forming dense bundles. However, carboxyl functionalized CNTs were cleaner and slightly disentangled as compared to the pristine CNTs. From the purity data presented in Table 3.1, it can be noticed that MWCNTs contained negligible amount of impurity. However, pristine SWCNTs contained about 4 wt.% impurities which were removed after the functionalization process. EDX data also showed higher oxygen % in case of functionalized CNTs due to formation of carboxylic groups.

3.3.2 Visual Inspection of Sedimentation

The condition of various CNT suspensions within 24 hrs of their preparation is shown in Figure 3.4.

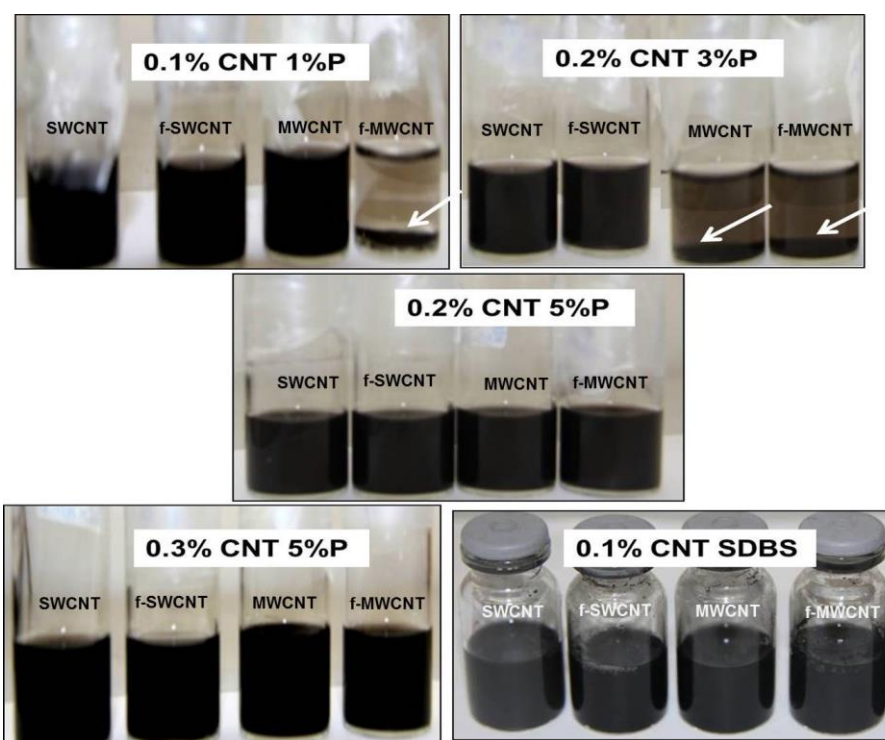


Figure 3.4 Visual observation of sedimentation of various CNT suspensions prepared using Pluronic and SDBS.

No visible sedimentation was observed in the CNT suspensions except for 0.1% f-MWCNT suspension prepared with 1% Pluronic and 0.2% MWCNT and f-MWCNT suspensions prepared using 3% Pluronic. An increase in Pluronic concentration to 5%, however, was able to avoid

sedimentation in case of 0.2% MWCNT and f-MWCNT suspensions. Sedimentation was observed in the case of 0.1% f-MWCNT suspensions even when Pluronic concentration was increased to 3% (not shown in the figure). In the case of SDBS, however, no visible sedimentation was observed for studied 0.1% and 0.3% CNT concentrations (0.3% CNT suspension is not shown in the figure). So, visual inspection indicates that f-MWCNTs at lower concentrations presented lower dispersion stability than other nanotubes when prepared using Pluronic and, overall, SWCNTs (both pristine and functionalized) showed better stability than MWCNTs. The reason for lower stability of f-MWCNT could be less adsorption of surfactant molecules on the functionalized nanotube surface leading to nanotube segregation and sedimentation.

3.3.2.1 Sedimentation after Ultracentrifugation

Sedimentation of CNT suspensions under ultracentrifugation is presented in Figure 3. 5. Only 0.1% and 0.3% CNT suspensions are shown in this figure.

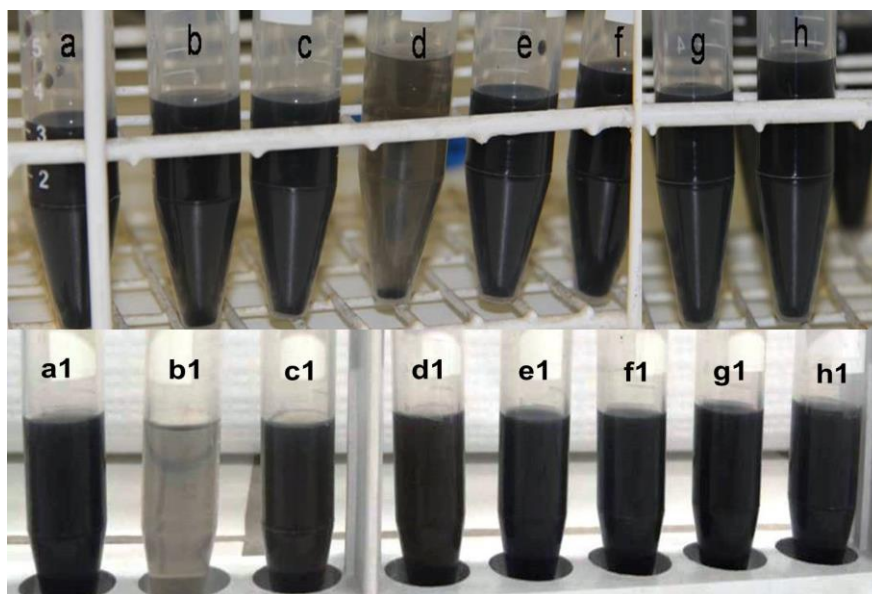


Figure 3. 5 Inspection of sedimentation of various CNT suspensions after ultracentrifugation: (a) 0.1% SWCNT-1% Pluronic, (b) 0.1% MWCNT-1% Pluronic, (c) 0.1% f-SWCNT-1% Pluronic, (d) 0.1% f-MWCNT-1% Pluronic, (e) 0.3% SWCNT-5% Pluronic, (f) 0.3% MWCNT-5% Pluronic, (g) 0.3% f-SWCNT-5% Pluronic and (h) 0.3% f-MWCNT-5% Pluronic, (a1) to (h1): same CNT conc. as (a) to (h), dispersed using SDBS.

As similar to the previous case, 0.1% f-MWCNT suspension exhibited significant sedimentation indicating inferior stability of f-MWCNT suspensions. However, although no immediate sedimentation was observed in case of 0.1% MWCNT suspension prepared using SDBS, after

ultracentrifugation this suspension showed visible sedimentation. All other suspensions prepared with Pluronic and SDBS exhibited good stability and exhibited no visible sedimentation under ultracentrifugation. However, it should be noted that slight sedimentation could not be clearly observed through visual inspection, especially in the suspensions containing high CNT concentrations. Further studies using optical and UV-Vis spectroscopy will provide a deeper understanding about the quality of prepared suspensions

3.3.3 Optical Microscopy: Qualitative study

Optical micrographs of MWCNT suspensions prepared using Pluronic and SDBS are presented in Figure 3. 6.

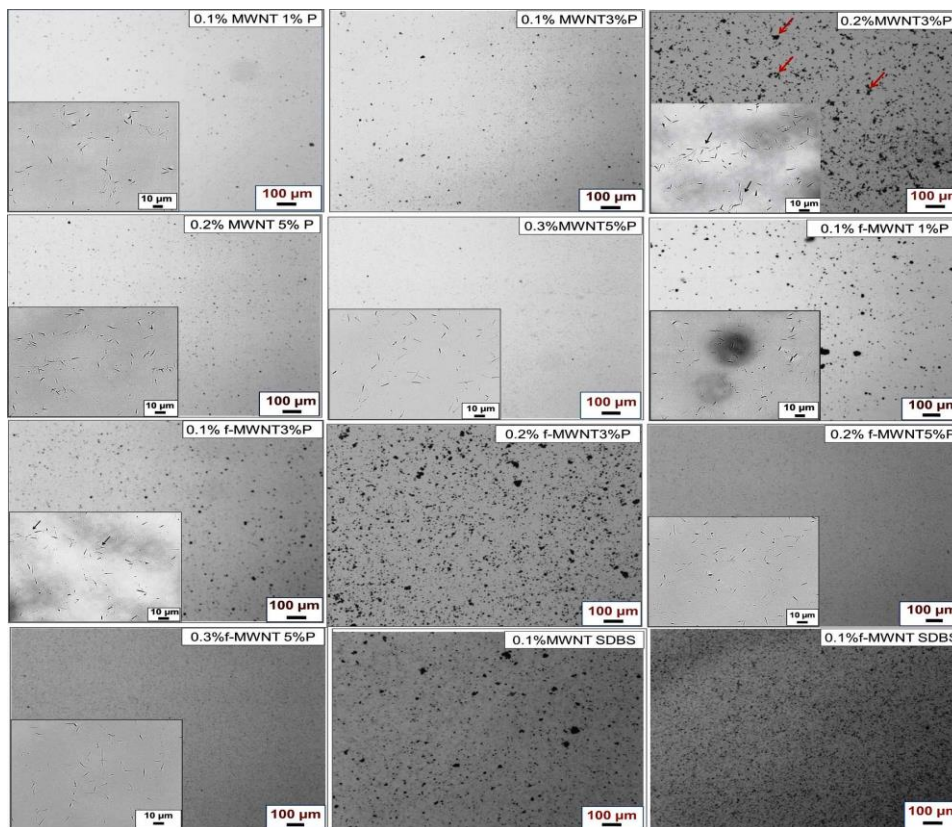


Figure 3. 6 Optical micrographs of MWCNT suspensions prepared using Pluronic F-127 and SDBS.

Optical micrographs at higher magnifications are also provided, unless they are very similar to the previous micrographs or difficult to capture due to presence of big CNT agglomerates. It can be noticed that the dispersion homogeneity and agglomeration were highly dependent on CNT and surfactant concentrations. 0.1% MWCNT could be dispersed very well using both 1% and 3% Pluronic, as can be noticed at both magnifications. A very few small CNT clusters were

visible. However, when 0.2% CNT was dispersed with 3% Pluronic, large number of CNT clusters could be noticed at lower magnification, and the dispersed phase also showed clustering of CNTs (indicated by arrows), as evident at high magnification. These CNT clusters flocculated and formed sedimentation, as observed during visual observation. So, Pluronic concentration was increased and it can be seen that 5% Pluronic was helpful to prepare excellent dispersion of 0.2% MWCNT. 5% Pluronic could also disperse 0.3% MWCNT homogeneously and therefore, no sedimentation was observed in these suspensions during visual inspection. Functionalized MWCNTs also showed similar dispersion behaviour except 0.1% MWCNT which formed some agglomerates when dispersed using 1% Pluronic and resulted in sedimentation. In contrast to Pluronic, functionalization helped in dispersion of CNTs using SDBS and consequently, 0.1% f-MWCNT (but not pristine CNTs) could be dispersed well using 0.4% SDBS. The formation of some CNT agglomerates in pristine MWCNT suspensions with SDBS resulted in sedimentation after ultracentrifugation, as observed in section 3.3.2.1.

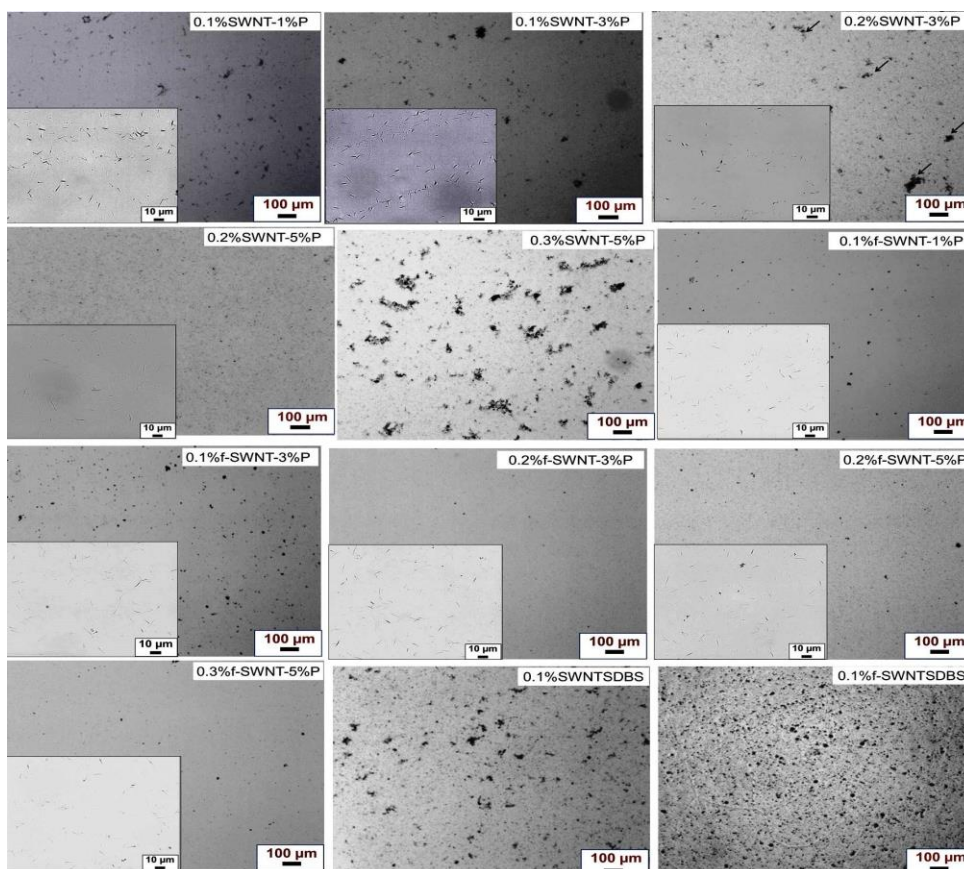


Figure 3. 7 Optical micrographs of SWCNT suspensions prepared using Pluronic F-127 and SDBS.

Optical micrographs of various SWCNT suspensions are presented in Figure 3. 7. Similar to the case of MWCNTs, dispersion of 0.1 and 0.2% SWCNT with very less agglomerates could be

prepared using 1% and 5% Pluronic, respectively. However, it can be noted that 0.3% pristine SWCNT could not be dispersed homogeneously using 5% Pluronic, resulting in numerous visible clusters. Therefore, at higher concentrations pristine SWCNTs were much more difficult to disperse as compared to MWCNTs. Another important difference between SWCNT and MWCNT suspensions using Pluronic was the effect of functionalization. Although functionalization had negative effect on MWCNT dispersion, it significantly helped in dispersing SWCNTs. Consequently, 0.3% f-SWCNTs could be dispersed well using 5% Pluronic. SWCNT suspensions prepared using SDBS, however, showed similar agglomeration and homogeneity to MWCNTs.

3.3.3.1 Quantitative Analysis of Agglomerates

The total area of agglomerates (calculated as the sum of the areas of all agglomerates measured for a given sample, divided by the total area of the image analysed and expressed in percentage) and maximum agglomerate size for various CNT suspensions are presented in Figure 3. 8 (the suspension 0.1%NT1%P indicates 0.1% CNT dispersed using 1% Pluronic and so on).

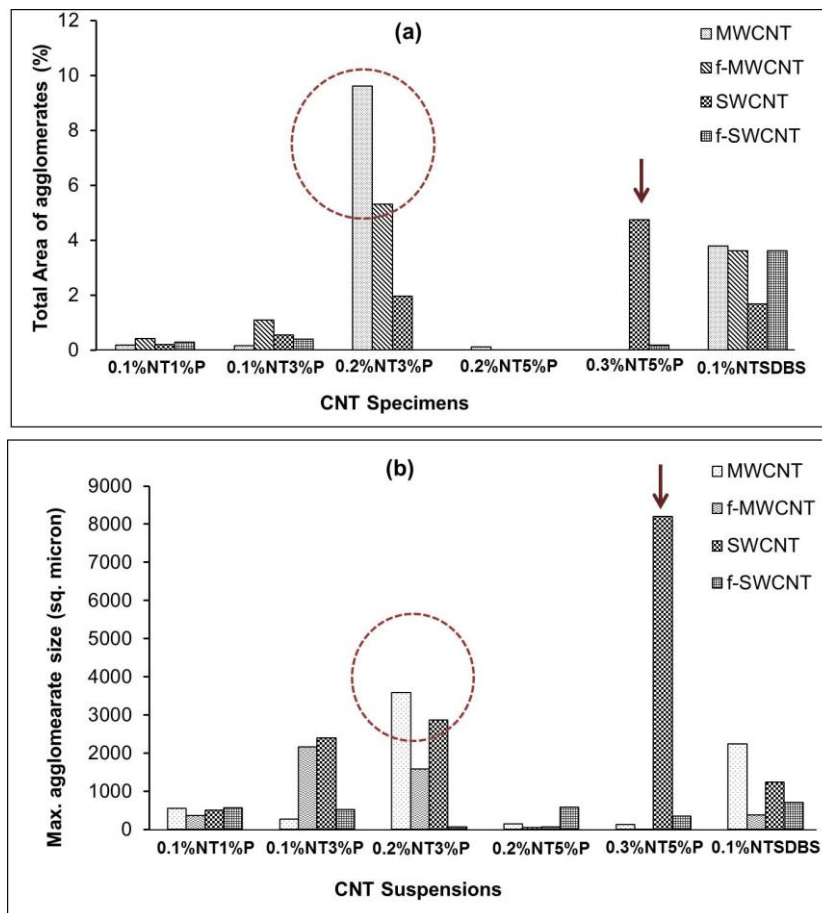


Figure 3. 8 Total area of agglomerates (a) and max. agglomerate size (b) of CNT suspensions.

It is clear that the suspensions with optimum Pluronic concentrations, i.e. 0.1% NT1%P, 0.2%NT5%P and 0.3%NT5%P (except pristine SWCNT, as indicated by arrow) exhibited very small area of agglomerates (only 1% or lower) indicating very good dispersion quality. Other pluronic suspensions (e.g. 0.2%NT3%P, as indicated by dotted circle) showed larger area of agglomerates. The suspensions prepared using SDBS showed higher area of agglomerates as compared to these optimized CNT/Pluronic suspensions. Similarly, maximum size of agglomerates in these optimum suspensions was significantly lower as compared to other Pluronic and SDBS suspensions, as shown in Figure 3. 8(b). Another interesting point to note here was that the use of 0.3% Pluronic for dispersing 0.1% SWCNT or MWCNT deteriorated the dispersion quality, suggesting that for each CNT concentration there existed an optimum Pluronic concentration, above or below which dispersion was inferior. At lower surfactant concentrations than optimum, the number of surfactant molecules was not sufficient for the debundling of CNTs; whereas when surfactant concentration was higher than optimum, the number of surfactant molecules increased in the suspensions leading to more micelle formation and segregation of CNTs.

Besides area % and maximum size of CNT agglomerates, the number of large agglomerates is also an important dispersion parameter, since large agglomerates are more likely to settle down and consequently, responsible for inferior stability of CNT suspensions. The plot of the cumulative agglomerate area ratio against the agglomerate areas, presented in Figure 3. 9, depicts this information. It clearly illustrates the differences in the agglomerate populations. The greater the range of CNT agglomerate sizes, the wider the statistical distribution will be. Consequently, the cumulative agglomerate area distribution will present a gentler slope for wide agglomerate size distributions and a steeper slope for narrower agglomerate size distributions. Thus, suspensions with small CNT agglomerates, or retaining a wide range of agglomerate sizes, may be differentiated by comparing their cumulative agglomerate area distribution.

In case of MWCNT (both pristine and functionalized), suspensions containing optimum Pluronic concentrations (i.e.0.1%CNT1%Pluronic, 0.2%CNT5%Pluronic, 0.3%CNT5%Pluronic) as well as 0.1%CNT3%Pluronic contained lower agglomerate area and most of the agglomerates were very small. Other Pluronic suspensions as well as 0.1% pristine CNT/SDBS suspension exhibited much higher agglomerate area and higher number of large agglomerates.

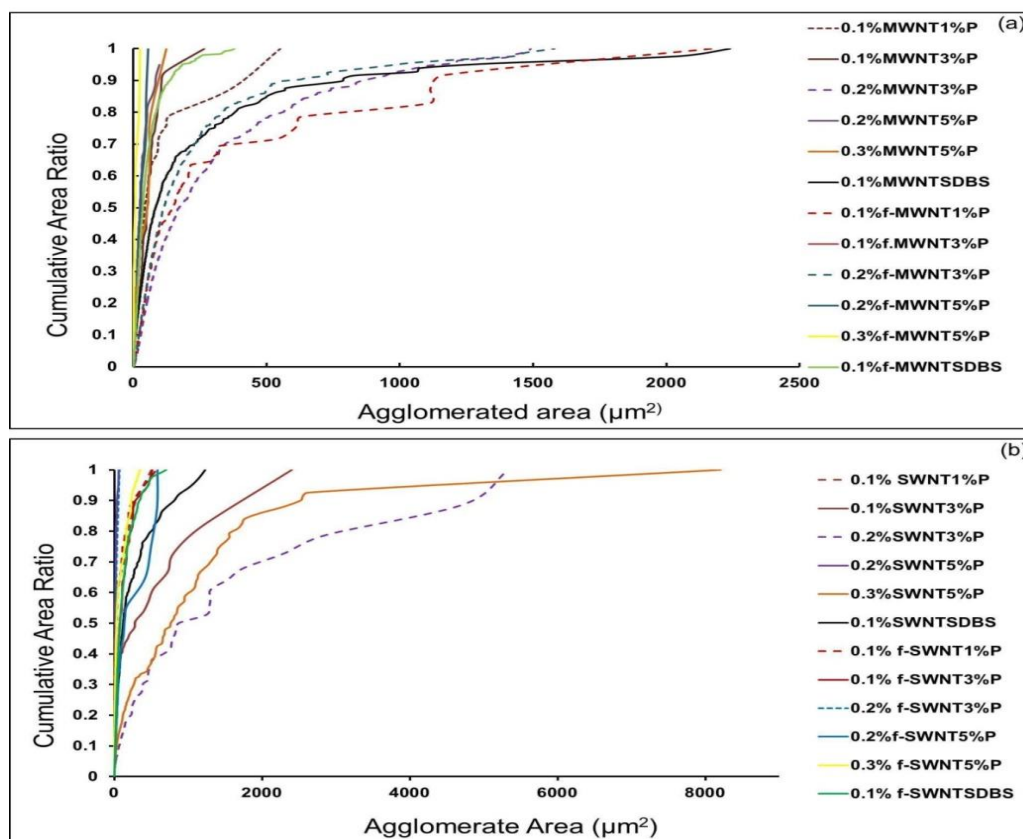


Figure 3. 9 Cumulative area ratio of (a) MWCNT and (b) SWCNT suspensions (P denotes Pluronic F-127).

Similar to MWCNTs, the optimum SWCNT suspensions, i.e. 0.1%SWCNT1%Pluronic, 0.1%f-SWCNT1%Pluronic, 0.2%SWCNT5%Pluronic, 0.2%f-SWCNT5%Pluronic, 0.3%f-SWCNT5%Pluronic and also 0.1%f-SWCNT3%Pluronic, 0.2%f-SWCNT3%Pluronic and 0.1%f-SWCNTSDBS showed low agglomerates area and lower number of large agglomerates. Other un-optimized Pluronic suspensions, i.e. 0.2%SWCNT3%Pluronic, 0.3%SWCNT5%Pluronic, 0.1%SWCNT3%Pluronic and 0.1%SWCNTSDBS suspensions showed considerably higher agglomerates area and large number of big agglomerates (much higher than the equivalent MWCNT suspensions). As pristine SWNTs were present as highly dense clusters, in which entry of surfactant molecules were more difficult, they exhibited relatively higher agglomerated area as well as higher size of agglomerates. This problem was even more when SWNT concentration was higher and consequently, 0.3% pristine SWNT suspensions exhibited high agglomerated area as well as higher agglomerate size and more number of large agglomerates. MWCNTs bundles and functionalized CNT bundles were seen to be more open, facilitating the entry of surfactant molecules and de-agglomeration process.

Based on the observations of sedimentation and optical microscopy (both qualitative and quantitative), it can be commented that the use of optimum Pluronic concentration ensured very good dispersion quality of CNT suspensions, i.e. (a) low agglomerated area, (b) smaller number of large agglomerates, (c) lower maximum agglomerate size, (d) no sedimentation under free standing or ultracentrifugation. However, all above parameters are related to the CNT agglomerates and does not reflect the state of dispersion of individual nanotubes. Further investigation of the suspensions using UV-Vis spectroscopy and TEM provided useful information about the individual dispersion state of nanotubes.

3.3.4 UV-Vis Spectroscopy: Extractability

The UV-Vis absorption spectra and calibration curves for MWCNT and SWCNT suspensions are provided in Figure 3. 10. The presented UV-Vis spectra are for the suspensions prepared by dilution of the original concentrated suspensions.

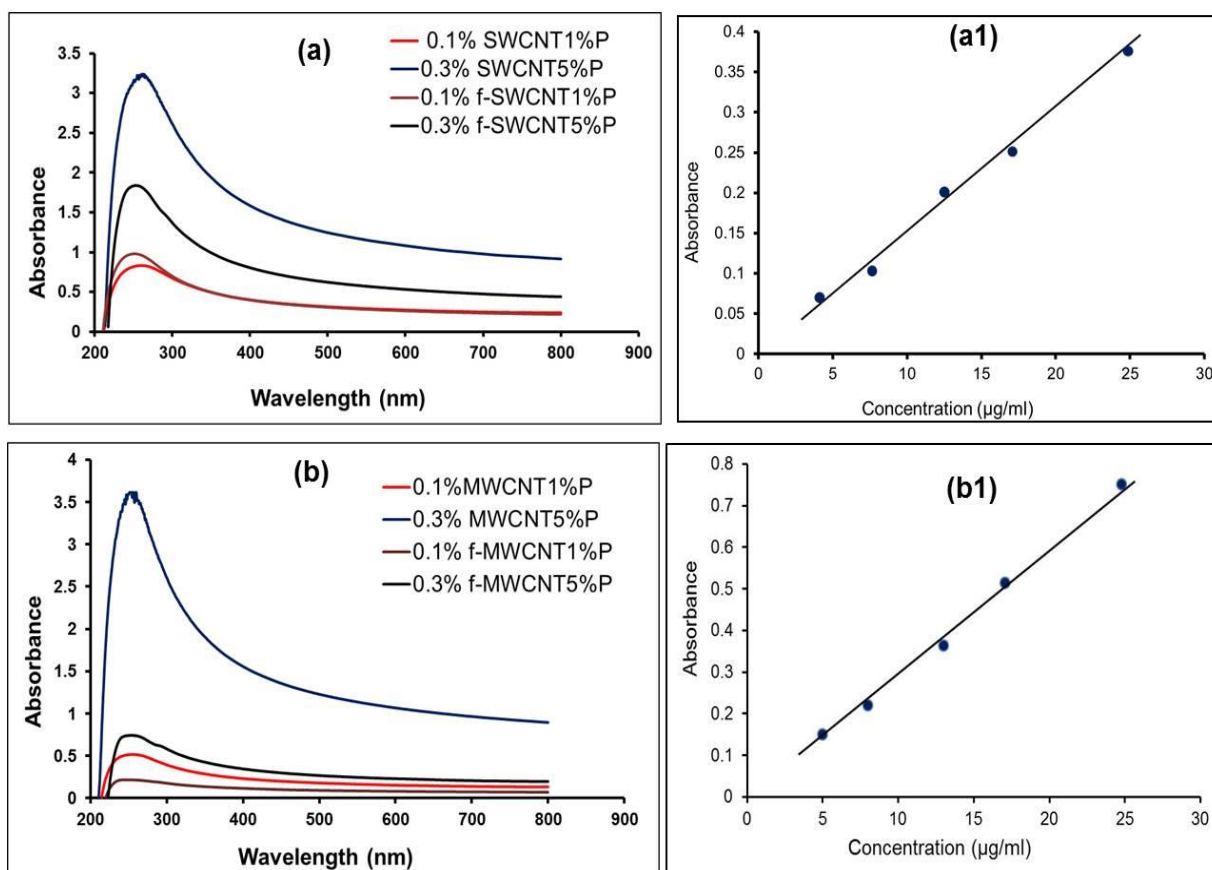


Figure 3. 10 UV-Vis absorption spectra of (a) MWCNT and (b) SWCNT suspensions prepared using Pluronic F-127.

As mainly the well dispersed nanotubes are active in the UV-Vis region, the CNT concentration calculated from UV-Vis spectroscopy provide information about the fraction of well dispersed CNTs. The calculated concentrations and extractability are presented in Table 3. 3. Extractability for SDBS suspensions is also provided for comparison purpose. It can be observed that the concentration of well dispersed CNTs after centrifugation remaining in the suspension was significantly lower than the initial concentration of CNT due to sedimentation of the CNT agglomerates. Overall, SWCNTs exhibited significantly higher extractability as compared to MWCNTs using Pluronic. Also, higher initial CNT concentration resulted in higher extractability for pristine CNTs, whereas the opposite was observed for functionalized nanotubes.

Table 3. 3 Concentration and Extractability of Various Types of CNT Dispersed in Aqueous Solution using Pluronic F-127 and SDBS

CNT Type	Initial conc. (%)	Pluronic, SDBS conc. (%)	Conc. After Centrifugation (%)	Extractability after centrifugation (%)	
				Pluronic	SDBS
MWCNT	0.3	5% P, 1.2% SDBS	0.22	73	87
MWCNT	0.1	1% P, 0.4% SDBS	0.03	30	-
f-MWCNT	0.3	5% P, 1.2% SDBS	0.04	13	80
f-MWCNT	0.1	1% P, 0.4% SDBS	0.02	15	-
SWCNT	0.3	5% P, 1.2% SDBS	0.15	50	80
SWCNT	0.1	1% P, 0.4% SDBS	0.04	40	-
f-SWCNT	0.3	5% P, 1.2% SDBS	0.10	33	70
f-SWCNT	0.1	1% P, 0.4% SDBS	0.05	50	-

In most of the cases, surface functionalization exhibited negative effect reducing the extractability. The use of SDBS led to much higher extractability as compared to Pluronic. The extractability obtained with SDBS was in the range obtained with other ionic surfactants such as Sodium dodecyl sulphate (SDS) investigated previously [17]. Similarly, extractability with Pluronic was also in the range found by previous researchers [12, 193].

3.3.5 Long Term Storage Stability

The long term stability of 0.2 wt. % SWCNT suspensions, with pristine and functionalized nanotubes, was evaluated. For that purpose, the first suspensions prepared were stored and were analyzed after 4 years in terms of SWCNT concentration in suspension. The suspensions were kept in storage for more than 4 years, providing a good estimate for the long term storage stability. Table 3. 4 lists the extractability of these suspensions and compares with equivalent SDBS suspensions. It can be observed that although SDBS led to higher initial extractability for pristine SWCNTs, the concentration of well dispersed CNTs after 4 years was similar to Pluronic.

Table 3. 4 Extractability of 0.2% SWCNT Suspensions after Storage for 4 years

CNT Type	Extractability % with Pluronic		Extractability % with SDBS	
	As prepared ¹	Long term ²	As prepared ³	Long term ²
SWCNT	40-50	17	80	17
f-SWCNT	33-50	55	70	21

¹ Range of results obtained for as-prepared Pluronic suspensions with 0.1 and 0.3 wt% of SWCNT

² Results obtained for stored suspensions with 0.2 wt% SWCNT

³ Results obtained for as-prepared SDBS suspensions with 0.3 wt% SWCNT

The extractability of the long term suspension of pristine SWCNT was lower than the as-prepared suspensions with both surfactants. The extractability after 4 years, however, was higher for the suspension produced with functionalized SWCNT as compared to pristine SWCNTs. This effect was particularly important for the Pluronic suspensions, where no f-SWCNT sedimentation was observed after 4 years of storage, meaning that total stability of the f-SWCNT was attained with this surfactant.

The long term suspensions prepared with SDBS (showing sedimentation) and Pluronic (indicating homogeneous suspension) are shown in Figure 3. 11a and b, respectively. The low concentration homogenous suspensions prepared by dilution of the suspension in Figure 3. 11b by hand shaking are shown in Figure 3. 11c.

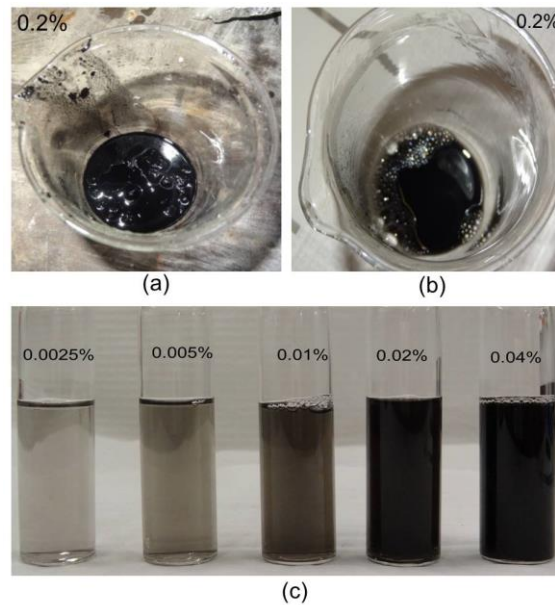


Figure 3. 11 Long term stability of CNT suspensions over a period of 4 years: (a) 0.2% SWCNT with 0.8% SDBS, (b) 0.2% SWCNT with 5% Pluronic and (c) 0.04-0.0025% SWCNT suspensions prepared through dilution of (b).

TEM micrographs of SWCNT and f-SWCNT collected from long term Pluronic suspensions are presented in Figure 3. 12a and b. It was generally observed that the SWCNT ropes (bundles of SWCNT) were thinner, or smaller in diameter, for the functionalized SWCNT suspensions compared to the pristine SWCNT suspensions. Pluronic was present at the surface of the SWCNT as also confirmed by FTIR-ATR analysis (Figure 3. 13).

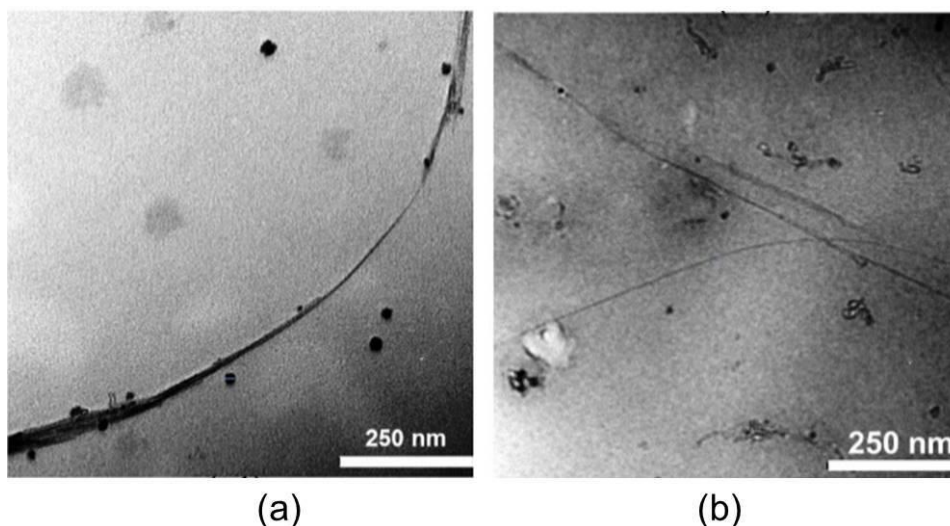


Figure 3. 12 TEM micrograph of 0.2% SWCNT suspensions prepared with 5% Pluronic: pristine SWCNT (a) and functionalized SWCNT (b).

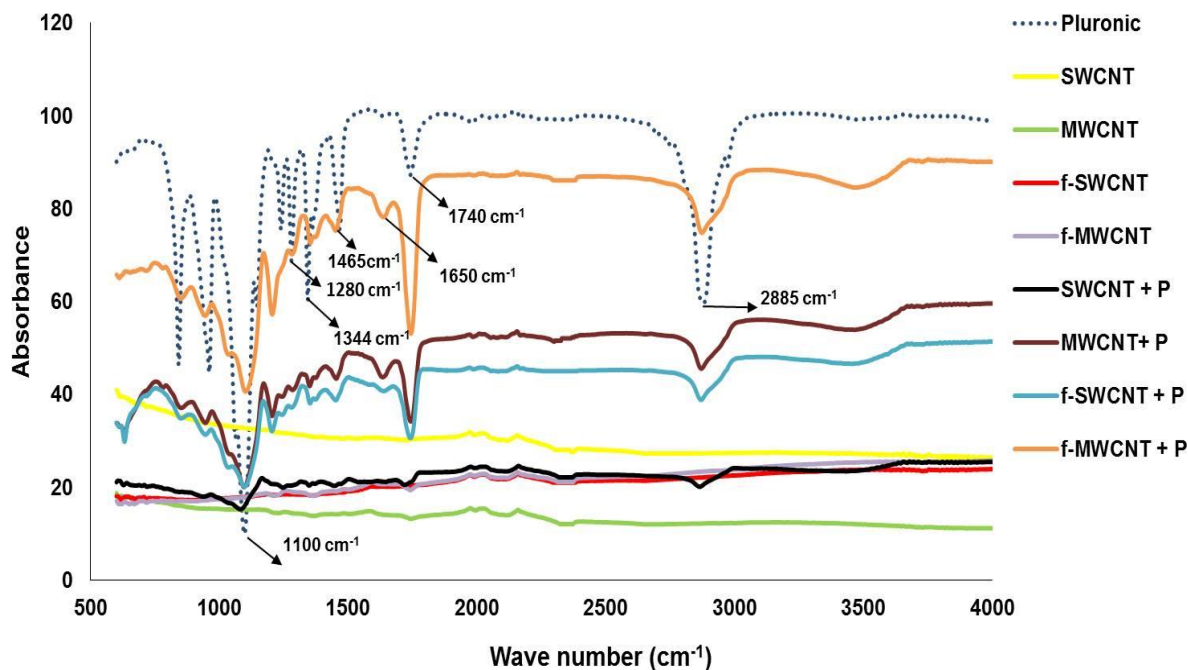


Figure 3. 13 ATR curves of Pluronic F-127 and various nanotubes.

3.3.6 Detection of Surfactant on CNT surface

To detect the presence of surfactant on CNT surface, CNTs were separated from the dispersed suspensions, washed and dried before ATR analysis. A typical ATR spectral band of tri-block copolymer, Pluronic F-127 is shown in Figure 3. 13. Pluronic F-127 shows amorphous state in aqueous solutions and crystalline state after evaporation of water [202]. The main distinguishing region for amorphous and crystalline state of Pluronic F-127 is from 1000 cm^{-1} to 1400 cm^{-1} . The characteristic peaks of Pluronic F-127 appear at 1111 cm^{-1} for C-O stretching, 1280 cm^{-1} for CH_2 out of plane bending (twisting region), 1344 cm^{-1} for CH_2 out of plane bending (wagging) and 2885 cm^{-1} for aliphatic C-H stretching. As ATR analysis was performed in dry form, ATR should show the bands for crystalline form of Pluronic F-127. The characteristic band for amorphous phase (aqueous solution of Pluronic F127) is a broad spectral band at 1100 cm^{-1} , but in the present case, the presence of an overlapped triplet band at 1060 cm^{-1} , 1111 cm^{-1} and at 1150 cm^{-1} indicated the presence of crystalline Pluronic F-127 [202]. Similarly, in CH_2 bending region, three different peaks were observed for crystalline Pluronic, namely a weak band at 1236 cm^{-1} and other intense bands at 1244 cm^{-1} and at 1280 cm^{-1} . Two bands observed at 1344 cm^{-1} and 1360 cm^{-1} were due to wagging of CH_2 , the band at 1465 cm^{-1} due to C-H in plane bending (scissor), at 2885 cm^{-1} due to symmetric stretch of C-H in CH_3/CH_2 structure and at 2890 cm^{-1} due to asymmetric stretch of C-H in CH_3/CH_2 structure. A characteristic aldehyde band at

1740 cm^{-1} was also observed due to oxidation of ether structure of Pluronic F-127 to aldehyde [202]. The presence of these characteristics peaks in the spectra of CNTs recovered from the solution confirmed that Pluronic was adsorbed on the surface of CNTs during the dispersion process.

3.3.7 Discussion: Carbon Nanotube Dispersion in Aqueous Surfactant Solutions

Carbon nanotube stability in aqueous suspension is governed by its ability to adsorb specific surfactants. The surfactant is typically an amphiphilic molecule with a non-polar moiety that strongly adsorbs at the nanotube surface and a polar moiety that is stable in water, keeping the nanotube in suspension if in sufficient concentration. The preparation of stable suspensions of MWCNT and SWCNT present different challenges, although based on similar principles. MWCNT have a larger diameter and higher specific weight compared to SWCNT, and form large agglomerates of entangled nanotubes. These agglomerates are difficult to stabilize in aqueous suspension, requiring the use of an effective mixing method to achieve the dispersion into individual tubes, combined with the surfactant action. The SWCNT tend to pack tightly along their length forming ropes that may contain hundreds of SWCNT. Their aqueous suspension requires the separation of these ropes into individual tubes, or into smaller ropes that may be stable in suspension. This process requires the use of a surfactant that strongly adsorbs at the nanotubes' surface and is able to intercalate between individual SWCNT, and a mixing method that assists the intercalation process and the exfoliation of the nanotube ropes.

The application of ultrasounds is known to be an efficient method for the dispersion of nanoparticles in solution. Vaisman et al. [8] interpreted the exfoliation of SWCNT induced by the high shear forces provided by the sonicator, concluding that the process started at the ends of the bundles with simultaneous intercalation of the surfactant. The adsorption of surfactant molecules continues along the SWCNT length allowing separation from the ropes. Pluronic F-127 is a non-ionic polymeric surfactant containing hydrophobic and hydrophilic segments of PPO and PEO, respectively, so that the PPO segments adsorb at the nanotube surface while the PEO segments extend into the water. The separation of the SWCNT is aided by the steric hindrance induced by the long PEO chains. SDBS is a low molecular weight anionic surfactant with a hydrophobic tail that adsorbs at the CNT surface, and a hydrophilic moiety for the stability in water. The separation of SWCNT from the ropes by adsorption of SDBS is aided by

the Coulombic repulsion between the SDBS anionic groups, averting the aggregation of neighboring nanotubes.

In the present work, it was observed that the preparation of suspensions with higher nanotube concentration required higher concentration of surfactant to achieve higher extractability. There is an optimum Pluronic concentration for each nanotube concentration level, in order to achieve maximum extractability. However, the optimum nanotube/surfactant ratio was not constant for different nanotube concentrations, and this observation is in agreement with previous studies [200].

Higher initial extractability was observed with SDBS, which may be due to its smaller molecular size and easier nanotube exfoliation, as compared to Pluronic F-127. For the dispersion of pristine MWCNT, the open structure of their agglomerates may enable their higher extractability compared to SWCNT. Higher long-term stability may be expected with Pluronic F-127 due to the stability of the long molecules wrapped around the nanotubes' surface, remaining adsorbed for long periods of time and hindering the re-aggregation of the nanotubes. This effect was observed for aqueous suspensions of SWCNT.

The CNT functionalization reduced, in general, the extractability. This effect may be assigned to the reduction of CNT surface available for adsorption of surfactant molecules, due to the covalently bonded functional groups. However, the oxygen-containing functional groups bonded to the CNT surface may still assist the dispersion process due to an increase in nanotube hydrophilicity. Overall, it was observed that f-SWCNT presented higher extractability as compared to f-MWCNTs when using Pluronic F-127 as surfactant.

3.4 Conclusions

In this chapter of the thesis, concentrated aqueous suspensions of different types of CNT prepared using Pluronic were investigated and the influence of CNT type, concentration, functionalization and surfactant concentration was studied. The aqueous suspensions were characterized in terms of CNT agglomeration, extractability and suspension stability. It was observed that the use of optimum Pluronic conc. (1% for 0.1% CNT and 5% for 0.2% and 0.3% CNT) resulted in highly homogeneous CNT dispersion with smaller CNT agglomerates. SWCNTs (both pristine and functionalized) provided significantly higher stability in Pluronic

solution, which may be assigned to stable wrapping of long Pluronic molecules around the small diameter nanotubes. Increasing the CNT concentration enhanced extractability for pristine CNTs, but reduced the extractability of functionalized CNTs. Surface functionalization resulted in reduced extractability for both Pluronic and SDBS suspensions due to lower adsorption of surfactant on the functionalized CNT surface. Nevertheless, long term stability improved significantly with surface functionalization, in Pluronic solution. SDBS provided higher initial extractability, however the long term stability of SDBS suspensions was considerably inferior compared to the Pluronic suspensions. Suspensions containing 0.2 wt% of f-SWCNT with very less agglomerates were produced, and were observed to be stable for more than 4 years.

Chapter 4

Development of Carbon Nanotube Reinforced Cementitious Composites

This chapter is based on the article:

Shama Parveen, Sohel Rana, Raul Figueiro, and Maria Conceição Paiva. Microstructure and mechanical properties of carbon nanotube reinforced cementitious composites developed using a novel dispersion technique. *Cement and Concrete Research* 73 (2015): 215-227.

4.1 Introduction

CNTs are getting tremendous attention for developing high performance and piezoresistive cementitious composites [42,43,48,192,203,204]. Although CNTs possess exceptional physical and chemical properties, the successful transfer of these properties into composite materials is strongly dependent on the state of CNT dispersion within the matrix. Due to their strong agglomeration tendency, it is extremely challenging to obtain a homogeneous CNT dispersion, which is, however, a prerequisite for successful utilization of CNT in most of the applications including composite materials. As discussed in detail in Chapter 2 (section 2.2), the approach of dispersing CNTs directly within cement paste during mixing is not feasible, as the thickening of cement paste begins within a short period after addition of water. The mixing process using a Hobart mixer, commonly used to prepare mortar paste cannot ensure proper dispersion of CNT within cementitious matrix [77]. To overcome this problem, the strategy commonly employed for mixing CNTs with cementitious matrices is to disperse these nanomaterials first in water, followed by mixing of nanomaterial/water suspensions with cement using a conventional mixer. Various physical and chemical techniques have been tried to prepare homogeneous aqueous dispersion of CNT such as ultrasonication, mechanical stirring, using surfactants, polymers, CNT functionalization, etc. [8-18]. CNT suspensions prepared using these various techniques can be subsequently mixed with the cement mixtures to prepare cementitious composites [76, 45, 46, 93, 97, 103, 111]. Alternative ways to improve dispersion of CNT within cementitious matrices are to use chemical admixtures during mixing process [47,89] or through fabricating cementitious composites by directly growing CNTs on the cement particles [95].

Among the various carbon nanotubes, SWCNTs are considered as the best reinforcement for different matrices due to their huge surface area and exceptional mechanical properties [42]. However, these nanotubes are expensive and obtaining homogeneous dispersion is a highly challenging task due to their strong agglomeration tendency. More often, they are dispersed using a very long dispersion route involving physical and chemical treatments, which either leads to nanotube's damage or make the process unsuitable for industrial application. Due to these reasons, very few research studies have been conducted till date on utilizing SWCNTs within cementitious matrices, but only for developing piezoresistive composites [205].

As discussed in Chapter 3, Pluronic F-127 could produce homogeneous and stable CNT aqueous suspensions and provided better results as compared to commonly used surfactant SDBS.

However, no attempt has been made to use Pluronic F-127 to disperse CNT for cementitious matrices. Therefore, an in-depth investigation is necessary to apply this new dispersant for cementitious composites, in which the challenge is to disperse relatively higher CNT concentrations without affecting the hydration behaviour of cement. So, in the present chapter of the thesis, development of CNT reinforced cementitious composites using Pluronic F-127 as the dispersing agent has been discussed. The optimum concentrations of Pluronic, as determined in Chapter 3, was used to develop cementitious composites and the influence of Pluronic and CNT on the microstructure and mechanical properties of cementitious composites were thoroughly investigated. In addition, the results obtained in case of optimum samples have been compared with those obtained using SDBS.

4.2 Materials and Methods

4.2.1 Raw Materials

The details of the raw materials (CNT, Pluronic F-127 and SDBS) used in this research are provided in Chapter 3, section 3.2.1.

4.2.2 Preparation of CNT Aqueous Suspensions

To prepare CNT suspensions, defoaming agent (1/3 or 1/2 of the surfactant weight) was first added to water, followed by addition of surfactant and magnetic stirring for 10 minutes for proper mixing. To disperse both 0.1% and 0.2 wt. % of CNT in water, 3% and 5% of Pluronic F-127 was used, in order to study the influence of surfactant concentration. On the other hand, a fixed surfactant to CNT weight ratio of 4:1 was used in case of SDBS, based on previous literature [76]. The CNT suspensions were then subjected to ultrasonication for 1 hour in a bath sonicator (CREST Ultrasonicator, CP 230T) operated at 45 kHz frequency.

4.2.3 Preparation of Plain Mortar and CNT/Mortar Composites

Plain mortar and CNT/mortar samples were prepared through mixing of prepared CNT suspensions with Ordinary Portland Cement (OPC) and standardized sand in a Hobart mixer. A cement to water ratio of 0.5 was used in all samples. Samples were prepared in rectangular moulds with dimensions of 160 mm × 40 mm × 40 mm. The moulds were kept in a moist atmosphere for 24 h and then the samples were de-moulded and kept under water for 28 days to carry out hydration or setting. The samples containing SDBS were kept in the moulds for 48h, since it was not possible to de-mould them without breakage after 24h. Some selected samples

were kept in water for 42 and 56 days also in order to investigate the influence of hydration period on mechanical properties.

4.2.4 Characterization of Plain Mortar and CNT/Mortar Composites

Consistence of freshly prepared mortar pastes was evaluated using a flow table according to EN 1015-3 standard. Consistence is a measure of the fluidity and/or wetness of the fresh mortar and gives a measure of the workability of the fresh mortar paste. The diameter of mortar paste at two perpendicular directions was measured, as shown in Figure 4. 1 and reported as flow values. Compressive and flexural testing was carried out according to BS EN 196-1:1995 standard. In addition, dry bulk density of plain mortar and samples containing only surfactant (without CNT), A , was evaluated using the following equations:

$$A = \frac{M_{s,dry}}{V_s} \quad (4.1)$$

$$V_s = \frac{M_{s,sat} - M_{s,i}}{\rho_w} \quad (4.2)$$

Where $M_{s,dry}$ is the oven dry mass of specimen of hardened mortar (kg), $M_{s,sat}$ is the mass of saturated specimen of hardened mortar (kg), $M_{s,i}$ is the apparent mass of saturated specimen of hardened mortar immersed in water (kg), ρ_w is the density of water (kg/m^3) and V_s is the volume of specimen of hardened mortar (m^3).



Figure 4. 1 Determination of flow diameter.

The fracture surfaces of plain mortar and CNT/mortar samples were characterized by SEM (FEG-SEM, NOVA 200 Nano SEM, FEI) using secondary electron mode and acceleration voltage of 10kV) after coating with a thin film (30 nm) of Au-Pd in a high resolution sputter coater (208HR Cressington) in order to investigate the microstructure. To further investigate the fracture behavior, flexural tests were also performed on plain mortar and CNT/mortar samples containing a notch of 6 mm. For the purpose of fracture testing, the surface of the specimens was painted with a white synthetic paint. Next, a black paint was sprayed onto the surface of the specimens to be studied using the digital image correlation technique (DIC), in order to obtain contrast black spots on the white background. A notch of 6 mm was introduced into the samples according to Single Edge Notched Bend (SENB) configuration. The flexural testing machine and the DIC setup were started simultaneously. Loads were recorded from the testing machine, whereas the corresponding mid-span deflection and crack tip opening displacement (CTOD) were recorded using the DIC system. The fracture energy was calculated from the load-CTOD curves following JCI-S-001-2003 standard.

Plain mortar and CNT/mortar composite samples were analyzed using Fourier Transform Infrared Spectroscopy (FTIR, 4100 Jasco), in order to detect any influence of CNT on the hydration behavior of cement. For FTIR study, thin pellets were prepared through mixing of plain mortar or CNT/mortar powder with KBr and applying pressure. The same type of samples were also characterized using Thermogravimetric Analyzer (TGA, Perkin Elmer) in nitrogen atmosphere at heating rate of 10°C/min up to 900°C. Derivative thermogravimetry (DTG) curves for these specimens were studied to obtain quantitative estimation of different products formed due to hydration such as C-S-H, Ca(OH)₂, CaCO₃, etc.

4.3 Results and Discussion

4.3.1 Consistence of Mortar Paste

Flow values of plain mortar, mortar containing Pluronic and defoamer and different types of CNT are listed in Table 4. 1. It can be noticed that all samples showed similar consistence to that of plain mortar samples, indicating that addition of CNT, surfactant or defoamer did not have much influence on the workability of mortar.

Table 4. 1 Consistence of Plain Mortar and CNT/Mortar Pastes

Samples*	Pluronic %	Defoamer: Pluronic	Flow values (mm)
Plain Mortar	-	-	189,187
Mortar 5%P1/3D	5	1:3	182, 183
Mortar 5%P1/2D	5	1:2	194, 190
0.1 %MWCNT5%P1/3D	5	1:3	185,183
0.1 %MWCNT5%P1/2D	5	1:2	183, 177
0.1 %MWCNT3%P1/2D	3	1:2	183, 184
0.08% MWCNT3%P1/2D	3	1:2	190, 185
0.1% SWCNT5%P1/2D	5	1:2	176, 175
0.1 %SWCNT3%P1/2D	3	1:2	177, 179
0.08 %SWCNT3%P1/2D	3	1:2	177,176
0.1 %f-SWCNT5%P1/2D	5	1:2	175,172
0.1% f-SWCNT3%P1/2D	3	1:2	192,187
0.08% f-SWCNT3%P1/2D	3	1:2	193,191
0.1% f-MWCNT5%P1/2D	5	1:2	181,182
0.1% f-MWCNT3%P1/2D	3	1:2	190,191
0.08% f-MWCNT3%P1/2D	3	1:2	186,185

*P and D denote Pluronic and defoaming agent, respectively

4.3.2 Effect of Pluronic on Dry Bulk Density

Table 4. 2 lists the dry bulk density of plain mortar and mortar containing 5% Pluronic and defoamer. It can be observed that density of mortar slightly increased due to addition of Pluronic F-127. This indicated lower porosity and formation of denser microstructure in presence of this surfactant [206]. It can be observed from Figure 3.2 that the chemical structure of Pluronic F-127 contains PEO side chains similar to commonly used polycarboxylate super plasticizers. PEO side chains are reported to be the main chemical components of these superplasticizers responsible for the dispersion of cement particles and the fluidity of mortar [206]. The presence of similar PEO side chains in the structure of Pluronic F-127 in the present research is probably the main factor that improved the cement particle dispersion and microstructure. This observation has been made for the first time in this PhD work.

Table 4. 2 Dry Bulk Density of Plain Mortar with and without Pluronic

Samples	Dry bulk density (Kg/m ³)
Plain mortar	2012.4
Mortar with 5% Pluronic and defoaming agent	2020.8

4.3.3 Mechanical Properties

4.3.3.1 Effect of Surfactant and CNT Type on Flexural Properties

Flexural stress-strain curves of plain mortar and CNT/mortar samples after setting for a period of 28 days are shown in Figure 4. 2.

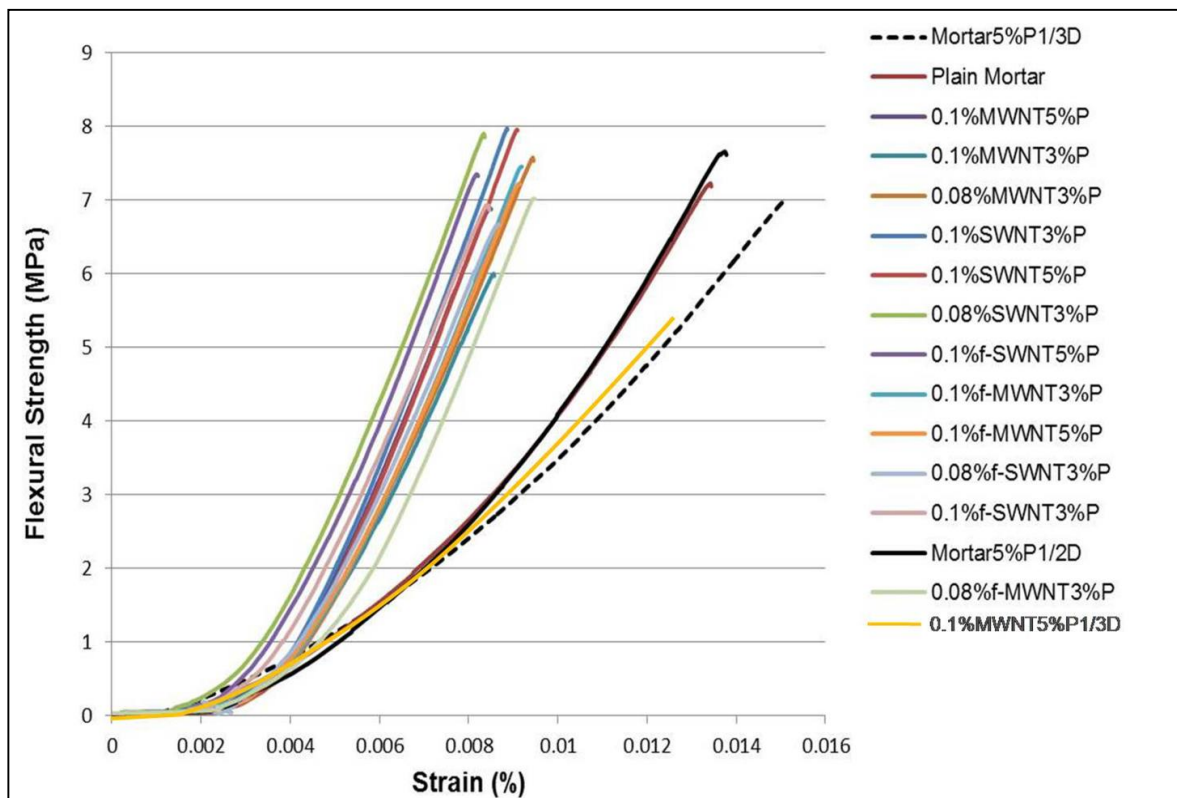


Figure 4. 2 Flexural stress-strain curves of plain mortar and CNT/cement composites.

It is very interesting to note that addition of Pluronic (containing ½ defoaming agent of Pluronic weight) within mortar led to improvement of flexural strength and stiffness. This was attributed to the formation of denser microstructure formed in presence of Pluronic. However, it was also

evident that addition of Pluronic with 1/3 defoaming agent led to significant reduction in both flexural strength and stiffness. Therefore, an optimized quantity of defoamer was extremely important to suppress the formation of froth due to use of Pluronic. If generation of froth is not suppressed, its presence leads to increase in porosity of mortar samples resulting in lower mechanical properties. It can be also clearly observed from Figure 4.2 that flexural stress-strain curves for CNT reinforced samples were much steeper as compared to the stress-strain curves of plain mortar samples. This indicated significantly higher flexural modulus of CNT/cement composites as compared to plain mortar. It is also clear that some of the CNT/mortar samples presented better flexural strength as compared to plain mortar, while flexural strength of some samples was inferior to plain mortar's strength. Flexural modulus of plain mortar and CNT/mortar composites are provided in Table 4. 3.

Table 4. 3 Flexural Properties of Plain Mortar and CNT/Mortar Samples

Samples	Flexural Modulus (GPa)	% Improvement	Flexural Strength (MPa)	% Improvement
Plain Mortar	15.0 ± 0.7*	-	7.15 ± 0.25*	-
Mortar 5%P 1/3D	10.9 ± 0.5	- 27	6.96 ± 0.07	-2.7
Mortar 5% P 1/2D	17.3 ± 0.5	15.3	7.41 ± 0.24	3.6
0.1%MWCNT5%P1/3D	10.2 ± 0.8	-32	5.21 ± 0.14	-27.1
0.1%MWCNT5%P1/2D	23.8 ± 0.7	58.7	6.35 ± 0.49	-11. 2
0.1%f-MWCNT5%P1/2D	22.5 ± 0.9	50.0	7.09 ± 0.21	-0.8
0.1%MWCNT3%P1/2D	21.3 ± 0.3	42.0	6.00 ± 0.35	-16.0
0.1%f-MWCNT3%P1/2D	23.8 ± 0.8	58.7	7.09 ± 0.37	-0.8
0.08% MWCNT 3%P1/2D	23.5 ± 0.5	56.7	7.37 ± 0.28	3.1
0.08% f-MWCNT 3%P1/2D	23.1 ± 0.8	54.1	6.71 ± 0.29	-6.1
0.1%SWCNT5%P1/2D	24.9 ± 0.6	66.0	7.59 ± 0.30	6.2
0.1%f-SWCNT5%P1/2D	25.8 ± 0.7	72.0	7.09 ± 0.21	-0.8
0.1%SWCNT3%P	24.5 0.9	63.3	7.63 ± 0.36	6.7
0.1%f-SWCNT3%P	22.3 ± 0.4	48.7	6.69 ± 0.25	-6.4
0.08% SWCNT 3%P	24.3 ± 0.9	62.0	7.55 ± 0.29	5.6
0.08% f-SWCNT 3% P	22.9 ± 0.7	52.7	6.42 ± 0.23	-10.2

* ± values are the 95% confidence intervals calculated from the modulus and strength data.

It can be observed that addition of Pluronic (with optimum defoamer ratio) within mortar led to improvement in flexural modulus by about 15%. Further enhancement of flexural modulus was noticed upon reinforcement with CNTs. The improvement in modulus was quite high reaching up to 72% in case of SWCNT reinforced samples. In general, flexural modulus improved more through reinforcement with SWCNTs as compared to MWCNTs due to the better mechanical properties of SWCNTs, unless they were dispersed using lower concentration of Pluronic. Figure 4. 3 shows the comparison between the experimental values of flexural modulus of selected SWCNT and MWCNT reinforced samples (0.08%SWCNT3%P, 0.1%SWCNT5%P, 0.08% MWCNT 3%P, 0.1%MWCNT5%P) and predicted values calculated using the properties of CNT and mortar applying rule of mixtures [76]. It can be noticed that the experimental values were always higher than the predicted modulus indicating that there were other factors besides reinforcing effect (such as improvement of microstructure), which has also played a vital role in enhancing the modulus of cementitious composites.

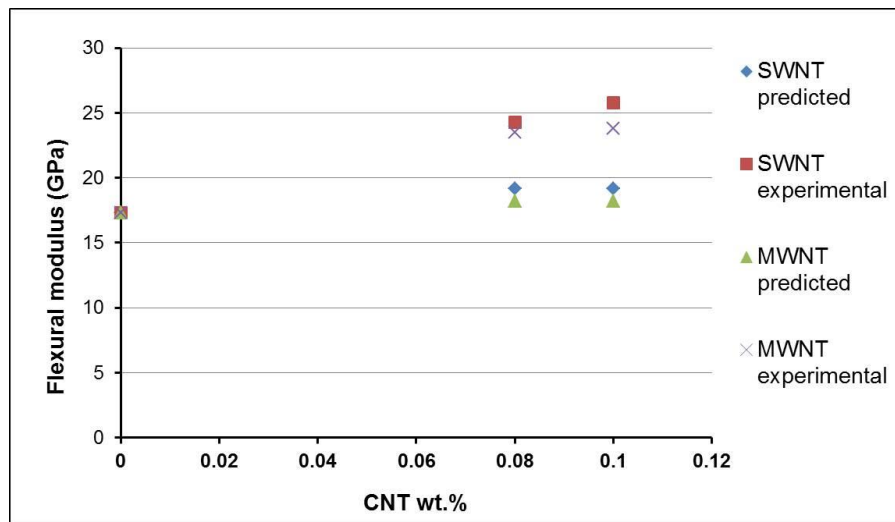


Figure 4. 3 Comparison between predicted and experimental values of flexural modulus.

Flexural strength of plain mortar and CNT reinforced mortar samples are listed in Table 4.3. It is clear that use of Pluronic with non-optimized defoamer concentration resulted in deterioration of flexural strength. This case was even worse when CNTs were dispersed using Pluronic with non-optimized defoamer concentration (0.1% MWCNT 5%P 1/3D), leading to significant deterioration of flexural strength. However, similar to flexural modulus, flexural strength also improved to some extent using Pluronic in combination with defoaming agent at optimized concentration. As mentioned previously, this reflected better microstructure and lower porosity

of mortar containing Pluronic. Among the various nanotubes, it can be observed that flexural strength was higher in case of SWCNTs as compared to MWCNTs. Highest improvement of ~7% was achieved in case of SWCNTs dispersed using 3% Pluronic. On the other hand, dispersion of MWCNTs led to deterioration of flexural strength, except lower concentration (0.08%) of MWCNT which resulted in slight improvement of flexural strength (3.1%). Further, functionalization of MWCNT helped to improve the flexural strength of MWCNT/mortar composites to the level of unreinforced cementitious composites, as can be commented from the mechanical properties of 0.1% f-MWCNT5%P and 0.1% f-MWCNT 3%P. Better mechanical properties at lower concentration and with functionalized MWCNTs indicates that some CNT clusters were still present at higher concentration dispersion of non-functionalized MWCNTs deteriorating the mechanical properties. On the contrary, although some agglomerates could also be present in case of SWCNTs, their size was too small (due to small dimensions of SWCNTs) to significantly influence the mechanical properties. In this case, use of higher CNT concentration led to slightly higher flexural strength and unlike MWCNTs, functionalization resulted in reduction of flexural strength. Deterioration of mechanical performance of CNT/cement composites using functionalized CNTs has been reported by other researchers also [103] and may be attributed to the retention of water by functional groups impairing the cement hydration process. For both SWCNTs and MWCNTs, the influence of chosen surfactant concentration (3% and 5%) on the flexural strength was not observed to be so significant.

4.3.3.2 Effect of Surfactant and CNT Type on Compressive Properties

Compressive strength of plain mortar and CNT/mortar samples are listed in Table 4. 4. Compressive strength was also influenced by different parameters similar to flexural strength. Highest compressive strength was also achieved in case of 0.1% SWCNTs dispersed with 3% Pluronic. The maximum improvement of compressive strength was 19.1%. On the contrary, addition of MWCNTs to mortar led to deterioration of compressive strength. However, functionalization showed positive influence on compressive strength in case of MWCNTs, whereas an opposite trend was noticed in case of SWCNTs similar to flexural strength.

4.3.3.3 Effect of Hydration Period on Mechanical Properties

Flexural strength

Flexural strength of plain mortar and CNT/mortar samples at different hydration periods (28, 42 and 56 days) are listed in Table 4. 5 and graphically presented in Figure 4. 4.

Table 4. 4 Compressive Strength of Plain Mortar and CNT/Mortar Composites

Samples	Compressive strength (MPa)	Improvement of compressive strength (%)
Plain Mortar	35.6 ± 1.6*	-
Mortar + 5% P+ 1/3 D	32.7 ± 1.3	-8.1
Mortar + 5% P + 1/2D	35.7 ± 1.0	0.2
0.1% MWCNT 5%P1/3D	20.4 ± 0.8	-42.7
0.1% MWCNT5%P	30.1 ± 2.0	-15.5
0.1%MWCNT3%P	32.4 ± 1.1	-8.9
0.08% MWCNT3%P	35.0 ± 1.4	-1.7
0.1% f-MWCNT5%P	32.0 ± 0.9	-10.1
0.1% f-MWCNT3%P	35.4 ± 0.7	-0.6
0.1% SWCNT3%P	42.4 ± 1.5	19.1
0.1% SWCNT5%P	39.1 ± 1.5	9.8
0.08% SWCNT3%P	41.1 ± 1.0	15.4
0.1% f-SWCNT 5%P	36.0 ± 1.7	1.1
0.1% f-SWCNT3%P	32.4 ± 1.5	-8.9
08% f-SWCNT3%P	31.1 ± 2.1	-12.6

* ± values are the 95% confidence intervals calculated from the strength data.

Table 4. 5 Flexural Strength (MPa) of Plain Mortar and CNT/mortar samples at 28, 42 and 56 Days of Hydration

Samples	28 days	42 days	56 days
Plain Mortar	7.15 ± 0.13*	6.54 ± 0.56*	7.29 ± 0.13*
Mortar + Pluronic	7.41 ± 0.24	7.12 ± 0.48	7.15 ± 0.15
Mortar +SDBS	6.64 ± 0.53	6.95 ± 0.34	6.68 ± 0.34
Mortar + 0.08% SWCNT+ Pluronic	7.55 ± 0.45	5.71 ± 0.44	8.09 ± 0.63
Mortar+ 0.08% f-SWCNT+ Pluronic	6.42 ± 0.28	8.01 ± 0.61	8.37 ± 0.45
Mortar + 0.08% SWCNT+SDBS	7.56 ± 0.42	7.74 ± 0.34	7.97 ± 0.21
Mortar + 0.08% f-SWCNT+SDBS	6.88 ± 0.66	7.47 ± 0.66	7.40 ± 0.78

* ± values are the 95% confidence intervals calculated from the strength data.

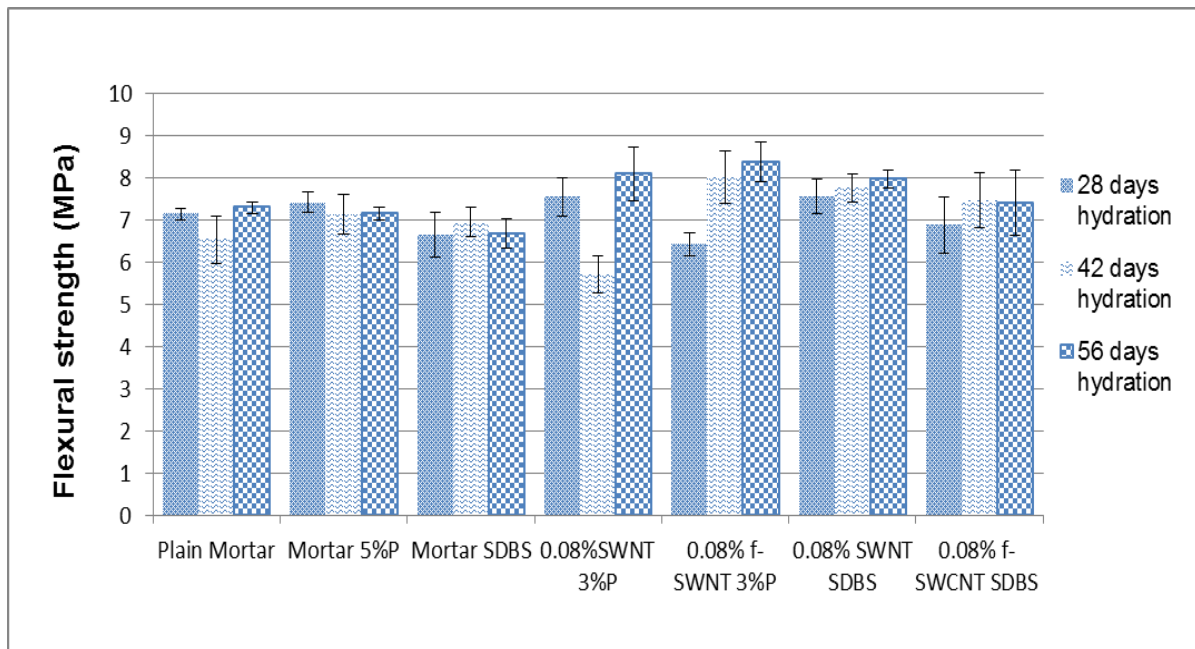


Figure 4. 4 Comparison of flexural strength of plain mortar and CNT/mortar samples at different periods of hydration.

For this study, only SWCNTs at lower concentration (0.08 %) dispersed using 3% Pluronic have been used, as these samples showed better flexural and compressive properties as compared to higher nanotube concentration samples. In addition, flexural strength of mortar/CNT samples prepared using SDBS at optimum concentration have been measured for comparison. It can be noticed that the difference in flexural strength at different hydration periods was not so significant or did not show clear trend, except for the samples prepared using functionalized CNTs. It was noteworthy that mortar/CNT samples containing functionalized SWCNTs showed gradual increase in flexural strength with the hydration time. This was true for both Pluronic and SDBS, although the change in flexural strength with hydration period was more prominent in case of Pluronic. The highest improvement in flexural strength (17%) was achieved with Pluronic for hydration period of 56 days.

Compressive Strength

Compressive strength of plain mortar and CNT/mortar samples at different hydration periods (28, 42 and 56 days) are listed in Table 4. 6 and graphically presented in Figure 4. 5.

Table 4. 6 Compressive Strength (MPa) of Mortar and CNT/Mortar Samples at 28, 42 and 56 Days of Hydration

Samples	28 Days	42 Days	56 Days
Plain Mortar	35.6 ± 1.1*	39.7 ± 1.4*	38.8 ± 2.0*
Mortar + Pluronic	34.4 ± 0.8	40.5 ± 0.8	36.1 ± 1.8
Mortar +SDBS	35.6 ± 1.0	36.7 ± 1.7	36.1 ± 0.4
Mortar + 0.08% SWCNT+ Pluronic	41.0 ± 0.8	39.6 ± 0.9	40.1 ± 0.7
Mortar+ 0.08% f-SWCNT+ Pluronic	32.9 ± 1.3	36.5 ± 0.7	43.8 ± 1.4
Mortar + 0.08% SWCNT+SDBS	39.9 ± 0.9	34.2 ± 1.1	38.0 ± 1.5
Mortar + 0.08% f-SWCNT+SDBS	36.0 ± 0.9	34.4 ± 1.7	35.9 ± 0.6

* ± values are the 95% confidence intervals calculated from the strength data.

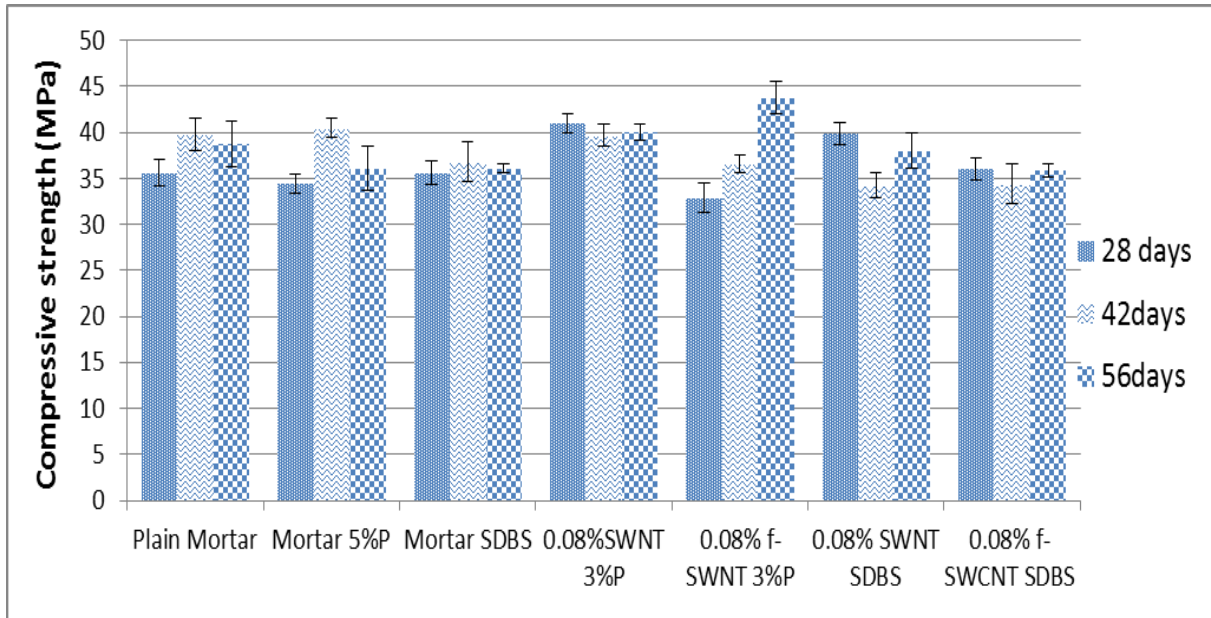


Figure 4. 5 Comparison of compressive strength of plain mortar and CNT/mortar samples at different periods of hydration.

Similar to flexural strength, the difference between compressive strength at different hydration periods was not significant except for the samples prepared using functionalized CNTs with Pluronic. Similar to flexural strength, compressive strength of functionalized SWCNT/mortar samples also showed sharp increase with hydration period and an improvement of 23% was achieved after 56 days of hydration. The reason for the increase in mechanical properties with hydration period in case of functionalized CNT was probably the release of water bound by CNT functional groups with time, resulting in slow progress in the cement hydration process.

Moreover, this fact was more evident in case of Pluronic, may be due to retention of water also by Pluronic molecules (through hydrogen bonding) which released water slowly as the hydration process proceeded.

Cement hydration is a very complex process involving severe reactions and is not fully understood till now. Cement hydration rate changes with the presence of foreign ions, clinkers and the additives present in cement during hydration process. C-S-H gel formed during hydration of cement is an amorphous two component solid solution consists of hexagonal crystals of $\text{Ca}(\text{OH})_2$ and calcium silicate hydrate. FT-IR spectra (Figure 4. 6) exhibited characteristic difference in the hydration behaviour of plain mortar and SWCNT reinforced mortar samples.

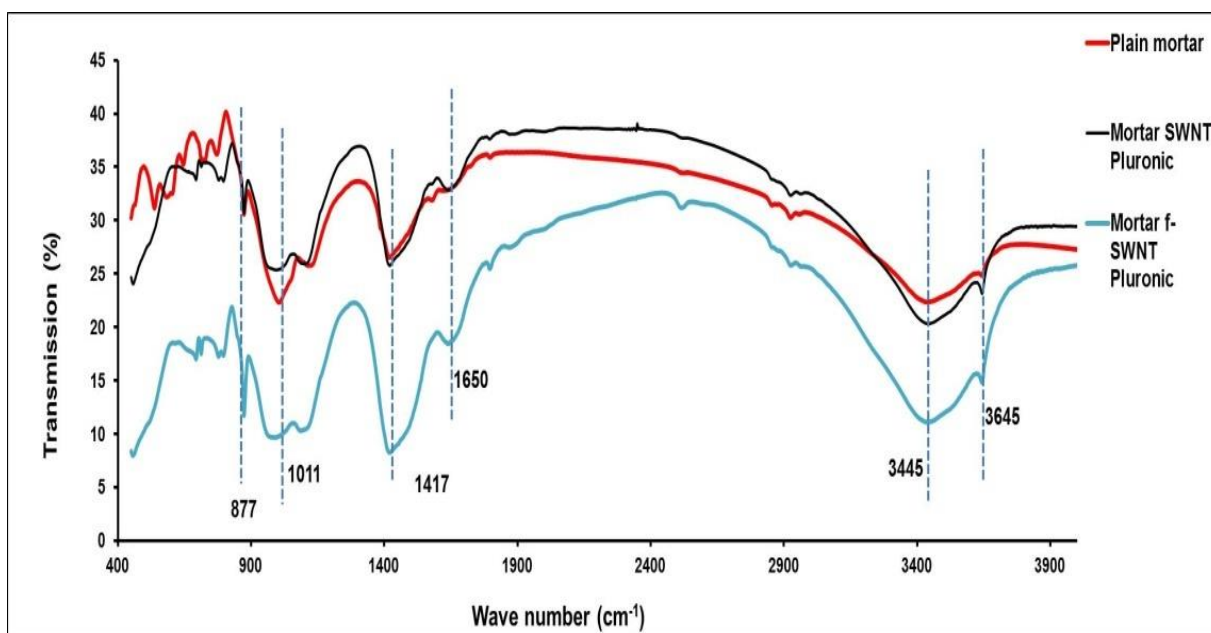


Figure 4. 6 FTIR curves of plain mortar and CNT/mortar samples.

FT-IR peak at 3645cm^{-1} corresponds to stretching vibration of O-H of $\text{Ca}(\text{OH})_2$ which was formed along with calcium silicate hydrate during cement hydration. In SWCNT reinforced cementitious composites, this peak was slightly enhanced showing marginal increase in the formation of crystalline $\text{Ca}(\text{OH})_2$. Therefore, the presence of CNT did not retard the hydration of cement. FT-IR peak at 1650cm^{-1} corresponds to the bending vibration of irregularly bound water. As the hydration proceeds, this peak becomes more prominent due to formation of C-S-H phase which holds the bound water. In case of CNT reinforced cementitious composites, the peak of bound water was more intense, especially in case of functionalized CNT reinforced

samples, probably due to retention of water by Pluronic and also by $-\text{COO}-$ groups in functionalized CNTs. Peak at 1417 cm^{-1} corresponds to the formation of asymmetric stretching vibration of CO_3^{2-} , which was formed due to absorption of atmospheric CO_2 during air hydration of samples. In case of CNT reinforced samples this peak was more prominent and intense, probably due to presence of more $\text{Ca}(\text{OH})_2$ forming CaCO_3 . The region between 970 cm^{-1} to 1100 cm^{-1} corresponds to the stretching vibration of polymerized silica during cement hydration. In case of plain cement mortar this region was stronger showing formation of more calcium silicate hydrate in plain cement mortar as compared to CNT reinforced samples.

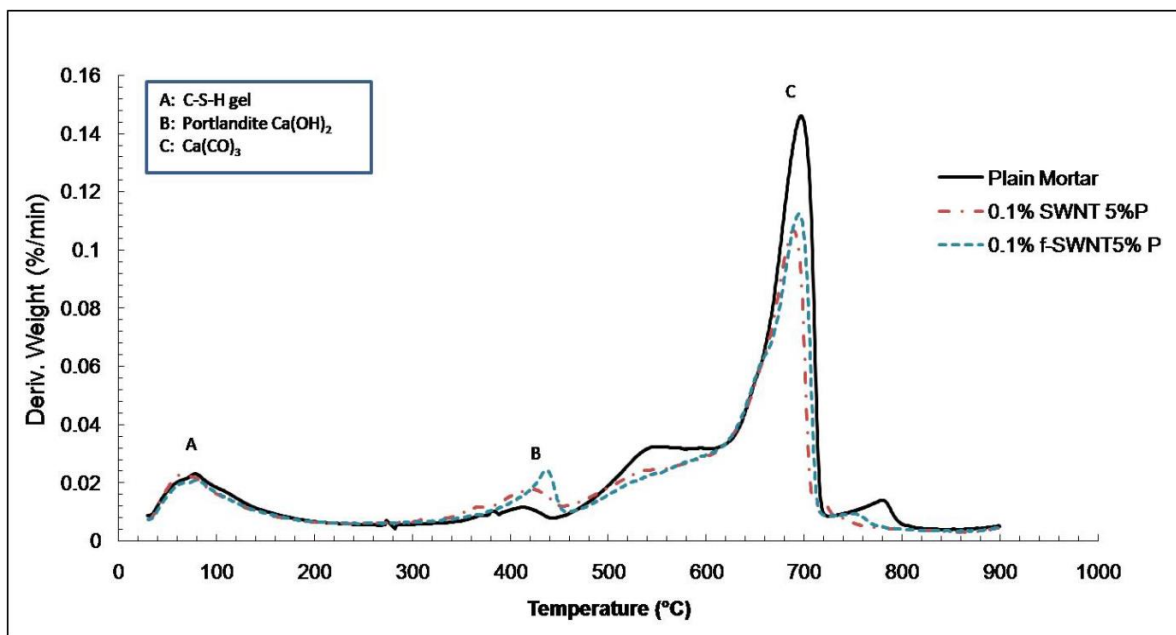


Figure 4. 7 DTG curves of plain mortar and CNT/mortar composites.

Similar comments can also be made from the DTG curves of plain mortar and CNT/mortar specimens, as presented in Figure 4. 7. The peak A represents the quantity of loss of water from C-S-H gel layers [103]. Both in plain mortar and CNT reinforced mortar samples, the height of peak A was nearly same confirming that CNT did not reduce the quantity of C-S-H phase or strength determining phase of cement, unlike the observations made in Ref. [103] which reported lower quantity of C-S-H formation in case of MWNT reinforced cement specimens. Peak B in the DTG curves was attributed to the decomposition of $\text{Ca}(\text{OH})_2$ [103]. Higher height of peak B in case of CNT reinforced composites demonstrated the formation of higher amount of $\text{Ca}(\text{OH})_2$, as also observed from FTIR analysis. Although peak C represents the quantity of calcium carbonate present in all samples, its amount can not be quantified reliably from DTG, as it strongly depends on storage conditions (i.e. availability of atmospheric CO_2 for formation of

CaCO₃ from Ca(OH)₂) as well as due to overlapping of peaks from mass loss of structural OH groups of C-S-H phase around this temperature range [207].

4.3.4 Microstructure

Scanning electron micrographs of fracture surface of plain cement and mortar/CNT samples are shown in Figure 4. 8. Presence of CNT all over the fracture surface (Figure 4. 8b and Figure 4. 8c) was identified indicating their homogeneous distribution within the cementitious matrix. It was also observed that CNTs were very tightly inserted between the hydration products of cement (C-S-H phases), as shown in Figure 4. 8(d).

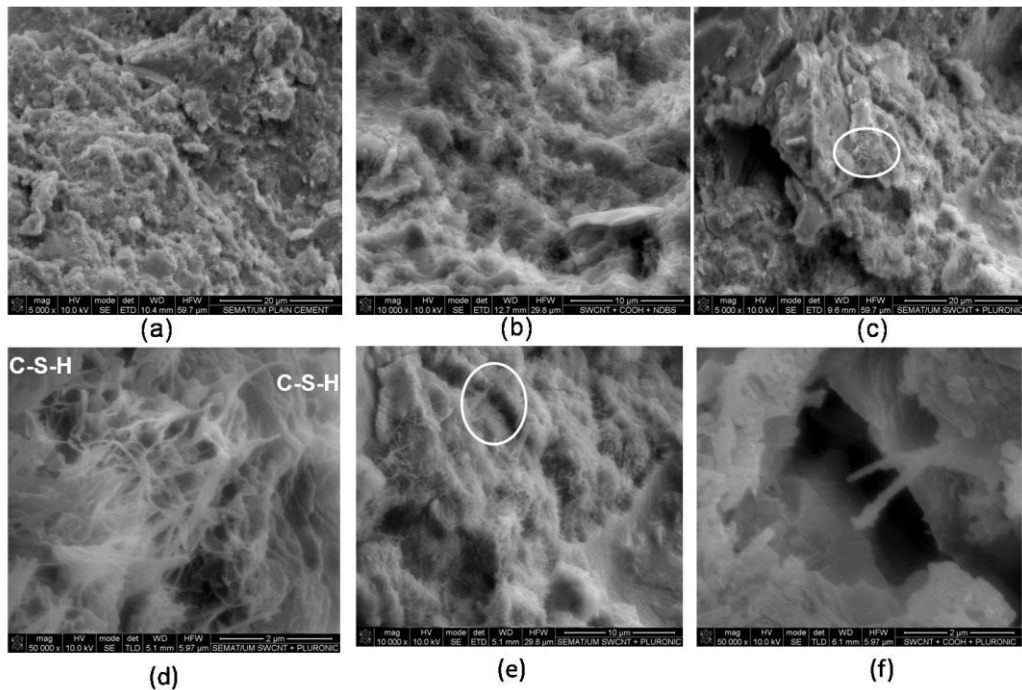


Figure 4. 8 Fracture surface of plain mortar (a) and CNT/mortar samples (b, c, d, e, f) at different magnifications.

It can be noticed that CNTs were well wetted by cement forming a dense reinforcing network. Additionally, the presence of CNTs within the cracks of cementitious matrix should be noted, as indicated in Figure 4. 8(e). At higher magnification it was possible to identify CNTs bridging the micro cracks within cementitious matrix, as shown in Figure 4. 8(f). Crack bridging mechanism offered by CNTs is possibly the primary reason for better mechanical strength of CNT reinforced cementitious composites.

4.3.5 Fracture Behaviour

To characterize the fracture behaviour, the load vs. crack tip opening displacement curves were obtained, and the fracture energy was calculated for the composites prepared. Typical load-CTOD curves obtained for plain mortar and SWCNT-mortar composites are presented in Figure 4. 9a. The overall results for the fracture energy of all the materials tested are presented in Figure 4. 9b.

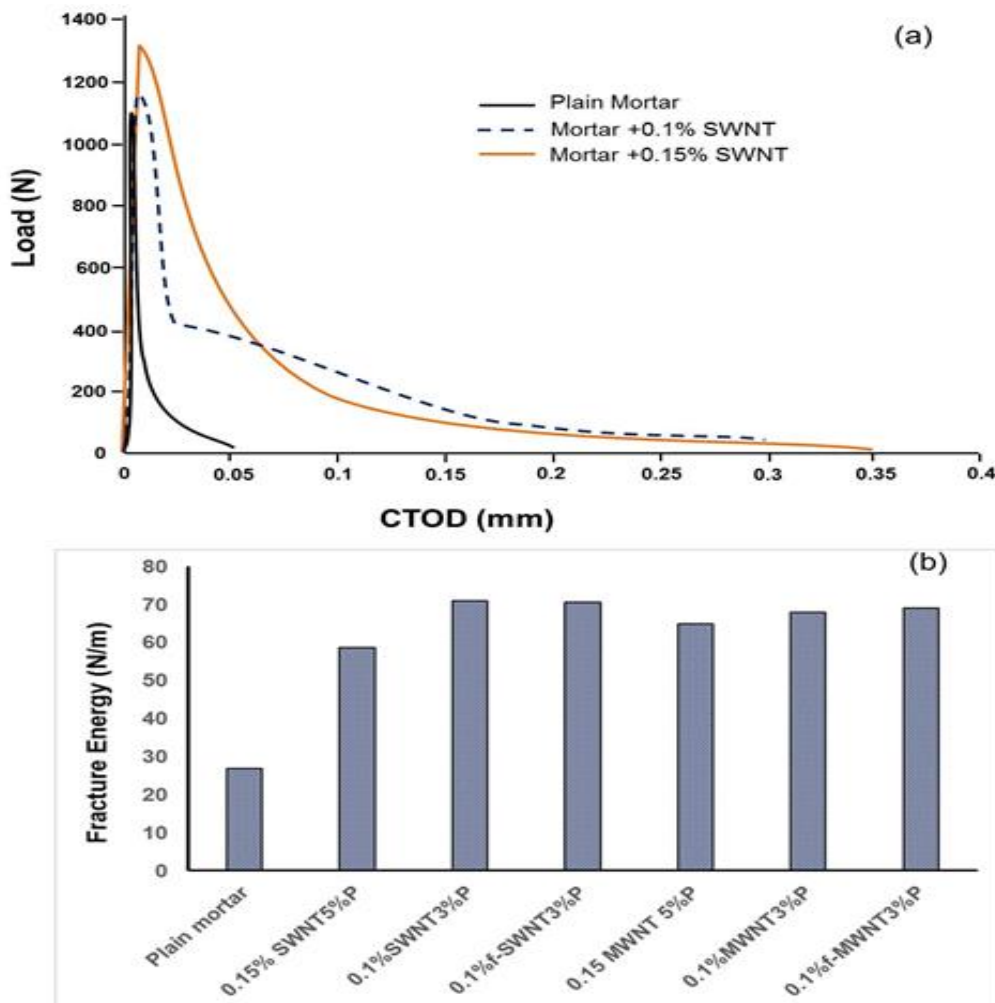


Figure 4. 9 Load-CTOD curves (a) and fracture energy (b) of plain cement mortar and CNT/cement composites.

It was observed that the plain mortar showed brittle failure behaviour and sharp drop of load after the specimen fracture. The fracture behaviour was considerably modified by the addition of either SWCNT or MWCNT. The CNT/cement composites showed post-peak fracture behaviour, sustaining a substantial amount of load after the peak and maintaining the structural integrity. Thus, the nanotubes were able to bridge the cracks and sustain load after fracture initiation in the

composites. The fracture energy of plain mortar and CNT/cement composites presented in Figure 4.9b shows that the incorporation of 0.1 wt% CNT increased the fracture energy of cement mortar up to 164% and considerably improved its ductility. The improvement observed may be attributed to the homogeneous dispersion of CNT within the cementitious matrix, resulting from the addition of stable surfactant-assisted suspensions of well dispersed SWCNT and MWCNT.

4.4 Comparison with Previous Studies

Table 4. 7 lists the main findings of previous studies carried out on CNT/reinforced cementitious composites prepared using alternative surfactants and compared with the results of present thesis. It is clear from Table 4.7 that these studies were mainly carried out using MWCNTs since it is relatively easier to disperse MWCNTs using conventional dispersion routes and also due to their lower cost. The extent of improvement in mechanical properties was also different in different studies depending on the dispersion route, type and concentration of CNTs and other parameters. It is also noteworthy that in some cases dispersion of CNT (more frequently functionalized CNTs) in cementitious composites resulted in considerable deterioration in mechanical properties, as also observed in this research. In the present study, Pluronic has been used for the first time to disperse SWCNTs within cementitious composites. It was possible to disperse both MWCNTs and SWCNTs using a short dispersion route (only 1 hour), but achieving very good dispersions in terms of both homogeneity and stability. This novel dispersion route provided enhanced mechanical performance for composites with SWCNT and lower improvement for MWCNT composites. Nevertheless, the later presented improved elastic modulus and fracture energy. With SWCNTs, the reinforced composites showed significant improvement in terms of elastic modulus, flexural and compressive strengths, microstructure and also ductility and fracture behaviour. The optimized samples developed within the present research showed much better mechanical properties as compared to those prepared using SDBS at optimum concentrations. Another important advantage of the dispersion route investigated in this research is the non-toxicity and bio-compatibility of Pluronic and its ability to prevent CNT agglomeration (which in turn reduces its toxicity) for very long time period. As a result, the developed dispersion route may prove to be more suitable for practical applications.

Table 4. 7 Comparison of Present Results with Those of CNT/Cement Composites Prepared Using Other Dispersion Routes

Reference	Dispersion technique	Improvement in mechanical properties
48	CNTs were directly mixed with mortar paste using a rotary mixer	Flexural strength of mortar improved by 25% using 0.5% MWCNT
46	Ultrasonication in presence of polymers	Flexural strength of cement paste improved by 10% using 0.042% MWCNT
76	Ultrasonication with surfactant	Flexural strength of cement improved by 25% using 0.08% MWCNTs
111	Ultrasonication of CNT/water suspension for 10 mins	With 0.5% MWCNT and fly ash: decrease in compressive strength by 2% With 1% MWCNT and fly ash: decrease in compressive strength by 1.4%
103	Using acetone and ultrasonication for 4 hours	With 0.5% pristine and annealed MWCNT, compressive strength improved by 11% and 17%. With functionalized MWCNT compressive strength reduced by 86%
208	Ultrasonication of CNT/water suspension for 5 mins	Compressive strength of Portland cement improved by 17% using 1% MWCNTs
209	Direct mixing	Compressive strength of white Portland cement improved by 10% using 1% MWCNTs.
Present work	Ultrasonication in presence of Pluronic F-127 for 1 hour	Flexural modulus improved up to 72% with 0.1% f-SWCNT and improved strongly with all CNT types. Flexural and compressive strengths improved up to 7% and 19% with SWCNTs after 28 days of hydration and 17% and 23% after 56 days. Fracture energy improved significantly with all CNT types with maximum increase up to 164% with SWCNTs. Improvement in mechanical properties of optimum samples was significantly higher than those prepared with SDBS

4.5 Conclusions

Following conclusions can be drawn from the present chapter:

- (1) Use of Pluronic along with optimized concentration of defoaming agent led to improvement of cement microstructure, density and mechanical properties. This was probably attributed to the presence of PEO side chains in the structure of Pluronic which helped in proper dispersion of cement particles improving the microstructure of cementitious composites.
- (2) All CNT reinforced cement composites showed significantly higher flexural modulus as compared to plain mortar. Among various nanotubes, pristine SWCNTs showed maximum improvement in flexural modulus (72%), flexural strength (7%) and compressive strength (19%) after 28 days of hydration. On the contrary, although MWCNTs led to significant enhancement of stiffness, their incorporation led to slight deterioration in mechanical strength. Functionalized CNTs showed gradual increase in flexural and compressive strengths with hydration period reaching up to 17% and 23% after 56 days. The improvement in mechanical properties using Pluronic was much higher as compared to the improvements using SDBS at optimized concentration. The fracture surface of CNT/mortar samples showed the evidence of crack bridging mechanism which was responsible for higher strength and fracture energy.
- (3) Cementitious composites prepared using CNT suspensions showed post-peak fracture behaviour and an increase in fracture energy up to 164% as compared to plain cement mortar.

Chapter 5

Development of Micro Crystalline Cellulose Reinforced Cementitious Composites

This chapter is based on the article:

Shama Parveen, Sohel Rana, Raul Figueiro, and Maria Conceição Paiva. A Novel Approach of Developing Micro Crystalline Cellulose Reinforced Cementitious Composites with Enhanced Microstructure and Mechanical Performance. Cement and Concrete Composites. Under Review.

5.1 Introduction

Recently, there is a growing interest on different bio-based technical fibres such as flax, jute, hemp, sisal, etc., for reinforcing polymeric as well as cementitious composites due to concern about environment and sustainability. Due to the same reason, the use of natural nano and micro reinforcements such as nanocellulose (e.g. NFC, NCC and BNC) and MCC are getting considerable attention in different industrial applications [119-121, 210]. MCC possesses excellent mechanical properties (axial elastic modulus 120-200 GPa, tensile strength 7.5 GPa) and already finds applications in food, cosmetics, medical and hygiene products, emulsions, etc [119-121]. Both nanocellulose and MCC have been extensively used as reinforcements of polymeric matrices [32, 211-213]. However, they have been rarely studied as reinforcements of cementitious composites for construction applications. Very recently, well dispersed nanocellulose (as received from the acid hydrolysis) was found to improve the flexural strength of cement by 30% [52]. BNC has also been used as fibre coating in bagasse fibre reinforced cement composites resulting in stronger fibre/cement interface and reduced fibre mineralization [214]. Similarly, MCC was also used for reinforcement of cementitious materials; however, no improvement in mechanical performance was achieved [51]. In the above work, MCC was saturated with water and mixed with cement without any dispersion step and therefore, non-homogeneous dispersion of MCC could be the main reason behind its ineffectiveness in enhancing mechanical performance. Similar to other nano and micro materials, dispersion of MCC is also believed to be highly important with respect to the mechanical properties, as MCC agglomeration can significantly reduce its reinforcing efficiency and leads to defects within cementitious materials. Therefore, to ensure homogeneous dispersion of MCC within cementitious matrix, this PhD work made the first attempt of using a surfactant (Pluronic F-127) to fabricate MCC reinforced cementitious composites.

Surfactants have been extensively used to disperse CNTs in polymers and cement [45, 46, 189, 215]. Pluronic F-127 is a biocompatible surfactant which has been widely used for dispersing CNTs [11,12]. Pluronic F-127 was found highly effective to homogeneously disperse CNTs within cementitious composites [199], as discussed in Chapter 3. In addition to superior ability of Pluronic F-127 to disperse CNTs, the possibility of obtaining better microstructure of cementitious composites using Pluronic was also observed in Chapter 4. Based on this positive finding, Pluronic F-127 has also been used in this research work to prepare aqueous MCC suspensions for fabricating cementitious composites. Additionally, CMC, which is frequently

used as stabilizing agent for MCC in industrial applications [216], has been used in order to compare its performance with Pluronic F-127. The effect of different conditions (e.g. use of superplasticizer, higher water ratio, magnetic stirring/ultrasonication and high temperature) on flexural and compressive performance of cementitious composites was investigated in order to find the optimum conditions to maximize mechanical performance.

5.2 Materials and Methods

5.2.1 Raw Materials

MCC, Pluronic F-127 and CMC, which were used to disperse MCC in water, were supplied by Sigma Aldrich (Portugal). The superplasticizer used for the fabrication of cementitious composites was MasterGlenium SKY 526, supplied by BASF. Table 5. 1 lists the important properties of these materials.

Table 5. 1 Properties of Raw Materials

Materials	Properties
MCC	Particle size ~50 μm
Pluronic F-127	Average molecular weight: 12,500, non-ionic surfactant, critical micelle conc.: 950-1000 ppm
CMC	Average molecular weight: 90,000, stabilizer
MasterGlenium SKY 526	Superplasticizer, polycarboxylic ether type

5.2.2. Preparation of Aqueous MCC Suspensions

The aqueous suspensions of MCC/Pluronic or CMC were prepared by first mixing MCC in water by the help of magnetic stirring, for 10 mins. The aqueous MCC suspensions were then stored for 2 days for soaking and subsequently, the surfactant Pluronic F-127 or stabilizer CMC was added through magnetic stirring for 5 mins. The MCC suspensions were then kept in a bath ultrasonicator (CREST Ultrasonicator, CP 230T) operated at 45 kHz frequency and 80W power for 15 mins. For a few suspensions, ultrasonication was avoided and only magnetic stirring (MS) was used for 30 mins, instead of ultrasonication. Also, for some suspensions an additional MS step of 30 mins at high temperature ($^{\circ}60\text{ C}$) was used after ultrasonication. The objective behind using these dispersion conditions was to study their influence on the mechanical performance of cementitious composites. For the suspensions prepared using Pluronic, a defoamer, tri butyl

phosphate ($\frac{1}{2}$ of surfactant weight) was used to suppress the formation of foam. For preparation of aqueous MCC suspensions, a CMC: MCC weight ratio of 1:5 has been used as recommended for commercial applications [216] and Pluronic was also used in the same ratio for comparison purpose.

5.2.3. Characterization of Aqueous MCC Suspensions through UV-Vis Spectroscopy

MCC aqueous suspensions prepared with Pluronic and CMC using ultrasonication were characterized by UV-Vis spectroscopy to measure the concentration of MCC suspended in the solution. The suspensions showing lower absorption indicate lower MCC concentration in the solution due to lower stability and sedimentation. Suspensions prepared by varying MCC concentration (0.4 to 1.5 wt. %) were studied by UV-Vis spectroscopy, in order to study the stability of the suspensions at different MCC concentrations. For each measurement, same concentrations of Pluronic/CMC solution (without MCC) were used as blank to eliminate the peaks due to Pluronic/CMC.

5.2.4. Characterization of Aqueous MCC Suspensions through Optical Microscopy

MCC suspensions prepared with Pluronic and CMC using ultrasonication were characterized for dispersion homogeneity and agglomerates using optical microscopy. For this purpose, a drop of the suspension was taken on glass slide and covered using a glass slip and observed under optical microscope at different magnifications. Observations were made from different parts of each suspension prepared repeated times in order to get clear idea about the dispersion quality. The overall homogeneity, presence of individually dispersed MCC and agglomerated MCC were observed and compared for different suspensions.

5.2.5. Fabrication of MCC/Cement Composites

The details of sample prepared using CMC and Pluronic are provided in Table 5. 2 and Table 5. 3, respectively. Fabrication of MCC/cement composites was done by mixing the prepared MCC aqueous suspensions with OPC and standardized sand using a standard mixer. The amounts of MCC added to the cement mixture were 0.25%, 0.75% and 1.5% (on the weight of cement mix), in case of Pluronic, and 0.5%, 1% and 1.5%, in case of CMC. As can be seen from Table 5. 2 and Table 5. 3, the cement: water ratio was always maintained at 0.5 except for one set of

5. Development of Micro Crystalline Cellulose Reinforced Cementitious Composites

samples, for which the water ratio was increased to 0.6 in order to study the effect of higher water ratio.

Table 5. 2 Details of Samples Prepared using CMC

Samples	CMC:MCC	Super-plasticizer	Water Ratio	Dispersion Conditions	Sample Code	Flow Values
Cement + 0.5% MCC+CMC	1:5	No	0.6	Ultrasonication	0.5 MC+CMC+0.6W	220, 215
Cement + 1.0% MCC+CMC	1:5	No	0.6	Ultrasonication	1 MC+CMC+0.6W	170, 170
Cement + 1.5% MCC+CMC	1:5	No	0.6	Ultrasonication	1.5 MC+CMC+0.6W	90, 94
Cement + 0.5% MCC+ CMC	1:5	Yes	0.5	Ultrasonication	0.5 MC+CMC+SP	180, 180
Cement + 1.0% MCC+CMC	1:5	Yes	0.5	Ultrasonication	1 MC+CMC+SP	156, 158
Cement + 1.5% MCC+CMC	1:5	Yes	0.5	Ultrasonication	1.5 MC+CMC+SP	170, 170
Cement + 0.5% MCC +CMC	1:5	Yes	0.5	Ultrasonication, MS at 60 °C	0.5 MC+CMC+SP+T	210, 210
Cement + 1.0% MCC+CMC	1:5	Yes	0.5	Ultrasonication, MS at 60 °C	1 MC+CMC+SP+T	150, 155
Cement + 1.5% MCC+CMC	1:5	Yes	0.5	Ultrasonication, MS at 60 °C	1.5 MC+CMC+SP+T	185, 184

The amount of superplasticizer was varied from 0-1.25 wt.% for Pluronic samples and from 0-3 wt.% for CMC samples. Due to higher MCC concentrations, samples prepared with CMC needed higher superplasticizer to achieve required flow values of the mortar paste suitable for mixing, compacting and moulding. Both for CMC and Pluronic, higher amount of superplasticizer was used for samples containing high MCC conc. to achieve the required flow values. The high water ratio (0.6) was used only in case of CMC to avoid using high amount of superplasticizer. Also, ultrasonication was avoided and only MS was used for one set of samples prepared using Pluronic, in order to study whether MS will be sufficient to disperse relatively lower amount of MCC using Pluronic. Prepared mortar mixes were poured in to rectangular moulds with dimensions of 160mm× 40mm× 40mm and kept for 24h in a humid atmosphere. Subsequently, the samples were demoulded and kept under water for hydration for 28 days. After 28 days, the samples were taken out from water, dried and tested for dry bulk density and mechanical properties. One set of plain mortar samples without MCC and dispersant was also prepared as reference samples for comparison purpose. The details of sample prepared are provided in Table 5.2 and 5.3, along with the flow values of prepared mortar mixes.

Table 5. 3 Details of Samples Prepared using Pluronic

Samples	Pluronic: MCC	Super- plasticizer	Water Ratio	Dispersion Conditions	Sample Code	Flow Values
Cement+0.25% MCC+ Pluronic	1:5	Yes	0.5	MS	0.25 MC+P+SP+MS	High
Cement + 0.5% MCC + Pluronic	1:5	Yes	0.5	MS	0.5 MC+P+SP+MS	High
Cement + 0.75% MCC+ Pluronic	1:5	Yes	0.5	MS	0.75 MC+P+SP+MS	170, 170
Cement +0.25% MCC+ Pluronic	1:5	Yes	0.5	Ultrasonication	0.25 MC+P+SP	200, 200
Cement + 0.5% MCC + Pluronic	1:5	Yes	0.5	Ultrasonication	0.5 MC+P+SP	170, 170
Cement + 0.75% MCC+ Pluronic	1:5	Yes	0.5	Ultrasonication	0.75 MC+P+SP	200, 200
Cement+0.25% MCC+ Pluronic	1:5	Yes	0.5	Ultrasonication, MS at 60 °C	0.25 MC+P+SP+T	185, 184

Cement + 0.5% MCC+ Pluronic	1:5	Yes	0.5	Ultrasonication, MS at 60 °C	0.5 MC+P+SP+T	High
Cement+ 0.75% MCC+ Pluronic	1:5	Yes	0.5	Ultrasonication, MS at 60 °C	0.75 MC+P+SP+T	High

5.2.6. Characterization of Mechanical Performance and Dry Bulk Density

Plain mortar and MCC/cement composites were characterized for flexural and compressive properties according to BS EN 196-1:1995 standard. The fracture energy of the samples was calculated from the area under the flexural load-deflection curves. Also, plain mortar, mortar containing Pluronic and CMC and MCC/mortar samples were characterized for dry bulk density according to BS EN 1015-10:1999 standard using equations 4.1 and 4.2.

5.2.7. Thermo-gravimetric Analysis of MCC/Cement Composites

Plain mortar and mortar containing MCC were characterized using Thermogravimetric Analyzer (TGA, Perkin Elmer) in nitrogen atmosphere at heating rate of 10°C/min up to 900°C. DTG curves of these samples were analyzed for obtaining quantitative estimation of various hydration products such as C-S-H, Ca(OH)₂ and CaCO₃. The influence of MCC on the hydration degree of cement was studied from this characterization.

5.2.8. Microstructural Characterization of MCC/Cement Composites

Microstructure of MCC/cement composites was characterized by investigating the fracture surface by SEM (FEG-SEM, NOVA 200 Nano SEM, FEI) using secondary electron mode and acceleration voltage of 10kV) after coating with a thin film (30 nm) of Au-Pd in a high resolution sputter coater (208HR Cressington).

5.3 Results and Discussion

5.3.1 Aqueous Dispersion of MCC: Visual Inspection

Figure 5.1 shows the state of aqueous MCC suspensions prepared with Pluronic and CMC using ultrasonication, as observed by visual inspection. Pluronic/CMC: MCC ratio of 1:5 has been used to prepare the aqueous suspensions. It can be clearly observed that up to 0.6%, the suspensions were clear without any sedimentation in case of Pluronic (Figure 5. 1a). However,

for 0.8% or higher concentrations, sedimentation can be clearly noticed, as indicated by the arrows. On the contrary, for suspensions prepared using CMC, sedimentation was observed in all concentrations (Figure 5. 1b) and the amount of settled MCC was similar. This indicates that at Pluronic: MCC ratio of 1:5, Pluronic could provide stable suspension up to 0.6% MCC and at higher concentrations, the stability of the suspensions was poor, similar to all CMC suspensions.

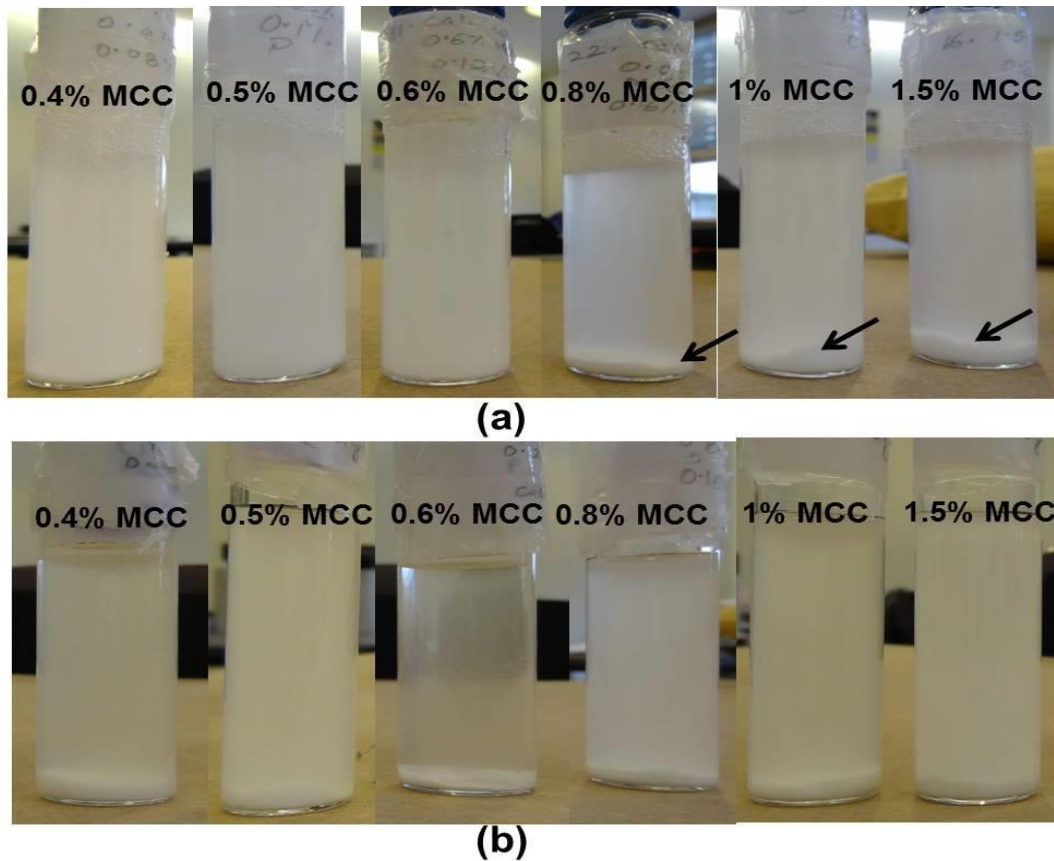


Figure 5. 1 Aqueous suspension of MCC with Pluronic (a) and CMC (b).

Pluronic was found to be more effective in providing stable suspension as compared to CMC, as it is a non-ionic surfactant containing hydrophobic and hydrophilic segments of PPO and PEO, among which PPO segments may be adsorbed on MCC while PEO segments extend into the water providing steric stabilization. However, at higher MCC conc., the number of surfactant molecules may not be sufficient to hinder agglomeration and subsequent sedimentation. Therefore, attempts were also made to disperse higher MCC concentrations using higher Pluronic ratio, as shown in Figure 5. 2.

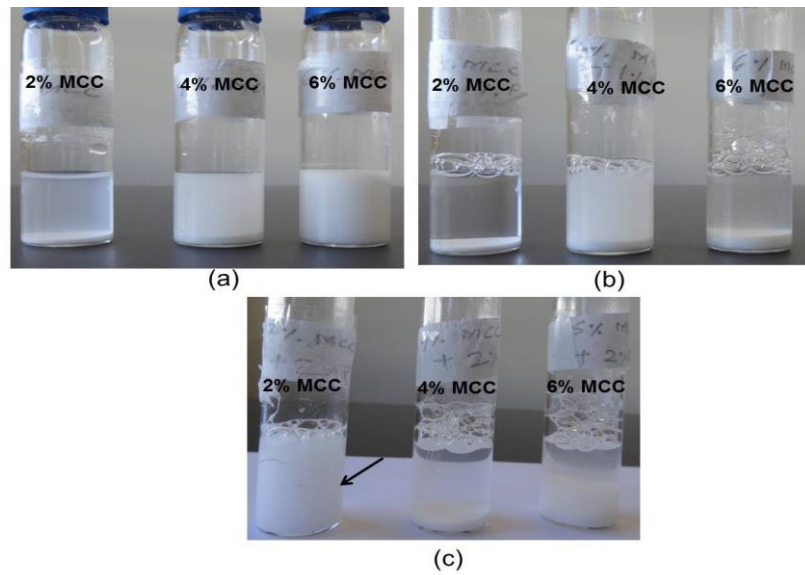


Figure 5. 2 MCC suspensions prepared using Pluronic: (a) 0% Pluronic and (b) 1% Pluronic and (c) 2% Pluronic.

The high concentration suspensions prepared without Pluronic showed considerable sedimentation, similar to those prepared using 1% Pluronic. However, 2% MCC could be dispersed well without any sedimentation using 2% Pluronic, i.e. using a Pluronic: MCC ratio of 1:1, as indicated by arrow in Figure 5.2c. Nonetheless, 4% and 6% Pluronic could not be dispersed well using 2% Pluronic. Increasing Pluronic concentration further may provide stable dispersion of these concentrated suspensions; however, this has been avoided in this research as too much use of Pluronic can have adverse effects (for example, can excessively increase flow values of cement mortar) on the performance of mortar paste.

5.3.2 Characterization of MCC Dispersion Quality using UV-Vis Spectroscopy

UV-Vis spectra of MCC suspensions are provided in Figure 5. 3. For Pluronic, higher absorption was obtained up to 0.8% MCC, indicating that higher amount of MCC was present in the suspensions in well dispersed condition. At higher MCC conc., i.e. 1.5% absorption reduced significantly. This was attributed to sedimentation of large amount of MCC leading to significant decrease in the MCC concentration in the suspension. This observation is in well agreement with the visual inspection of sedimentation, as discussed in section 5.3.1.

In case of CMC, however, similar absorption was noticed for MCC concentrations ranging from 0.4-0.6%. Visual observation also showed similar sedimentation in the suspensions prepared using CMC indicating similar concentration of MCC in all suspensions. Higher absorption was

obtained in case of higher MCC concentrations, i.e. 0.8 % and 1.5%, indicating higher amount of dispersed MCC in the suspensions. As observed in visual inspection, higher MCC concentrations did not increase sedimentation significantly and therefore, increased the amount of MCC in the suspensions. Based on these observations, higher amount of MCC has been dispersed using CMC as compared to Pluronic for fabricating cementitious composites.

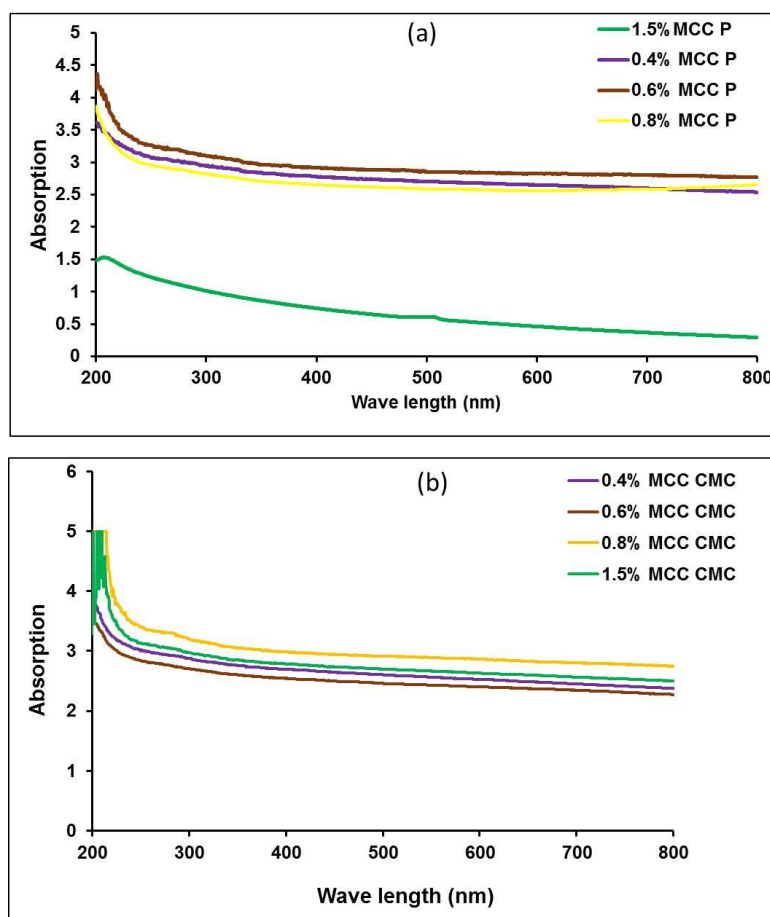


Figure 5. 3 UV-Vis absorption spectra for (a) Pluronic and (b) CMC suspensions.

5.3.3 Characterization of Dispersion Quality through Optical Microscopy

The state of MCC dispersion using Pluronic (using Pluronic: MCC ratio of 1:5) can be observed from the optical micrographs presented in Figure 5. 4. It can be noticed that at 0.5% conc., cellulose crystals were homogeneously dispersed and many individually dispersed crystals can be observed in the suspension. This can be clearly observed at high magnification (Figure 5.4a). At 1% also, significant number of individual MCC could be observed along with agglomerated crystals. At 1.5%, however, most of the cellulose micro crystals were highly agglomerated.

The dispersion quality was inferior in case of CMC, as can be observed from optical micrographs provided in Figure 5. 5. Even at 0.5%, numerous MCC agglomerates were observed. Further, the suspensions containing 1% and 1.5% MCC exhibited highly agglomerated crystals of cellulose.

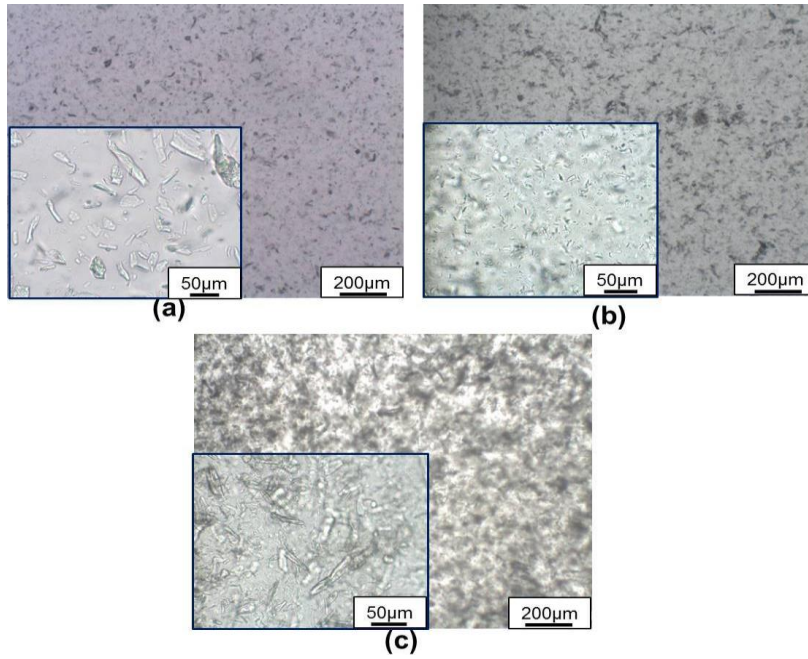


Figure 5. 4 Optical micrographs of MCC suspensions: (a) 0.5% MCC, (b) 1% MCC, and (c) 1.5% MCC.

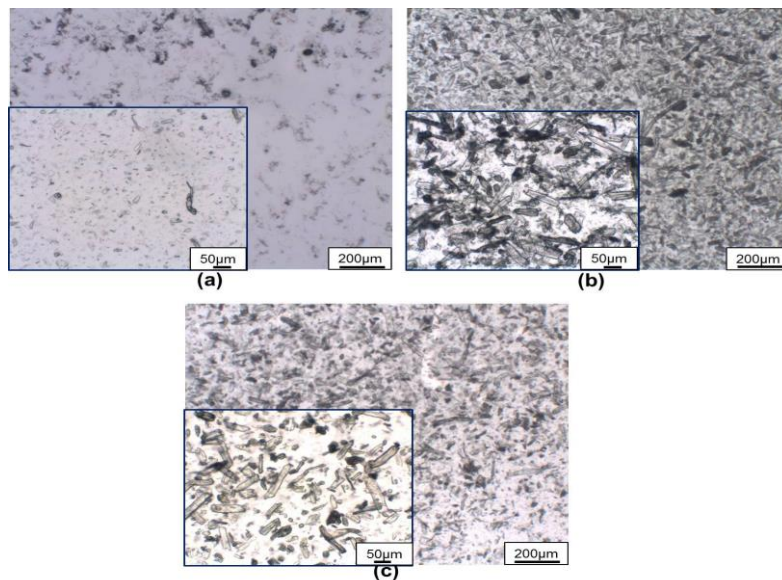


Figure 5. 5 Optical micrographs of MCC suspensions prepared using CMC: (a) 0.5% MCC, (b) 1% MCC and (c) 1.5% MCC.

5.3.4 Dry Bulk Density of Cement and MCC/Cement Composites

Dry bulk density of plain cement mortar and mortar containing Pluronic and CMC, with or without MCC, is listed in Table 5. 4. It can be observed that bulk density improved significantly with the addition of both Pluronic and CMC. In Chapter 4, it was observed that the presence of PEO side chains in Pluronic led to better dispersion of cement particles resulting in reduced porosity and improved mortar’s bulk density [199]. Similarly, CMC contains carboxymethyl groups, which probably led to better dispersion of cement through steric stabilization mechanism, as also observed in case of polycarboxylate superplasticizers. As a result, bulk density of mortar containing CMC increased significantly. Addition of MCC also improved bulk density of mortar, similar to CMC or Pluronic, due to the same reason, i.e. steric stabilization of cement particles resulting in better dispersion. This type of mechanism has been already proposed for NCC [52] and is believed to be true for MCC as well as both of them have the same chemical structure. However, improvement of bulk density was not observed when MCC was dispersed using CMC due to inferior MCC dispersion and increased porosity due to presence of MCC agglomerates.

Table 5. 4 Bulk Density of Plain Mortar and MCC/Mortar Composites

Samples	Dry Bulk Density (Kg/m ³)
Plain cement mortar	2012.4
Mortar + 0.1% Pluronic	2020.8
Mortar + 0.1% CMC	2189.4
Mortar + 0.5% MCC+ 0.1% CMC	2178.4
Mortar + 0.5% MCC + 0.1% Pluronic	2158.5

5.3.5 Mechanical Properties of MCC/Cement Composites

The flexural stress-strain curves of plain mortar and MCC/mortar samples are presented in Figure 5. 6. It can be observed that MCC addition to plain mortar has strongly improved its elastic modulus. Flexural strength has also improved significantly for most of the samples. Maximum improvements of 106% and 103.3% in flexural modulus were achieved through addition of 0.5% MCC using CMC and Pluronic, respectively, as listed in Table 5. 5. Such a strong enhancement in flexural modulus was possible, due to very high modulus of MCC and uniform dispersion of 0.5% MCC using Pluronic and CMC.

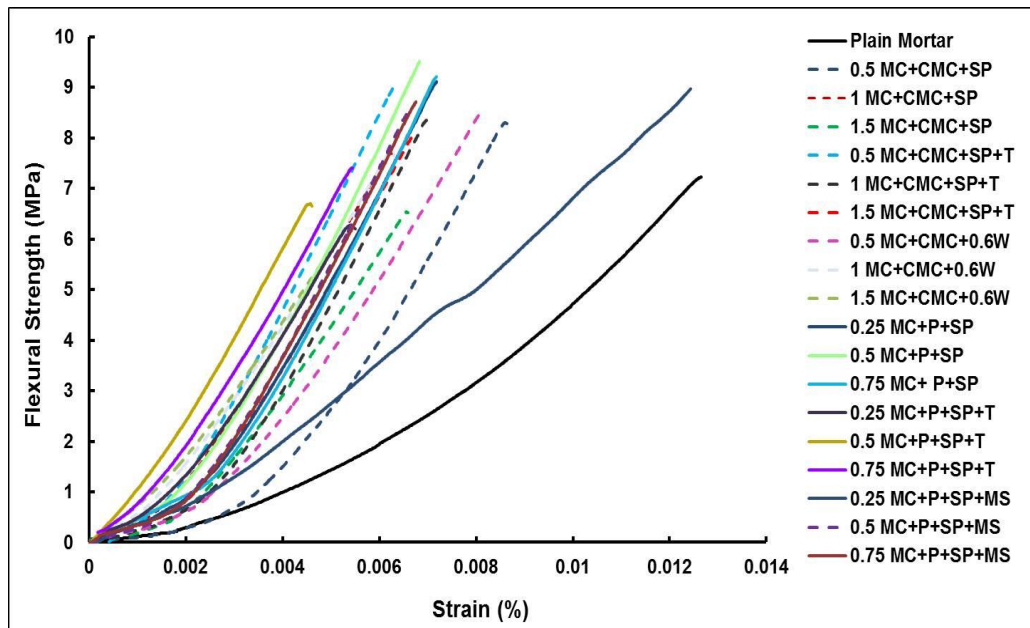


Figure 5. 6 Flexural stress-strain curves of plain mortar and MCC/cement composites.

Table 5. 5 Flexural Modulus and Fracture Energy of Plain Cement Mortar and MCC/Cement Composites

Samples	Elastic modulus (GPa)	Modulus increase (%)	Fracture energy (N.mm)
Plain Mortar	15.0	-	804.3
0.5MC+CMC+SP	27.7	84.7	408.6
1 MC + CMC + SP	25.8	72.0	347.0
1.5 MC + CMC + SP	22.8	52.0	289.9
0.5 MC+CMC+SP+ T	30.9	106.0	421.3
1 MC+CMC+SP+T	29.9	99.3	373.6
1.5MC+CMC+SP+T	27.6	84.0	365.2
0.5 MC + CMC + 0.6W	25.2	68.0	454.2
1 MC+ CMC+ 0.6W	24.2	61.3	373.0
1.5MC+CMC+0.6W	25.2	68.0	217.9
0.25MC+P+SP	29.0	93.3	438.3
0.5MC+P+SP	30.3	102.0	449.7
0.75 MC+P+SP	27.7	84.7	432.1
0.25MC+P+SP+T	25.6	70.7	243.8
0.5MC+P+SP+T	27.3	82.0	248.5

0.75 MC+P+SP+T	26.9	79.3	317.3
0.25MC+P+SP+MS	14.5	-3.3	861.5
0.5MC+P+SP+MS	30.5	103.3	368.1
0.75 MC+P+SP+MS	26.7	78.0	417.0

However, as can be noticed in Table 5.5, fracture energy of mortar reduced significantly through addition of MCC. Flexural strength, however, increased significantly for most of the samples, as can be observed from Figure 5. 6. The improvements in flexural and compressive strengths of mortar due to MCC incorporation are listed in Table 5. 6.

Table 5. 6 Improvement of Flexural and Compressive Strengths of Mortar due to MCC Addition

Samples	Flexural strength increase (%)	Compressive strength increase (%)
Plain Mortar	-	-
0.5 MC+CMC+SP	13.3	14.4
1 MC+CMC+SP	6.2	3.5
1.5 MC+CMC+SP	-9.7	-5.3
0.5 MC+CMC+SP+T	19.2	3.2
1 MC+CMC+SP+T	12.5	-4.4
1.5MC+CMC+SP+T	8.9	-5.8
0.5 MC+CMC+ 0.6W	8.5	-5.6
1 MC+CMC+ 0.6W	3.0	-8.2
1.5 MC+CMC+ 0.6W	-26.7	-21.9
0.25 MC+P+ SP	25.9	59.9
0.5 MC+ P + SP	31.2	65.6
0.75 MC+ P + SP	22.4	66.2
0.25 MC+P+SP+MS	15.0	11.5
0.5 MC+P+SP+MS	8.7	10.8
0.75 MC+P+SP+MS	17.5	-9.2
0.25 MC+P+SP+T	-17.6	-0.3
0.5 MC+P+SP+T	-8.5	3.2
0.75 MC+P+SP+T	-1.8	10.5

Improvement of 31% in mortar's flexural strength was achieved with 0.5% MCC addition using Pluronic. Similarly, compressive strength of mortar also improved strongly with MCC addition in most of the cases (Figure 5. 7) and a maximum improvement of 66% in compressive strength was achieved through 0.5% MCC addition using Pluronic.

5.3.5.1 Influence of Processing Parameters on Mechanical Properties

The influence of processing parameters such as addition of superplasticizer, water ratio, ultrasonication/magnetic stirring, dispersion temperature as well as MCC concentration on flexural and compressive strengths can be understood from Figure 5. 7 and Figure 5. 8. It is clear that in most of the cases, the samples showed decreased flexural and compressive strengths at high MCC concentrations. This was attributed to increased agglomeration of MCC at high concentrations, as observed from optical micrographs and UV-Vis spectroscopy results. The only exception to this was observed for the samples in which dispersion was carried out using Pluronic at higher temperature. In this case, high conc. MCC could be dispersed well due to high temperature and consequently, flexural and compressive strengths improved with MCC concentration.

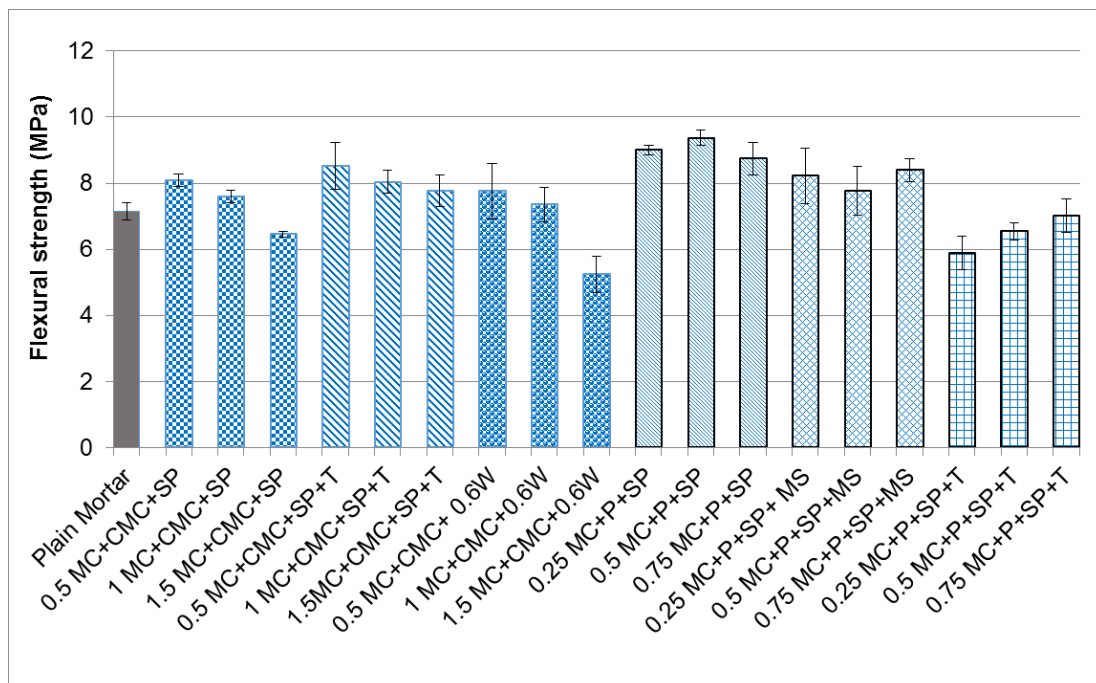


Figure 5. 7 Flexural strength of plain mortar and MCC/cement composites.

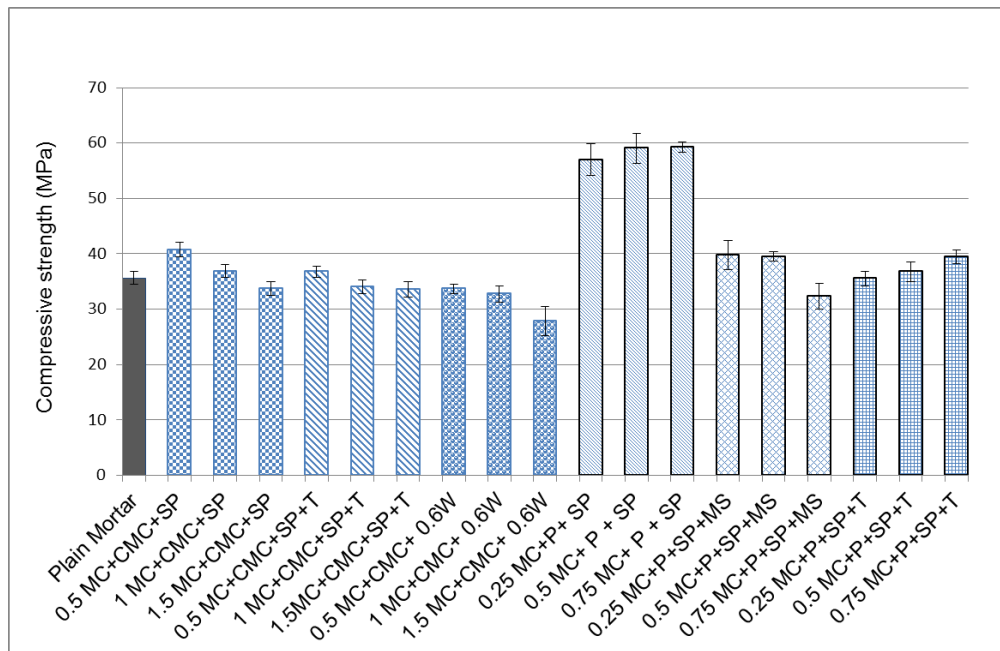


Figure 5. 8 Compressive strength of plain mortar and MCC/cement composites.

Also, overall better flexural and compressive strengths were obtained using Pluronic (even at lower MCC concentrations) as compared to CMC, mainly owing to better MCC dispersion achieved in case of Pluronic than CMC. The highest flexural and compressive strengths were achieved with Pluronic and superplasticizer combination using the ultrasonication process. The use of magnetic stirring, instead of ultrasonication, resulted in lower mechanical performance due to its lower dispersion ability as compared to ultrasonication. The addition of mechanical stirring step at high temperature also reduced the mechanical performance. This was due to the fact that MCC retained significant amount of water during high temperature stirring, reducing available water required for proper mixing with cement and sand during preparation MCC/cement composites. Therefore, improper mixing and compaction of cement paste increased the mortar's porosity and reduced the mechanical performance. In case of CMC also, the use of superplasticizer and ultrasonication process resulted in better mechanical properties. The use of higher water ratio, instead of using superplasticizer, was not found helpful, due to absence of positive effects of superplasticizer, i.e. dispersion of cement particles and also owing to increased porosity due to high water content in cement. Similar to Pluronic, the use of mechanical stirring at high temperature was not found to be beneficial for CMC also.

5.3.6 Influence of MCC on Cement Hydration

The derivative weight loss curves of pure cement mortar and mortar containing 0.75% MCC (dispersed using Pluronic) are presented in Figure 5. 9.

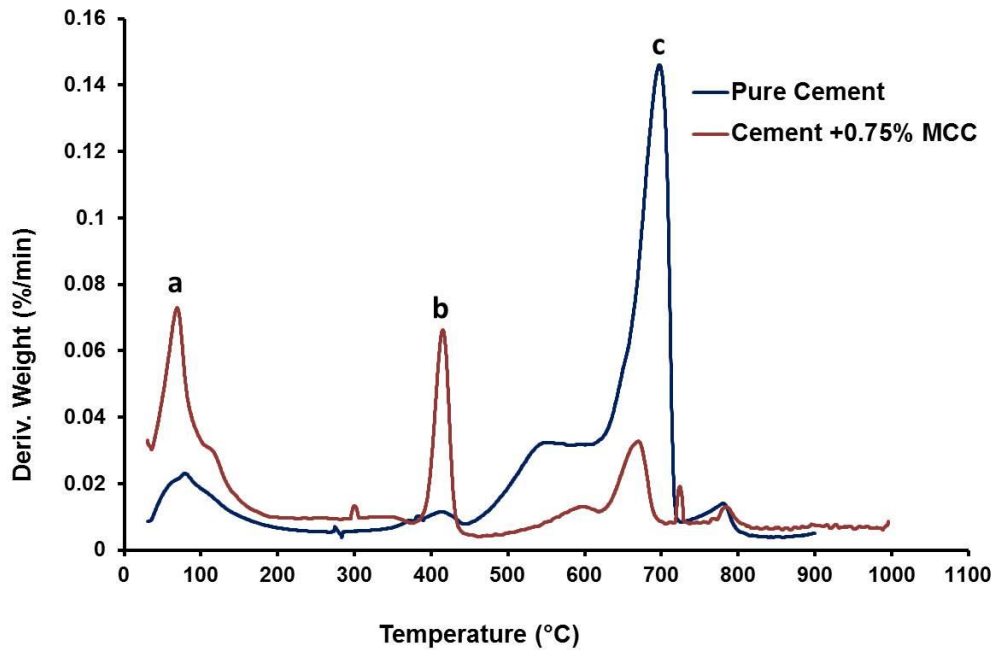


Figure 5. 9 Derivative weight loss curves for plain cement mortar and mortar containing MCC.

The first peak ‘a’ near 100°C represents the evaporation of free water and water present on the C-S-H surface [51]. The second peak ‘b’ is associated with the decomposition of $\text{Ca}(\text{OH})_2$. The third peak ‘c’ represents the amount of CaCO_3 present in all samples. However, peak ‘c’ is not a reliable measure for CaCO_3 , as its formation is also dependant on storage conditions (mainly the availability of atmospheric CO_2) and overlapping peaks from mass loss of structural OH groups of C-S-H gel. It can be clearly observed that the intensity of the peaks ‘a’ and ‘b’ was much higher in case of mortar containing MCC. It implies that the formation of C-S-H gel and $\text{Ca}(\text{OH})_2$ was significantly higher in case of MCC reinforced cement samples due to higher degree of hydration. This finding is in well agreement with the previous studies [51]. Owing to higher water retention capacity, MCC can release and supply water as the hydration proceeds, leading to higher degree of hydration. The enhanced mechanical performance of mortar due to MCC addition could, therefore, be due to increased degree of cement hydration, besides the reinforcing effect of MCC.

5.3.7 Microstructure of MCC/Cement Composites

Fracture surface of MCC/cement composites is presented in Figure 5. 10. It can be clearly observed that MCC was well embedded within the structure of cement, as indicated by arrows. This was attributed to the growth of cement hydration products on the surface of cellulose crystals. The water retained by MCC was released and used in the hydration process of cement. Also, formation of hydrogen bonds between the hydroxyl groups of MCC and cement hydration products could led to strong bonding between them. The strong interfacial bonding resulted in very good load transfer between MCC and cement matrix leading to considerable improvement in mechanical performance.

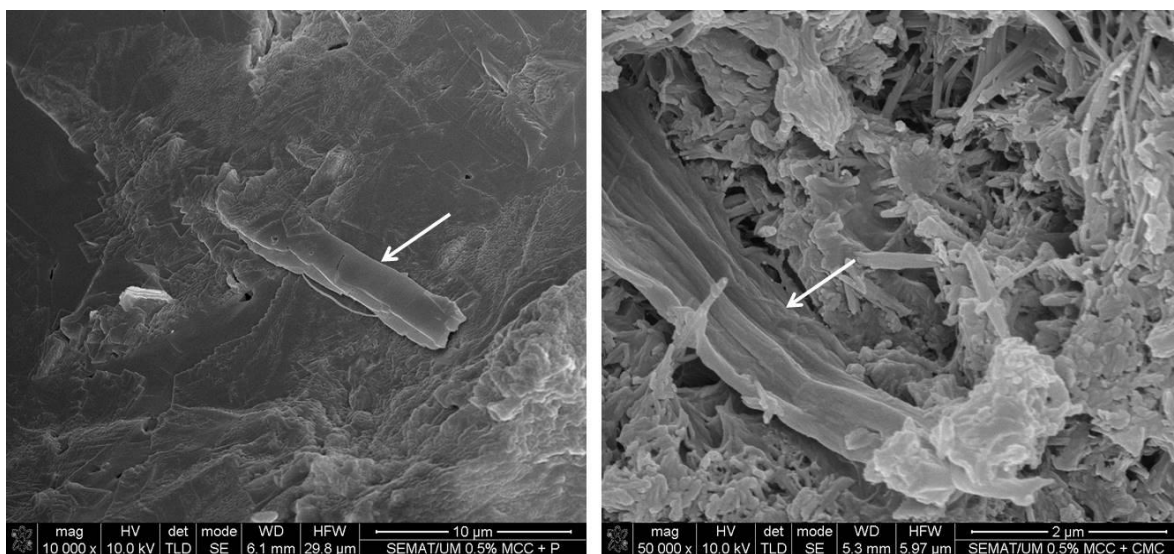


Figure 5. 10 Microstructure of MCC reinforced cementitious composites.

5.3.8 Main Findings

In Table 5. 7, the main findings of this part of PhD thesis has been compared with the previous studies on nanocellulose and MCC reinforced cementitious composites and also with the previous study on CNT reinforced cementitious composites prepared using Pluronic. It can be noticed that till now for fabricating nanocellulose and MCC reinforced cementitious composites no dispersion technique was used. As a result, CNC could be incorporated within cement composites without much agglomeration only up to 0.2 vol.%, leading to a maximum increase in flexural strength by 30% [52]. On the other hand, incorporation of MCC up to 3 wt.% could not improve mechanical properties of cementitious composites probably due to MCC agglomeration [51].

Table 5. 7 Comparison of Main Findings of Present Research with the Previous Studies on Nanocellulose, MCC and CNT Reinforced Cementitious Composites

Type of reinforcement	Dispersion technique	Main results	Reference
NCC	No. As received NCC suspension was directly mixed with cement	Flexural strength improved by 30% through addition of 0.2 vol.% NCC. At higher NCC loading, flexural strength decreased due to agglomeration. Degree of cement hydration increased with NCC addition	52
MCC	No. Saturated MCC suspension was directly added to cement mixture	Addition of MCC to cement paste led to reduction of mechanical properties in case of standard curing process. Using accelerated curing, mechanical properties of 0.3 wt.% MCC added cement mortar reached close to the mechanical properties of plain mortar. Hydration degree of cement improved with MCC addition	51
MCC	Ultrasonication in presence of Pluronic F-127 for 15 min. Superplasticizer was used during fabrication of cementitious composites	Flexural modulus, flexural strength and compressive strength improved by 106%, 31% and 66%, respectively. Hydration of cement improved due to MCC addition	Present thesis

SWCNT	Ultrasonication in presence of Pluronic F-127 for 1 hour	Flexural modulus improved up to 72% with 0.1% SWCNT. Flexural and compressive strengths improved up to 7% and 19% after 28 days of hydration and 17% and 23% after 56 days of hydration. Fracture energy improved up to 164%	Present thesis
-------	--	--	----------------

In this PhD work, homogeneous dispersion of MCC up to only 0.5 wt. %, achieved with ultrasonication process in presence of Pluronic, along with improved bulk density and microstructure obtained with superplasticizer combination resulted in 106% improvement in flexural modulus, 31% improvement in flexural strength and 66% improvement in compressive strength. The improvement in mechanical properties was even higher as compared to 0.1% SWCNT reinforced cementitious composites fabricated using the same dispersion technique, i.e. ultrasonication in presence of Pluronic (Chapter 4). However, a strong improvement in fracture energy was also obtained with SWCNT due to high extensibility of SWCNT along with high strength and stiffness. On the contrary, a decrease in fracture energy was observed in case of MCC reinforced cementitious composites developed in this PhD work.

5.4 Conclusions

In this part of the thesis, MCC was dispersed in water using Pluronic F-127 and CMC and cementitious composites were fabricated using these suspensions. The influence of Pluronic/CMC concentration, superplasticizer, dispersion technique and temperature on the mechanical performance of cementitious composites was thoroughly studied. Major conclusions of this work are as follows:

- MCC can be well dispersed using Pluronic up to 0.6% using Pluronic: MCC ratio of 1:5. Using this ratio, no sedimentation of MCC was noticed and MCC was dispersed homogeneously without agglomeration. Above 0.6% MCC concentration, significant agglomeration occurred leading to sedimentation and considerable decrease in MCC concentration in solution.
- Overall, the dispersion quality of MCC using CMC (at CMC: MCC ratio of 1:5) was inferior to Pluronic. For 0.4% to 0.6% MCC, the conc. of MCC in suspension was

similar and lower as compared to Pluronic. However, at higher conc., i.e. 1.5%, the conc. of dispersed MCC was higher with CMC indicating that the use of CMC may be preferable for higher MCC concentrations.

- The bulk density of cement mortar increased significantly due to addition of Pluronic, CMC and MCC dispersed using Pluronic. This was attributed to the better dispersion of cement particles through steric stabilization mechanism.
- The addition of MCC to cementitious composites led to strong improvement in elastic modulus. The maximum improvement in flexural modulus was 106%. The addition of MCC, however, reduced the breaking strain and fracture energy of cementitious matrix.
- Flexural and compressive strengths were highly dependent on various parameters. Higher mechanical properties were obtained with Pluronic due to better MCC dispersion as compared to CMC. The highest mechanical performance was achieved with Pluronic in combination with ultrasonication and superplasticizer. Maximum improvements in flexural and compressive strengths were 31% and 66%, respectively obtained through addition of 0.5% MCC using Pluronic.
- When added to cement matrix, MCC could be well wetted by the matrix leading to strong interface between MCC and cement hydration products.

The present work, therefore, shows the possibility of developing high performance cementitious composites through homogeneous dispersion of MCC using Pluronic F-127 and the findings will, therefore, be highly useful for construction applications.

Chapter 6

Conclusions and Future Work

This thesis aims at improving the microstructure and mechanical performance of cementitious materials by incorporating CNT and MCC as reinforcements. Pluronic F-127 was used as surfactant, for the first time, to improve the dispersion of CNT and MCC within cementitious matrices, in order to maximize the performance enhancement. The microstructure and mechanical properties of CNT and MCC reinforced cementitious composites were thoroughly investigated and the best processing conditions for achieving maximum performance improvement were identified. The major conclusions of this thesis are:

1. Different types of CNT at concentrations up to 0.3 wt.% could be dispersed in water homogeneously using optimum concentration of Pluronic F-127 with the help of a short (1hr) and medium energy (80W) ultrasonication process. The optimum suspensions presented good homogeneity, agglomerates with small areas, significant amount of well dispersed tubes (up to 55% of the initial CNT concentration) and high storage stability over 4 years. Pluronic F-127 provided better long term stability than the commonly used surfactant, SDBS and the stability was better for SWCNTs compared to MWCNTs and also with surface functionalization. Therefore, these highly homogeneous and stable CNT suspensions can be stored for long time period and used for developing cementitious composites for construction applications.
2. The use of Pluronic as a surfactant for CNT dispersion also improved the microstructure and bulk density of cement. Incorporation of CNT within cement mortar using Pluronic resulted in significant improvements in stiffness, fracture energy and ductility of cement mortar. The improvement in mechanical properties was higher with Pluronic as compared to SDBS and with SWCNTs than MWCNTs. For functionalized CNTs, mechanical properties improved with the hydration period. Maximum improvements of flexural modulus of mortar up to 72% and flexural and compressive strengths up to 7% and 19% were achieved with 0.1% SWCNT after 28 days of hydration. Flexural and compressive strengths with functionalized SWCNT increased up to 17% and 23% after 56 days of hydration.
3. MCC, up to 0.6 wt.%, could be well dispersed (without agglomeration and sedimentation) using Pluronic using Pluronic: MCC ratio of 1:5. A short (15 mins) and medium energy (80W) ultrasonication process could be used for this purpose. In this

concentration range, the dispersion quality of MCC using CMC (at CMC: MCC ratio of 1:5) was inferior to Pluronic. However, the use of CMC was found beneficial at higher MCC conc.

4. Similar to Pluronic, the addition of CMC and MCC (using Pluronic) resulted in significant improvement of bulk density and hydration degree of cement mortar, owing to better dispersion of cement particles. The addition of MCC using Pluronic to cement mortar led to strong improvement in elastic modulus (up to 106%), flexural strength (up to 31%) and compressive strength (up to 66%). The property enhancements were much higher with Pluronic than CMC. The addition of MCC, however, reduced the breaking strain and fracture energy of cementitious matrix.
5. Among CNTs and MCC, MCC could be dispersed in water and subsequently, within cementitious matrices using a shorter ultrasonication process and the improvements in mechanical properties was significantly higher. However, CNT presented one distinct advantage over MCC and that was the strong improvement in fracture energy of cement mortar with CNT addition. On the contrary, MCC reduced the breaking strain and fracture energy of cement mortar. Therefore, the selection between these two reinforcements should depend on the requirements of the targeted applications. If the civil engineering structure has to be designed to possess high ductility along with high strength and stiffness and higher processing cost can be afforded, CNT will be better reinforcing agent as compared MCC. On the other hand, if the objective is to develop structures with high strength and stiffness at lower cost and a low breaking strain can be tolerated, MCC can be considered as the better reinforcing material.

Future Scope of Work

- As both CNTs and MCC can be dispersed well using Pluronic F-127, in future, multi-scale cementitious composites can be developed using the same dispersion route through incorporation of both CNTs (nano-scale reinforcement) and MCC (micro-scale reinforcement) within cementitious matrices. These multi-scale composites are expected to provide high strength and stiffness (due to MCC and CNTs) as well as high fracture energy and ductility (due to CNTs). However, for this purpose, the dispersion technique developed in this thesis has to be optimized further to process the hybrid reinforcements

and the concentrations of Pluronic F-127 as well as CNT and MCC have to be optimized to achieve the maximum enhancement in the performance.

- The same dispersion approach can be followed in future to develop CNT reinforced or CNT-MCC reinforced multi-scale cementitious composites with piezoresistive properties for structural health monitoring. However, the concentration of the reinforcements and Pluronic has to be optimized to achieve the desired self-sensing performance.

References

1. Akkaya Y, Shah SP, Ghandehari M. Influence of fiber dispersion on the performance of microfiber reinforced cement composites. *Special Publication*. 2003;216:1-8.
2. Qing Y, Zenan Z, Deyu K, Rongshen C. Influence of nano-SiO₂ addition on properties of hardened cement paste as compared with silica fume. *Construction and building materials*. 2007;21(3):539-45.
3. Lin KL, Chang WC, Lin DF, Luo HL, Tsai MC. Effects of nano-SiO₂ and different ash particle sizes on sludge ash–cement mortar. *Journal of Environmental Management*. 2008;88(4):708-14..
4. Li H, Xiao HG, Yuan J, Ou J. Microstructure of cement mortar with nano-particles. *Composites Part B: Engineering*. 2004;35(2):185-9.
5. Li H, Zhang MH, Ou JP. Abrasion resistance of concrete containing nano-particles for pavement. *Wear*. 2006;260(11):1262-6.
6. Han B, Guan X, Ou J. Specific Resistance and Pressure-Sensitivity of Cement Paste Admixing with Nano-TiO₂ and Carbon Fiber. *Journal-Chinese Ceramic Society*. 2004;32(7):884-7.
7. Xiong G, Deng M, Xu L, Tang M. Properties of Cement-Based Composites by Doping Nano-TiO₂. *Journal-Chinese Ceramic Society*. 2006;34(9):1158.
8. Vaisman L, Marom G, Wagner HD. Dispersions of Surface-Modified Carbon Nanotubes in Water-Soluble and Water-Insoluble Polymers. *Advanced Functional Materials*. 2006;16(3):357-63.
9. Piret JP, Detriche S, Vigneron R, Vankoningsloo S, Rolin S, Mendoza JM, Masereel B, Lucas S, Delhalle J, Luizi F, Saout C. Dispersion of multi-walled carbon nanotubes in biocompatible dispersants. *Journal of Nanoparticle Research*. 2010;12(1):75-82.
10. Pang J, Xu G, Tan Y, He F. Water-dispersible carbon nanotubes from a mixture of an ethoxy-modified trisiloxane and pluronic block copolymer F127. *Colloid and Polymer Science*. 2010;288(18):1665-75.

11. Ciofani G, Raffa V, Pensabene V, Menciassi A, Dario P. Dispersion of Multi-walled Carbon Nanotubes in Aqueous Pluronic F127 Solutions for Biological Applications. *Fullerenes, Nanotubes and Carbon Nanostructures*. 2009;17(1):11-25.
12. Arutyunyan NR, Baklashev DV, Obraztsova ED. Suspensions of single-wall carbon nanotubes stabilized by pluronic for biomedical applications. *The European Physical Journal B*. 2010;75(2):163-6.
13. Bystrzejewski M, Huczko A, Lange H, Gemming T, Büchner B, Rummeli MH. Dispersion and diameter separation of multi-wall carbon nanotubes in aqueous solutions. *Journal of colloid and interface science*. 2010;345(2):138-42.
14. Pang J, Xu G, Yuan S, Tan Y, He F. Dispersing carbon nanotubes in aqueous solutions by a silicon surfactant: experimental and molecular dynamics simulation study. *Colloids and Surfaces A: Physicochemical and Engineering Aspects*. 2009;350(1):101-8.
15. Lavskaya YV, Bulusheva LG, Okotrub AV, Yudanov NF, Vyalikh DV, Fonseca A. Comparative study of fluorinated single-and few-wall carbon nanotubes by X-ray photoelectron and X-ray absorption spectroscopy. *Carbon*. 2009;47(7):1629-36.
16. Wang Y, Iqbal Z, Mitra S. Rapidly functionalized, water-dispersed carbon nanotubes at high concentration. *Journal of the American Chemical Society*. 2006;128(1):95-9.
17. Lee JU, Huh J, Kim KH, Park C, Jo WH. Aqueous suspension of carbon nanotubes via non-covalent functionalization with oligothiophene-terminated poly(ethylene glycol). *Carbon* 2007;45(5):1051-7.
18. Nativ-Roth E, Shvartzman-Cohen R, Bounioux C, Florent M, Zhang D, Szleifer I, Yerushalmi-Rozen R. Physical Adsorption of Block Copolymers to SWNT and MWNT: A Nonwrapping Mechanism. *Macromolecules* 2007;40(10):3676-85.
19. Pellenq RJ, Kushima A, Shahsavari R, Van Vliet KJ, Buehler MJ, Yip S, Ulm FJ. A realistic molecular model of cement hydrates. *Proceedings of the National Academy of Sciences*. 2009 Sep 22;106(38):16102-7.
20. Allen AJ, Thomas JJ, Jennings HM. Composition and density of nanoscale calcium–silicate–hydrate in cement. *Nature materials*. 2007;6(4):311-6.
21. Makar JM, Beaudoin JJ. Carbon nanotubes and their application in the construction industry. *Special Publication-Royal Society Of Chemistry*. 2004;292:331-42.

-
22. Li G. Properties of high-volume fly ash concrete incorporating nano-SiO₂. *Cement and Concrete research*. 2004;34(6):1043-9.
 23. Kroto HW, Allaf AW, Balm SP. C60: Buckminsterfullerene. *Chemical Reviews*. 1991 Sep;91(6):1213-35.
 24. Iijima S. Helical microtubules of graphitic carbon. *Nature*. 1991;354(6348):56-8.
 25. Odom TW, Huang JL, Kim P, Lieber CM. Structure and electronic properties of carbon nanotubes. *The Journal of Physical Chemistry B*. 2000;104(13):2794-809.
 26. W. Czernin, *Chemistry and Physics of Cement for Civil Engineers Co*, Chemical Publishing, New York, NY, USA, 1962
 27. Beyea SD, Balcom BJ, Bremner TW, Prado PJ, Cross AR, Armstrong RL, Grattan-Bellew PE. The influence of shrinkage-cracking on the drying behaviour of White Portland cement using Single-Point Imaging (SPI). *Solid state nuclear magnetic resonance*. 1998;13(1):93-100.
 28. Rana S, Alagirusamy R, Joshi M. A review on carbon epoxy nanocomposites. *Journal of Reinforced Plastics and Composites*. 2008.
 29. A.F. Turbak, F.W. Snyder, and K.R. Sandberg. "Microfibrillated Cellulose, a New Cellulose Product: Properties, Uses, and Commercial Potential." *Proceedings of the Ninth Cellulose Conference*, pp. 815–827, Applied Polymer Symposia, New York, USA: Wiley, 1983.
 30. Herrick FW, Casebier RL, Hamilton JK, Sandberg KR. Microfibrillated cellulose: morphology and accessibility. In *J. Appl. Polym. Sci.: Appl. Polym. Symp.*; (United States) 1983 (Vol. 37, No. CONF-8205234-Vol. 2). ITT Rayonier Inc., Shelton, WA.
 31. Turbak AF, Snyder FW, Sandberg KR, inventors; International Telephone, Telegraph Corporation, assignee. Microfibrillated cellulose. United States patent US 4,374,702. 1983 Feb 22.
 32. Eichhorn SJ, Dufresne A, Aranguren M, Marcovich NE, Capadona JR et. al. Review: current international research into cellulose nanofibres and nanocomposites. *Journal of Materials Science*. 2010;45(1):1-33.
 33. Kvien I, Tanem BS, Oksman K. Characterization of cellulose whiskers and their nanocomposites by atomic force and electron microscopy. *Biomacromolecules*. 2005;6(6):3160-5.

34. Angles MN, Dufresne A. Plasticized starch/tunicin whiskers nanocomposites. 1. Structural analysis. *Macromolecules*. 2000;33(22):8344-53.
35. Fleming K, Gray D, Prasannan S, Matthews S. Cellulose crystallites: a new and robust liquid crystalline medium for the measurement of residual dipolar couplings. *Journal of the American Chemical Society*. 2000;122(21):5224-5.
36. Habibi Y, Goffin AL, Schiltz N, Duquesne E, Dubois P, Dufresne A. Bionanocomposites based on poly (ϵ -caprolactone)-grafted cellulose nanocrystals by ring-opening polymerization. *Journal of Materials Chemistry*. 2008;18(41):5002-10.
37. Siqueira G, Bras J, Dufresne A. Cellulose whiskers versus microfibrils: influence of the nature of the nanoparticle and its surface functionalization on the thermal and mechanical properties of nanocomposites. *Biomacromolecules*. 2008;10(2):425-32.
38. Helbert W, Cavaille JY, Dufresne A. Thermoplastic nanocomposites filled with wheat straw cellulose whiskers. Part I: processing and mechanical behavior. *Polymer composites*. 1996;17(4):604-11.
39. Grunert M, Winter WT. Nanocomposites of cellulose acetate butyrate reinforced with cellulose nanocrystals. *Journal of Polymers and the Environment*. 2002;10(1-2):27-30.
40. Azizi Samir MA, Alloin F, Sanchez JY, Dufresne A. Cross-linked nanocomposite polymer electrolytes reinforced with cellulose whiskers. *Macromolecules*. 2004 Jun 29;37(13):4839-44.
41. J.M. Abdoveis An examination of concrete durability. Master Thesis. MIT. June 2003.
42. Parveen S, Rana S, Fanguero R. A review on nanomaterial dispersion, microstructure, and mechanical properties of carbon nanotube and nanofiber reinforced cementitious composites. *Journal of Nanomaterials*. 2013;2013:80.
43. Chen SJ, Collins FG, Macleod AJN, Pan Z, Duan WH, Wang CM. Carbon nanotube–cement composites: A retrospect. *The IES Journal Part A: Civil & Structural Engineering* 2011;4(4):254-65.
44. Gopalakrishnan K, Birgisson B, Taylor P, Attoh-Okine NO. *Nanotechnology in civil infrastructure a paradigm shift*. Springer-Verlag, Berlin Heidelberg, 2011.

-
45. Luo J, Duan Z, Li H. The influence of surfactants on the processing of multi-walled carbon nanotubes in reinforced cement matrix composites. *physica status solidi (a)*. 2009;206(12):2783-90.
46. Cwirzen A, Habermehl-Cwirzen K, Penttala V. Surface decoration of carbon nanotubes and mechanical properties of cement/carbon nanotube composites. *Advances in cement research*. 2008;20(2):65-74.
47. Collins F, Lambert J, Duan WH. The influences of admixtures on the dispersion, workability, and strength of carbon nanotube–OPC paste mixtures. *Cement and Concrete Composites*. 2012;34(2):201-7.
48. Li GY, Wang PM, Zhao X. Mechanical behavior and microstructure of cement composites incorporating surface-treated multi-walled carbon nanotubes. *Carbon*. 2005;43(6):1239-45.
49. Hubbe MA, Rojas OJ, Lucia LA, Sain M. Cellulosic nanocomposites: a review. *BioResources*. 2008;3(3):929-80.
50. Klemm D, Kramer F, Moritz S, Lindström T, Ankerfors M, Gray D, Dorris A. Nanocelluloses: A New Family of Nature-Based Materials. *Angewandte Chemie International Edition*. 2011;50(24):5438-66.
51. Hoyos CG, Cristia E, Vázquez A. Effect of cellulose microcrystalline particles on properties of cement based composites. *Materials & Design*. 2013 Oct 31;51:810-8.
52. Cao Y, Zavaterra P, Youngblood J, Moon R, Weiss J. The influence of cellulose nanocrystal additions on the performance of cement paste. *Cement and Concrete Composites*. 2015 Feb 28;56:73-83.
53. Ausman KD, Piner R, Lourie O, Ruoff RS, Korobov M. Organic solvent dispersions of single-walled carbon nanotubes: toward solutions of pristine nanotubes. *The Journal of Physical Chemistry B*. 2000;104(38):8911-5.
54. Paredes JI, Burghard M. Dispersions of individual single-walled carbon nanotubes of high length. *Langmuir*. 2004;20(12):5149-52.
55. Peng H, Alemany LB, Margrave JL, Khabashesku VN. Sidewall carboxylic acid functionalization of single-walled carbon nanotubes. *Journal of the American Chemical Society*. 2003;125(49):15174-82.

56. Wang Y, Iqbal Z, Malhotra SV. Functionalization of carbon nanotubes with amines and enzymes. *Chemical Physics Letters*. 2005;402(1):96-101.
57. Felten A, Bittencourt C, Pireaux JJ, Van Lier G, Charlier JC. Radio-frequency plasma functionalization of carbon nanotubes surface O₂, NH₃, and CF₄ treatments. *Journal of Applied Physics*. 2005;98(7):074308.
58. Utegulov ZN, Mast DB, He P, Shi D, Gilland RF. Functionalization of single-walled carbon nanotubes using isotropic plasma treatment: resonant Raman spectroscopy study. *Journal of applied physics*. 2005 May 15;97(10):104324.
59. Gonzalez-Dominguez JM, Martinez-Rubi Y, M Diez-Pascual A, Anson-Casaos A, Gomez-Fatou M. et al. Reactive fillers based on SWCNTs functionalized with matrix-based moieties for the production of epoxy composites with superior and tunable properties. *Nanotechnology* 2012;23(28):285702.
60. Xin X, Xu G, Zhao T, Zhu Y, Shi X, Gong H, Zhang Z. Dispersing carbon nanotubes in aqueous solutions by a starlike block copolymer. *The Journal of Physical Chemistry C*. 2008;112(42):16377-84.
61. Haggemueller R, Rahatekar SS, Fagan JA, Chun J, Becker ML, et al. Comparison of the Quality of Aqueous Dispersions of Single Wall Carbon Nanotubes Using Surfactants and Biomolecules. *Langmuir* 2008;24(9):5070-8.
62. Sabba Y, Thomas EL. High-concentration dispersion of single-wall carbon nanotubes. *Macromolecules* 2004;37(13):4815–20.
63. Zhu J, Yudasaka M, Zhang M, Iijima S. Dispersing carbon nanotubes in water: a noncovalent and nonorganic way. *The Journal of Physical Chemistry B*. 2004;108(31):11317-20.
64. Ma PC, Kim JK, Tang BZ. Effects of silane functionalization on the properties of carbon nanotube/epoxy nanocomposites. *Composites Science and Technology*. 2007;67(14):2965-72.
65. Sahoo NG, Jung YC, Yoo HJ, Cho JW. Effect of functionalized carbon nanotubes on molecular interaction and properties of polyurethane composites. *Macromolecular chemistry and physics*. 2006;207(19):1773-80.
66. Yuen SM, Ma CC, Lin YY, Kuan HC. Preparation, morphology and properties of acid and amine modified multiwalled carbon nanotube/polyimide composite. *Composites Science and Technology*. 2007;67(11):2564-73.

-
67. Koval'chuk AA, Shevchenko VG, Shchegolikhin AN, Nedorezova PM, Klyamkina AN, Aladyshev AM. Effect of carbon nanotube functionalization on the structural and mechanical properties of polypropylene/MWCNT composites. *Macromolecules* 2008;41:7536–42.
68. Byrne MT, McNamee WP, Gun'ko YK. Chemical functionalization of carbon nanotubes for the mechanical reinforcement of polystyrene composites. *Nanotechnology* 2008;19:415707.
69. Kim KH, Jo WH. Improvement of tensile properties of poly (methyl methacrylate) by dispersing multi-walled carbon nanotubes functionalized with poly (3-hexylthiophene)-graft-poly (methyl methacrylate). *Composites Science and Technology*. 2008;68(9):2120-4.
70. Liao YH, Marietta-Tondin O, Liang Z, Zhang C, Wang B. Investigation of the dispersion process of SWNTs/SC-15 epoxy resin nanocomposites. *Materials Science and Engineering: A*. 2004;385(1):175-81.
71. Cota FD, Panzera TH, Schiavon MA, Christoforo AL, Borges PH, Bowen C, Scarpa F. Full factorial design analysis of carbon nanotube polymer-cement composites. *Materials Research*. 2012;15(4):573-80.
72. Yazdanbakhsh A, Grasley ZC, Tyson B, Al-Rub RA. Carbon nano filaments in cementitious materials: some issues on dispersion and interfacial bond. *Special Publication*. 2009;267:21-34.
73. Yazdanbakhsh A, Grasley Z, Tyson B, Abu Al-Rub R. Distribution of carbon nanofibers and nanotubes in cementitious composites. *Transportation Research Record: Journal of the Transportation Research Board*. 2010 (2142):89-95.
74. Bentz DP, Garboczi EJ, Haecker CJ, Jensen OM. Effects of cement particle size distribution on performance properties of Portland cement-based materials. *Cement and Concrete Research*. 1999;29(10):1663-71.
75. Yazdanbakhsh A, Grasley Z. The theoretical maximum achievable dispersion of nano inclusions in cement paste. *Cement and Concrete Research*. 2012;42(6):798-804.
76. Konsta-Gdoutos MS, Metaxa ZS, Shah SP. Highly dispersed carbon nanotube reinforced cement based materials. *Cement and Concrete Research*. 2010;40(7):1052-9.
77. Metaxa ZS, Konsta-Gdoutos MS, Shah SP. Mechanical properties and nanostructure of cement-based materials reinforced with carbon nanofibers and polyvinyl alcohol (PVA) microfibers. *Special Publication*. 2010;270:115-24.

78. Islam MF, Rojas E, Bergey DM, Johnson AT, Yodh AG. High weight fraction surfactant solubilization of single-wall carbon nanotubes in water. *Nano letters*. 2003;3(2):269-73.
79. Yu X, Kwon E. A carbon nanotube/cement composite with piezoresistive properties. *Smart Materials and Structures*. 2009;18(5):055010.
80. Veedu VP. Multifunctional cementitious nanocomposite material and methods of making the same. Patent: US 7666327 B1 (2010).
81. Azhari F. Cement-based sensors for structural health monitoring. Dissertation for the Master Degree of Applied Science. University of British Columbia, Vancouver, Canada, (2008).
82. Azhari F, Banthia N. Structural Health Monitoring Using Piezoresistive Cementitious Composites. In: *Second International Conference on Sustainable Construction Materials and Technologies*, Ancona, Italy; June 28 -30.
83. Rixom R, Mailvaganam N. *Chemical admixtures handbook for concrete*. 3rd ed. London: E & FN Spon; 1999.
84. Chung DD. Review: improving cement-based materials by using silica fume. *Journal of Materials Science*. 2002;37(4):673-82.
85. Neville AM. *Properties of concrete*. New York: Pearson Education Limited; 2005.
86. Bentz DP, Jensen OM, Coats AM, Glasser FP. Influence of silica fume on diffusivity in cement-based materials: I. Experimental and computer modeling studies on cement pastes. *Cement and Concrete research*. 2000 Jun 30;30(6):953-62.
87. Toutanji H, McNeil S, Bayasi Z. Chloride permeability and impact resistance of polypropylene-fiber-reinforced silica fume concrete. *Cement and Concrete Research*. 1998;28(7):961-8.
88. Chung DD. Dispersion of short fibers in cement. *Journal of materials in civil engineering*. 2005 Aug;17(4):379-83.
89. Sanchez F, Ince C. Microstructure and macroscopic properties of hybrid carbon nanofiber/silica fume cement composites. *Composites Science and Technology*. 2009;69(7):1310-8.
90. Sanchez F. Carbon nanofibre/cement composites: challenges and promises as structural materials. *International Journal of Materials and Structural Integrity*. 2009;3(2-3):217-26.

91. Li GY, Wang PM, Zhao X. Pressure-sensitive properties and microstructure of carbon nanotube reinforced cement composites. *Cement and Concrete Composites*. 2007;29(5):377-82.
92. Sanchez F, Zhang L, Ince C. Multi-scale performance and durability of carbon nanofiber/cement composites. In: *Proc 3rd International Symposium on Nanotechnology in Construction*, vol. 3; 2009. p. 345-50.
93. Nasibulina LI, Anoshkin IV, Nasibulin AG, Cwirzen A, Penttala V, Kauppinen EI. Effect of carbon nanotube aqueous dispersion quality on mechanical properties of cement composite. *Journal of Nanomaterials*. 2012;2012:35.
94. Han B, Zhang K, Yu X, Kwon E, Ou J. Electrical characteristics and pressure-sensitive response measurements of carboxyl MWNT/cement composites. *Cement and Concrete Composites*. 2012;34(6):794-800.
95. Nasibulin AG, Shandakov SD, Nasibulina LI, Cwirzen A, Mudimela PR, Habermehl-Cwirzen K, et al. A novel cement-based hybrid material. *New Journal of Physics*. 2009; 11:023013.
96. Mudimela PR, Nasibulina LI, Nasibulin AG, Cwirzen A, Valkeapa`a M, Habermehl-Cwirzen K, et al. Synthesis of carbon nanotubes and nanofibers on silica and cement matrix materials. *Journal of Nanomaterials*. 2009;526128:1-4.
97. Metaxa ZS, Seo JWT, Konsta-Gdoutos MS, Hersam MC, Shah SP. Highly concentrated carbon nanotube admixture for nano-fiber reinforced cementitious materials. *Cement and Concrete Composites*. 2012; 34(5):612-17.
98. Nochaiya T, Chaipanich A. Behavior of multi-walled carbon nanotubes on the porosity and microstructure of cement-based materials. *Applied Surface Science*. 2011; 257(6):1941-45.
99. Makar J, Margeson J, Luh J. Carbon nanotube/cement composites-early results and potential applications. In: *Third International Conference on Construction Materials: Performance, Innovations and Structural Implications*, Vancouver; 2005. p. 1-10.
100. Al-Rub RKA, Ashour AI, Tyson BM. On the aspect ratio effect of multi-walled carbon nanotube reinforcements on the mechanical properties of cementitious nanocomposites. *Construction and Building Materials*. 2012;35:647-55.

101. Metaxa ZS, Konsta-Gdoutos MS, Shah SP. Carbon nanofiber cementitious composites: effect of debulking procedure on dispersion and reinforcing efficiency. *Cement and Concrete Composites*. 2013;36:25-32.
102. Yazdanbakhsh A, Grasley Z, Tyson B, Al-Rub RA. Challenges and Benefits of Utilizing Carbon Nanofilaments in Cementitious Materials. *Journal of Nanomaterials*. 2012;371927:1-8
103. Musso S, Tulliani JM, Ferro G, Tagliaferro A. Influence of carbon nanotubes structure on the mechanical behavior of cement composites. *Composites Science and Technology*. 2009;69(11):1985-90.
104. Yakovlev G, Kerienė J, Gailius A, Girmienė I. Cement based foam concrete reinforced by carbon nanotubes. *Materials Science*. 2006; 12(2):147–51.
105. Langan BW, Weng K, Ward MA. Effect of silica fume and fly ash on heat of hydration of Portland cement. *Cement and Concrete Research*. 2002; 32(7):1045–51.
106. Saraswathy V, Song HW. Evaluation of corrosion resistance of Portland pozzolana cement and fly ash blended cements in pre-cracked reinforced concrete slabs under accelerated testing conditions. *Materials chemistry and physics*. 2007; 104(2-3):356–61.
107. Yen T, Hsu TH, Liu YW, Chen SH. Influence of class F fly ash on the abrasion–erosion resistance of high-strength concrete. *Construction and Building Materials*. 2007; 21(2):458–63.
108. Zuquan J, Wei S, Yunsheng Z, Jinyang J, Jianzhong L. Interaction between sulfate and chloride solution attack of concretes with and without fly ash. *Cement and Concrete Research*. 2007; 37(8):1223–32.
109. Miranda JM, Jimenez AF, Gonzalez JA, Palomo A. Corrosion resistance in activated fly ash mortars. *Cement and Concrete Research*. 2005; 35(6):1210–17.
110. Yazici H. The effect of silica fume and high-volume Class C fly ash on mechanical properties, chloride penetration and freeze–thaw resistance of self-compacting concrete. *Construction and Building Materials*. 2008; 22(4):456–62.
111. Chaipanich A, Nochaiya T, Wongkeo W, Torkittikul P. Compressive strength and microstructure of carbon nanotubes-fly ash cement composites. *Materials Science and Engineering: A*. 2010; 527(4-5):1063–67.

112. Morsy MS, Alsayed SH, Aqel M. Hybrid effect of carbon nanotube and nano-clay on physico-mechanical properties of cement mortar. *Construction and Building Materials*. 2011;25(1):145–9.
113. Wild S, Khatib JM, Jones A. Relative strength, pozzolanic activity and cement hydration in superplasticised metakaolin concrete. *Cement and concrete research*. 1996; 26(10):1537–44.
114. Jones TR, Walters GV, Kostuch JA. Role of metakaolin in suppressing ASR in concrete containing reactive aggregate and exposed to saturated NaCl solution. In: *Proc 9th Int Conf alkali–aggregate react concr*, vol. 1; 1992. p. 485–96.
115. Khatib J, Wild S. Sulfate resistance of metakaolin mortar. *Cement and concrete research*. 1998;28(1):83–92.
116. Dubey A, Banthia N. Influence of high-reactivity metakaolin and silica fume on the flexural toughness of high-performance steel fiber reinforced concrete. *ACI Materials Journal*. 1998;95(3):284–92.
117. Hunashyal AM, Tippa SV, Quadri SS, Banapurmath NR. Experimental Investigation on Effect of Carbon Nanotubes and Carbon Fibres on the Behavior of Plain Cement Mortar Composite Round Bars under Direct Tension. *ISRN Nanotechnology*. 2011;856849:1-6.
118. Galao O, Zornoza E, Baeza FJ, Bernabeu A, Garces P. Effect of carbon nanofiber addition in the mechanical properties and durability of cementitious materials. *Materiales de Construcción*. 2012;62(307):343-57.
119. Dufresne A. Nanocellulose: a new ageless bionanomaterial. *Materials Today*. 2013;16(6):220-7.
120. Peng BL, Dhar N, Liu HL, Tam KC. Chemistry and applications of nanocrystalline cellulose and its derivatives: a nanotechnology perspective. *The Canadian Journal of Chemical Engineering*. 2011;89(5):1191-206.
121. Rebouillat, Serge, and Fernand Pla. "State of the art manufacturing and engineering of nanocellulose: a review of available data and industrial applications." *Journal of Biomaterials and Nanobiotechnology* 4, no. 2 (2013): 165.
122. Klemm D, Kramer F, Moritz S, Lindström T, Ankerfors M, Gray D, Dorris A. Nanocelluloses: A New Family of Nature-Based Materials. *Angewandte Chemie International Edition*. 2011;50(24):5438-66.

123. Habibi Y, Lucia LA, Rojas OJ. Cellulose nanocrystals: chemistry, self-assembly, and applications. *Chemical reviews*. 2010;110(6):3479-500.
124. Klemm D, Schumann D, Kramer F, Heßler N, Hornung M, Schmauder HP, Marsch S. Nanocelluloses as innovative polymers in research and application. In *Polysaccharides II 2006* (pp. 49-96). Springer Berlin Heidelberg.
125. Henriksson M, Berglund LA. Structure and properties of cellulose nanocomposite films containing melamine formaldehyde. *Journal of Applied Polymer Science*. 2007 Nov 15;106(4):2817-24.
126. Iguchi M, Yamanaka S, Budhiono A. Bacterial cellulose—a masterpiece of nature's arts. *Journal of Materials Science*. 2000 Jan 1;35(2):261-70.
127. Brinchi L, Cotana F, Fortunati E, Kenny JM. Production of nanocrystalline cellulose from lignocellulosic biomass: technology and applications. *Carbohydrate Polymers*. 2013 Apr 15;94(1):154-69.
128. Lam E, Male KB, Chong JH, Leung AC, Luong JH. Applications of functionalized and nanoparticle-modified nanocrystalline cellulose. *Trends in biotechnology*. 2012;30(5):283-90.
129. Beck S, Bouchard J, Berry R. Dispersibility in water of dried nanocrystalline cellulose. *Biomacromolecules*. 2012;13(5):1486-94.
130. Bondeson D, Mathew A, Oksman K. Optimization of the isolation of nanocrystals from microcrystalline cellulose by acid hydrolysis. *Cellulose*. 2006;13(2):171-80.
131. Lin N, Huang J, Dufresne A. Preparation, properties and applications of polysaccharide nanocrystals in advanced functional nanomaterials: a review. *Nanoscale*. 2012;4(11):3274-94.
132. Dong XM, Revol JF, Gray DG. Effect of microcrystallite preparation conditions on the formation of colloid crystals of cellulose. *Cellulose*. 1998 Mar 1;5(1):19-32.
133. Lu P, Hsieh YL. Preparation and properties of cellulose nanocrystals: rods, spheres, and network. *Carbohydrate Polymers*. 2010;82(2):329-36.
134. Cao X, Chen Y, Chang PR, Stumborg M, Huneault MA. Green composites reinforced with hemp nanocrystals in plasticized starch. *Journal of Applied Polymer Science*. 2008 Sep 15;109(6):3804-10.

-
135. Jackson JK, Letchford K, Wasserman BZ, Ye L, Hamad WY, Burt HM. The use of nanocrystalline cellulose for the binding and controlled release of drugs. *International journal of nanomedicine*. 2011;6:321.
136. Wang N, Ding E, Cheng R. Thermal degradation behaviors of spherical cellulose nanocrystals with sulfate groups. *Polymer*. 2007;48(12):3486-93.
137. Wang N, Ding E, Cheng R. Preparation and liquid crystalline properties of spherical cellulose nanocrystals. *Langmuir*. 2008 Jan 1;24(1):5-8.
138. Noishiki Y, Nishiyama Y, Wada M, Kuga S, Magoshi J. Mechanical properties of silk fibroin–microcrystalline cellulose composite films. *Journal of applied polymer science*. 2002 Dec 20;86(13):3425-9.
139. Svagan AJ, Hedenqvist MS, Berglund L. Reduced water vapour sorption in cellulose nanocomposites with starch matrix. *Composites Science and Technology*. 2009 Mar 31;69(3):500-6.
140. Viguié J, Molina-Boisseau S, Dufresne A. Processing and characterization of waxy maize starch films plasticized by sorbitol and reinforced with starch nanocrystals. *Macromolecular bioscience*. 2007 Nov 12;7(11):1206-16.
141. Kvien I, Sugiyama J, Votrubic M, Oksman K. Characterization of starch based nanocomposites. *Journal of Materials Science*. 2007 Oct 1;42(19):8163-71.
142. Angellier H, Molina-Boisseau S, Dole P, Dufresne A. Thermoplastic starch-waxy maize starch nanocrystals nanocomposites. *Biomacromolecules*. 2006 Feb 13;7(2):531-9.
143. Orts WJ, Shey J, Imam SH, Glenn GM, Guttman ME, Revol JF. Application of cellulose microfibrils in polymer nanocomposites. *Journal of Polymers and the Environment*. 2005 Oct 1;13(4):301-6.
144. Voronova MI, Zakharov AG, Kuznetsov OY, Surov OV. The effect of drying technique of nanocellulose dispersions on properties of dried materials. *Materials letters*. 2012;68:164-7.
145. Roy D, Semsarilar M, Guthrie JT, Perrier S. Cellulose modification by polymer grafting: a review. *Chemical Society Reviews*. 2009;38(7):2046-64.
146. Heux L, Chauve G, Bonini C. Nonflocculating and chiral-nematic self-ordering of cellulose microcrystals suspensions in nonpolar solvents. *Langmuir*. 2000 Oct 17;16(21):8210-2.

147. Ljungberg N, Bonini C, Bortolussi F, Boisson C, Heux L, Cavaillé JY. New nanocomposite materials reinforced with cellulose whiskers in atactic polypropylene: effect of surface and dispersion characteristics. *Biomacromolecules*. 2005 Sep 12;6(5):2732-9.
148. Fortunati E, Armentano I, Zhou Q, Iannoni A, Saino E, Visai L, Berglund LA, Kenny JM. Multifunctional bionanocomposite films of poly (lactic acid), cellulose nanocrystals and silver nanoparticles. *Carbohydrate Polymers*. 2012;87(2):1596-605.
149. Kaboorani A, Riedl B. Surface modification of cellulose nanocrystals (CNC) by a cationic surfactant. *Industrial Crops and Products*. 2015 Mar;65:45-55.
150. Salajková M, Berglund LA, Zhou Q. Hydrophobic cellulose nanocrystals modified with quaternary ammonium salts. *Journal of Materials Chemistry*. 2012;22(37):19798-805.
151. Beaupré, James J. “Chemically enhanced water removal in papermaking”, a dissertation submitted in fulfillment of the requirements for the degree in the Doctor of Philosophy (in Chemical Engineering), University of Maine, Orono, ME (May 2012).
152. Padalkar S, Capadona JR, Rowan SJ, Weder C, Won YH, Stanciu LA, Moon RJ. Natural biopolymers: novel templates for the synthesis of nanostructures. *Langmuir*. 2010;26(11):8497-502.
153. Fairman E. Avoiding Aggregation During Drying and Rehydration of Nanocellulose. Honors thesis. University of Maine, May 2014.
154. Hu Z, Ballinger S, Pelton R, Cranston ED. Surfactant-enhanced cellulose nanocrystal Pickering emulsions. *Journal of colloid and interface science*. 2015 Feb 1;439:139-48.
155. Kim J, Montero G, Habibi Y, Hinestroza JP, Genzer J, Argyropoulos DS, Rojas OJ. Dispersion of cellulose crystallites by nonionic surfactants in a hydrophobic polymer matrix. *Polymer Engineering & Science*. 2009;49(10):2054-61.
156. Emami Z, Meng Q, Pircheraghi G, Manas-Zloczower I. Use of surfactants in cellulose nanowhisker/epoxy nanocomposites: effect on filler dispersion and system properties. *Cellulose*. 2015 Oct 1;22(5):3161-76.
157. Sassi JF, Chanzy H. Ultrastructural aspects of the acetylation of cellulose. *Cellulose*. 1995 Jun 1;2(2):111-27.

158. Yuan H, Nishiyama Y, Wada M, Kuga S. Surface acylation of cellulose whiskers by drying aqueous emulsion. *Biomacromolecules*. 2006 Mar 13;7(3):696-700.
159. Çetin NS, Tingaut P, Özmen N, Henry N, Harper D, Dadmun M, Sèbe G. Acetylation of cellulose nanowhiskers with vinyl acetate under moderate conditions. *Macromolecular bioscience*. 2009 Oct 8;9(10):997-1003.
160. Braun B, Dorgan JR. Single-step method for the isolation and surface functionalization of cellulosic nanowhiskers. *Biomacromolecules*. 2008 Dec 22;10(2):334-41.
161. Berlioz S, Molina-Boisseau S, Nishiyama Y, Heux L. Gas-phase surface esterification of cellulose microfibrils and whiskers. *Biomacromolecules*. 2009 Jul 2;10(8):2144-51.
162. de Menezes AJ, Siqueira G, Curvelo AA, Dufresne A. Extrusion and characterization of functionalized cellulose whiskers reinforced polyethylene nanocomposites. *Polymer*. 2009 Sep 10;50(19):4552-63.
163. Hasani M, Cranston ED, Westman G, Gray DG. Cationic surface functionalization of cellulose nanocrystals. *Soft Matter*. 2008 Nov 1;4(11):2238-44.
164. Dong S, Roman M. Fluorescently labeled cellulose nanocrystals for bioimaging applications. *Journal of the American Chemical Society*. 2007 Nov 14;129(45):13810-1.
165. Goussé C, Chanzy H, Excoffier G, Soubeyrand L, Fleury E. Stable suspensions of partially silylated cellulose whiskers dispersed in organic solvents. *Polymer*. 2002 Apr 30;43(9):2645-51.
166. Li B, Xu W, Kronlund D, Määttänen A, Liu J, Smått JH, Peltonen J, Willför S, Mu X, Xu C. Cellulose nanocrystals prepared via formic acid hydrolysis followed by TEMPO-mediated oxidation. *Carbohydrate polymers*. 2015 Nov 20;133:605-12.
167. Saito T, Isogai A. TEMPO-mediated oxidation of native cellulose. The effect of oxidation conditions on chemical and crystal structures of the water-insoluble fractions. *Biomacromolecules*. 2004 Sep 13;5(5):1983-9.
168. Saito T, Hirota M, Tamura N, Isogai A. Oxidation of bleached wood pulp by TEMPO/NaClO/NaClO₂ system: effect of the oxidation conditions on carboxylate content and degree of polymerization. *Journal of wood science*. 2010 Jun 1;56(3):227-32.
169. Habibi Y, Chanzy H, Vignon MR. TEMPO-mediated surface oxidation of cellulose whiskers. *Cellulose*. 2006 Dec 1;13(6):679-87.

170. Montanari S, Roumani M, Heux L, Vignon MR. Topochemistry of carboxylated cellulose nanocrystals resulting from TEMPO-mediated oxidation. *Macromolecules*. 2005 Mar 8;38(5):1665-71

171. Araki J, Wada M, Kuga S, Okano T. Flow properties of microcrystalline cellulose suspension prepared by acid treatment of native cellulose. *Colloids and Surfaces A: Physicochemical and Engineering Aspects*. 1998 Nov 30;142(1):75-82.

172. Hoeng F, Denneulin A, Neuman C, Bras J. Charge density modification of carboxylated cellulose nanocrystals for stable silver nanoparticles suspension preparation. *Journal of Nanoparticle Research*. 2015 Jun 1;17(6):1-4.

173. Cao X, Habibi Y, Lucia LA. One-pot polymerization, surface grafting, and processing of waterborne polyurethane-cellulose nanocrystal nanocomposites. *Journal of Materials Chemistry*. 2009;19(38):7137-45.

174. Mangalam AP, Simonsen J, Benight AS. Cellulose/DNA hybrid nanomaterials. *Biomacromolecules*. 2009 Feb 2;10(3):497-504.

175. Azzam F, Heux L, Putaux JL, Jean B. Preparation by grafting onto, characterization, and properties of thermally responsive polymer-decorated cellulose nanocrystals. *Biomacromolecules*. 2010 Nov 8;11(12):3652-9.

176. Wang JS, Matyjaszewski K. Controlled/" living" radical polymerization. Atom transfer radical polymerization in the presence of transition-metal complexes. *Journal of the American Chemical Society*. 1995 May;117(20):5614-5.

177. Morandi G, Heath L, Thielemans W. Cellulose nanocrystals grafted with polystyrene chains through surface-initiated atom transfer radical polymerization (SI-ATRP). *Langmuir*. 2009 Apr 6;25(14):8280-6.

178. Yi J, Xu Q, Zhang X, Zhang H. Chiral-nematic self-ordering of rodlike cellulose nanocrystals grafted with poly (styrene) in both thermotropic and lyotropic states. *Polymer*. 2008 Sep 23;49(20):4406-12.

179. Yi J, Xu Q, Zhang X, Zhang H. Temperature-induced chiral nematic phase changes of suspensions of poly (N, N-dimethylaminoethyl methacrylate)-grafted cellulose nanocrystals. *Cellulose*. 2009 Dec 1;16(6):989-97.

-
180. Xu Q, Yi J, Zhang X, Zhang H. A novel amphotropic polymer based on cellulose nanocrystals grafted with azo polymers. *European Polymer Journal*. 2008 Sep 30;44(9):2830-7.
181. Chen G, Dufresne A, Huang J, Chang PR. A novel thermoformable bionanocomposite based on cellulose nanocrystal-graft-poly (ϵ -caprolactone). *Macromolecular Materials and Engineering*. 2009 Jan 14;294(1):59-67.
182. Lin N, Chen G, Huang J, Dufresne A, Chang PR. Effects of polymer-grafted natural nanocrystals on the structure and mechanical properties of poly (lactic acid): A case of cellulose whisker-graft-polycaprolactone. *Journal of Applied Polymer Science*. 2009 Sep 5;113(5):3417-25.
183. Siqueira G, Bras J, Dufresne A. New process of chemical grafting of cellulose nanoparticles with a long chain isocyanate. *Langmuir*. 2009 Nov 18;26(1):402-11.
184. De Volder, Michael FL, et al. "Carbon nanotubes: present and future commercial applications." *Science* 339.6119 (2013): 535-539.
185. Endo, Morinobu, Michael S. Strano, and Pulickel M. Ajayan. "Potential applications of carbon nanotubes." *Carbon nanotubes*. Springer Berlin Heidelberg, 2008. 13-61.
186. Madni, I., Hwang, C. Y., Park, S. D., Choa, Y. H., & Kim, H. T. (2010). Mixed surfactant system for stable suspension of multiwalled carbon nanotubes. *Colloids and Surfaces A: Physicochemical and Engineering Aspects*, 358(1), 101-107.
187. Liu, Y., Yu, L., Zhang, S., Yuan, J., Shi, L., & Zheng, L. (2010). Dispersion of multiwalled carbon nanotubes by ionic liquid-type Gemini imidazolium surfactants in aqueous solution. *Colloids and Surfaces A: Physicochemical and Engineering Aspects*, 359(1), 66-70.
188. Figueiredo, D. T., Correia, A. A. S., Hunkeler, D., & Rasteiro, M. G. B. (2015). Surfactants for dispersion of carbon nanotubes applied in soil stabilization. *Colloids and Surfaces A: Physicochemical and Engineering Aspects* 480: 405–412.
189. Li, C. C., Lin, J. L., Huang, S. J., Lee, J. T., & Chen, C. H. (2007). A new and acid-exclusive method for dispersing carbon multi-walled nanotubes in aqueous suspensions. *Colloids and Surfaces A: Physicochemical and Engineering Aspects*, 297(1), 275-281.

190. Clark, Michael D., Sachin Subramanian, and RamananKrishnamoorti. "Understanding surfactant aided aqueous dispersion of multi-walled carbon nanotubes." *Journal of colloid and interface science* 354.1 (2011): 144-151.
191. Rastogi, Richa, et al. "Comparative study of carbon nanotube dispersion using surfactants." *Journal of colloid and interface science* 328.2 (2008): 421-428.
192. Shin, Ji-Yong, Thathan Premkumar, and Kurt E. Geckeler. "Dispersion of Single-Walled Carbon Nanotubes by Using Surfactants: Are the Type and Concentration Important?." *Chemistry-A European Journal* 14.20 (2008): 6044-6048.
193. Blanch, Adam J., Claire E. Lenehan, and Jamie S. Quinton. "Optimizing surfactant concentrations for dispersion of single-walled carbon nanotubes in aqueous solution." *The Journal of Physical Chemistry B* 114.30 (2010): 9805-9811.
194. Najeeb, Choolakadavil Khalid, et al. "Highly efficient individual dispersion of single-walled carbon nanotubes using biocompatible dispersant." *Colloids and Surfaces B: Biointerfaces* 102 (2013): 95-101.
195. Arutyunyan, N. R., D. V. Baklashev, and E. D. Obraztsova. "Suspensions of single-wall carbon nanotubes stabilized by Pluronic for biomedical applications." *The European Physical Journal B-Condensed Matter and Complex Systems* 75.2 (2010): 163-166.
196. Moore, Valerie C., et al. "Individually suspended single-walled carbon nanotubes in various surfactants." *Nano Letters* 3.10 (2003): 1379-1382.
197. Farbod, M., Tadavani, S. K., &Kiasat, A. (2011). Surface oxidation and effect of electric field on dispersion and colloids stability of multiwalled carbon nanotubes. *Colloids and Surfaces A: Physicochemical and Engineering Aspects*, 384(1), 685-690.
198. Dresel, A., &Teipel, U. (2016). Influence of the wetting behavior and surface energy on the dispersibility of multi-wall carbon nanotubes. *Colloids and Surfaces A: Physicochemical and Engineering Aspects*, 489, 57-66.
199. Parveen, Shama, Sohail Rana, Raul Fanguero, and Maria Conceição Paiva. "Microstructure and mechanical properties of carbon nanotube reinforced cementitious composites developed using a novel dispersion technique." *Cement and Concrete Research* 73 (2015): 215-227.
200. Yu J, Grossiord N, Koning CE, Loos J. Controlling the dispersion of multi-wall carbon nanotubes in aqueous surfactant solution. *Carbon*. 2007 Mar 31;45(3):618-23

-
201. Jiang, Linqin, Lian Gao, and Jing Sun. "Production of aqueous colloidal dispersions of carbon nanotubes." *Journal of Colloid and Interface Science* 260, no. 1 (2003): 89-94.
202. Zhou Q, Zhang Z, Chen T, Guo X, Zhou S. Preparation and characterization of thermosensitive pluronic F127-b-poly (ϵ -caprolactone) mixed micelles. *Colloids and Surfaces B: Biointerfaces*. 2011;86(1):45-57
203. Pacheco-Torgal F, Jalali S. Nanotechnology: Advantages and drawbacks in the field of construction and building materials. *Constr Build Mater* 2011;25(2):582–90.
204. Singh AP, Gupta BK, Mishra M, Chandra A, Mathur RB, Dhawan SK. Multiwalled carbon nanotube/cement composites with exceptional electromagnetic interference shielding properties. *Carbon*. 2013;56:86-96.
205. Saafi M. Wireless and embedded carbon nanotube networks for damage detection in concrete structures. *Nanotechnology*. 2009;20(39):395502.
206. Yamada K, Takahashi T, Hanehara S, Matsuhisa M. Effects of the chemical structure on the properties of polycarboxylate-type superplasticizer. *Cement and concrete research*. 2000;30(2):197-207.
207. Gabrovšek R, Vuk T, Kaučič V. Evaluation of the hydration of Portland cement containing various carbonates by means of thermal analysis. *Acta Chim. Slov*. 2006;53:159-65.
208. Nochaiya T, Tolkittikul P, Singjai P, Chaipanich A. Microstructure and characterizations of Portland-carbon nanotubes pastes. In *Advanced Materials Research* 2008; 55: 549-52.
209. Torkittikul P, Chaipanich A. Bioactivity and mechanical properties of White Portland cement paste with carbon nanotubes. In *Nanoelectronics Conference (INEC), 2010 3rd International* 2010 Jan 3 (pp. 838-839). IEEE.
210. Hamzaoui R, Guessasma S, Mecheri B, Eshtiaghi AM, Bennabi A. Microstructure and mechanical performance of modified mortar using hemp fibres and carbon nanotubes. *Materials & Design*. 2014;56:60-8.
211. Spoljaric S, Genovese A, Shanks RA. Polypropylene–microcrystalline cellulose composites with enhanced compatibility and properties. *Composites Part A: Applied Science and Manufacturing*. 2009 Jul 31;40(6):791-9.

212. Haafiz MM, Hassan A, Zakaria Z, Inuwa IM, Islam MS, Jawaid M. Properties of polylactic acid composites reinforced with oil palm biomass microcrystalline cellulose. Carbohydrate polymers. 2013 Oct 15;98(1):139-45.

213. Kiziltas A, Gardner DJ, Han Y, Yang HS. Mechanical Properties of Microcrystalline Cellulose (MCC) Filled Engineering Thermoplastic Composites. Journal of Polymers and the Environment. 2014;22(3):365-72.

214. Mohammadkazemi F, Doosthoseini K, Ganjian E, Azin M. Manufacturing of bacterial nano-cellulose reinforced fiber– cement composites. Construction and Building Materials. 2015;101:958-64.

215. Rana S, Alagirusamy R, Joshi M. Development of carbon nanofibre incorporated three phase carbon/epoxy composites with enhanced mechanical, electrical and thermal properties. Composites Part A: Applied Science and Manufacturing. 2011;42(5):439-45.

216. <http://www.hawkinswatts.com/documents/DispersionofcolloidalgradesofAvicel.pdf>. Accessed on 15.02.2016.